Title
The Feeding Morphology and Ecology of Stomatopod Crustaceans

Author
Devries, Maya Susanna

Publication Date
2012

Peer reviewed|Thesis/dissertation

The Feeding Morphology and Ecology of Stomatopod Crustaceans

by

Maya Susanna deVries

A dissertation submitted in partial satisfaction of the

requirements for the degree of

Doctor of Philosophy

in

Integrative Biology

in the

Graduate Division

of the

University of California, Berkeley

Committee in charge:

Professor Sheila N. Patek, Co-Chair
Professor Todd E. Dawson, Co-Chair
Professor Roy L. Caldwell
Professor Steven E. Beissinger
Professor Peter C. Wainwright

Fall 2012

The Feeding Morphology and Ecology of Stomatopod Crustaceans

by

Maya Susanna deVries

Abstract

The Feeding Morphology and Ecology of Stomatopod Crustaceans

by

Maya Susanna deVries

Doctor of Philosophy in Integrative Biology

Professors Sheila N. Patek and Todd E. Dawson, Co-Chairs

The paradigm that animals with specialized feeding morphology consume specific prey types is central to current understanding of ecological and evolutionary processes seen in nature. Mantis shrimp, or stomatopod crustaceans, are often hailed as having highly specialized feeding morphology; their raptorial appendages produce among the fastest, most powerful strikes ever reported in the animal kingdom, allowing species to capture fast-moving prey or to crush hard-shelled prey. While all stomatopods have appendages that produce fast movements, their appendage forms differ dramatically, which has led researchers to divide stomatopods into two groups: *spearers* that unfurl streamlined appendages to capture soft-bodied, evasive prey, and *smashers* that generate enough force to crush hard-shelled prey with hammer-like appendages. Smashing appendages are thought to be more specialized for generating high speeds and accelerations, but some smasher species have been observed consuming everything from gastropods to evasive fish. Counter to expectation, this observation suggests that morphological specialization allows smashers to consume a wider range of prey compared to spearers. Thus, the classic notion of a one-to-one relationship between "specialized morphology" and diet may not apply to stomatopods.

This dissertation lays the foundation for testing the hypothesis that stomatopods with appendages specialized for speed and acceleration have broad rather than narrow diets. Specifically, this dissertation addresses three fundamental questions in three chapters: 1) what are the kinematics of the spearing mantis shrimp, 2) do different stomatopod tissues integrate diet over a variety of timescales, and 3) does morphological specialization for speed and acceleration correspond with a broad or narrow diet in a smashing mantis shrimp?

The first question addresses a key gap in current knowledge of stomatopod mechanics by providing the first in depth analysis of strike kinematics in a spearer. High speed and field videos of prey capture events were used to quantify appendage movements and behavior. Morphology was analyzed with Computed Tomography scans of the appendage. The results from these analyses were then compared to previous research on a smashing species. I found that the spearer exhibited greater reach but lower speeds and accelerations than the smasher, which implies a trade-off between reach and speed.

The second question aims to develop methods in stable isotope ecology that determine the diet breadth of smashing mantis shrimp, because stable isotope analysis measures and compares intra- and interspecific patterns of diet breadth. The isotopic incorporation rates and isotopic discriminations of carbon and nitrogen in tissues are essential for correctly interpreting stable isotope data. I measured these variables in the smashing mantis shrimp, *Neogonodactylus*

bredini, by feeding individuals a single species of prey and periodically sampling their muscle and hemolymph. I found variation in incorporation rates between and within tissues, and discrimination factors that were different than expected based on published literature values. *N. bredini*'s rate of carbon incorporation was consistent with rates predicted by an allometric equation correlating incorporation rate to body mass for teleost fishes and sharks.

The third question builds on the previous study and seeks to determine the diet breadth of *N. bredini*. Specifically, I combined abundance studies of prey items, a laboratory feeding experiment that examined which prey *N. bredini* would consume, a stable isotope analysis of diet, and field observations of feeding behavior. I conducted these studies in a sea grass habitat and a coral rubble habitat over two different seasons to determine whether diet changed spatially and temporally. The abundance study revealed that prey abundances vary between habitats. The feeding experiment showed that *N. bredini* was capable of consuming both hard- and soft-bodied prey. The stable isotope analysis showed that *N. bredini* consumed a wide range of different prey in the field, including snapping shrimp and soft-bodied worms. Thus, in contrast with the hypothesis that specialized feeding morphology corresponds to a narrow diet, this suite of observations demonstrates that *N. bredini*'s smashing appendage does not limit this predator to a diet of hard-shelled prey.

Together, the answers to these questions provide novel insight into the relationship between appendage morphology and diet specialization in mantis shrimp and lay the foundation for examining the ecomorphology of this diverse group of animals.

Dedicated to my loving parents,
Joyce and Jan de Vries,
who have believed in me from the beginning.

Table of Contents

Acknowledgements

I would never have come this far with my dissertation nor had such a wonderful time in the process without the support of the following people and funding agencies.

Funding was provided by the Fulbright Student Research Grant (Panama), the Phi Beta Kappa Graduate Fellowship, the Society of Integrative and Comparative Biology Grants-In-Aid-of-Research, the Smithsonian Tropical Research Institute's Short-Term Fellowship Award, the American Museum of Natural History Lerner-Gray Fund, the Berkeley and National Sigma Xi Scientific Honors Societies' Grants-In-Aid-of-Research, the UC Berkeley Department of Integrative Biology Endowment, the Department of Integrative Biology Gray Endowment Research Fellowship, the UC Museum of Paleontology Graduate Student Research Award. Funding was also provided by the National Science Foundation (IOS-1014573 to Sheila Patek).

I am so thankful to my dissertation co-chair, Sheila N. Patek, for sharing her expertise and love of nature with me. Her intellect, pro-active nature, thoughtfulness, and fun-loving spirit are the qualities that make her a truly inspiring mentor. During graduate school, Sheila taught me more about how to be a good scientist and an active citizen than she will ever know.

Todd E. Dawson, my dissertation co-chair, has been so encouraging and insightful throughout my graduate school career. I am so thankful that he accepted me into his lab as a full graduate student member and that he was excited to turn his plant lab into an "invertebrate lab." I am proud to be able to call myself a Dawsonite!

My dissertation and qualifying exam committees were critical to the intellectual development of this research. If my naturalist skills are half as keen as Roy L. Caldwell's one day, then I know I will have succeeded. I thank Roy for sharing his field site in Panama with me and for his never-ending knowledge of mantis shrimp biology. I also thank him for encouraging me to explore my interests in science outreach. Peter C. Wainwright has believed in me since I was an undergraduate in his lab and has been a motivating force for me to continue in science since then. I thank him for supporting me and fostering my many interests in evolutionary biology all of these years. Steven E. Beissinger, was so helpful and patient during my preparation for my qualifying exam and he has continued to be an encouraging voice throughout the writing of my dissertation. I am so grateful for his support. I also thank Robert Dudley for insightful discussions about broad topics in functional morphology and evolutionary biology and David Ackerly for teaching me about the intricacies of niche theory.

In addition to my committee members, several other professors were an important influence on my research and development as a scientist. John H. Christy was my advisor at the Smithsonian Tropical Research Center in Panama. I thank John for his invaluable support with everything from logistics in Panama to the theoretical basis of my dissertation. John was especially helpful with making Chapter III a success by giving critical consideration to every question I asked. In the process, he taught me how to be a thoughtful field biologist. Carlos Martínez del Rio was critical to the success of Chapter II. I am very grateful for the time and effort that he gave to this project.

I am truly lucky to have been a member of two amazing lab groups, The Patek Lab and Dawson Lab. The Patek Lab has made me the scientist that I am today. Marco Mendoza, Michael Rosario, and Patrick Green read many drafts of my writing and kept spirits high. I also thank Joe Baio and Lauren Shipp for being wonderful lab mates all around. The spearer kinematics paper would never have come as far as it did without Elizabeth Murphy and our meetings in Café Milano. I am forever indebted to Jennifer R. A. Taylor who became my

guiding light intellectually and emotionally. Thomas "Big Body" Claverie taught me how to be a careful field biologist while having a wonderful time in the process. Erica Staaterman is an amazing woman, scientist, and friend who knows how to keep me motivated.

The Dawson Lab took me under their wing as one of their own. I thank Cameron Williams for his supportive discussions and smiles and Allison Kidder for being a wonderful listener and friend. Greg Goldsmith was critical to the intellectual development of Chapter III and truly a guiding force during the last phase of my dissertation. What more can I say but, palabra. I thank Adam Roddy for supporting me in all of my scientific endeavors, from helping me to develop my fieldwork, to participating in and encouraging my many outreach projects in Panama. I value our many late night discussions and delicious dinners. I am forever grateful to one of my closest friends, Michal Shuldman, who is beyond supportive, honest, and helpful. Michal and I began this journey together and I am so proud to end it with her too.

The Caldwell Lab has also been incredibly supportive, and I thank all lab members with whom I have had the pleasure to work, for being such an integral part of my graduate school experience. Many other graduate students have helped me through this process, including Stephanie Bush and David Hembry, who made Moorea 2009 an unforgettable experience, and Stephanie Stuart, who was a wonderful housemate.

My undergraduate assistants were critical to the success of this research and I am sincerely grateful for their help. They are all incredibly kind, smart, and hard-working individuals, and I know they will be successful in whatever paths they choose. I thank Randy Tigue for assistance with kinematic data collection, Muniba Mohammad for endless time in the library and at the scanner, to Eric O. Campos, Eric Chan, Tiffany Chang, Danielle Desmet, Claire Liivoja, Maria Perez, Al Pickard, Alana Reece, Annie Stother, and Wendy Turner for assistance with animal care and stable isotope sample preparation. I thank the amazing undergraduates at the University of Panama in Colón, Claire Liivoja, and Vy Duong for watching many hours of video. I am especially grateful for Samantha Lu for assistance with animal care and dissections and for Julia Hassen for dissections and sample preparation.

My fieldwork would not have been possible without the invaluable support staff at the Smithsonian Tropical Research Institute's Galeta Marine Laboratory. I thank Franklin Guerra, Edgardo Gonzalez-Ulloa, Alfredo Lanuza, and especially Gabriel Thomas, Yiriana Romero Mejia, Jorge Morales, and the undergraduates at the University of Panama in Colón for all of their support. I am so grateful to Illia Grenald for helping me in all of my endeavors in Panama. All stable isotope analyses occurred at the UC Berkeley Center for Stable Isotope Biogeochemisty by Stefania Mambelli and Paul Brooks, to whom I am very grateful.

I would never have survived without my wonderful support network of friends outside of graduate school, including Becky, Emi, Keeley, Illeana, and Bernidet. I thank Bridie, Molly, and LCC for keeping me sane during the last phase of my dissertation, Megan for keeping me laughing, Lilah for always knowing how to keep my spirits high, Josephine for encouraging me to dream big and to have adventures, and Mika for supporting me in the face of any challenge.

My dissertation is as much an accomplishment of my family's as it is mine. My mother, Joyce, taught me how to be a good writer and to be patient, kind, and compassionate. She was also an excellent field assistant! My father, Jan, taught me how to enjoy life and to both appreciate and question the world around me. I thank both of them for their unending love and support. My loving husband, Tate Tunstall, experienced all of the ups and downs of graduate school with me. I thank him for supporting me in all of my endeavors from helping me to fix my R-code to counting invertebrates with me in Panama. I feel so lucky to have him as my rock.

Introduction

A tenet in ecology is that animals with specialized feeding morphology consume specific prey types (Darwin 1859, Wainwright & Reilly 1994). The powerful seed-crushing beak of the Galapagos finch (Darwin 1859, Grant & Grant 1993) and the long nectar-sucking proboscis of the hawkmoth (Darwin 1862) provide classic examples of the tight link between feeding morphology and ecology. Mantis shrimp (Stomatopoda) are a third group of organisms that biologists often tout as having highly specialized feeding morphology; their raptorial appendages produce among the fastest and most powerful strikes in the animal kingdom. Depending on their appendage morphology, they can either capture elusive fish and crustaceans or crush hard-shelled molluscs (Caldwell & Dingle 1976, Patek & Caldwell 2005, Patek, Korff & Caldwell 2004).

With the advent of new technology for accurately measuring prey consumption, however, recent research suggests that highly specialized feeding morphology is not necessarily an indicator of diet specialization (Barnett, Bellwood & Hoey 2006, Bellwood *et al.* 2006, Liem 1980). This discordance between morphology and diet was first noticed in African cichlids which have jaw morphologies that are considered remarkably specialized to consume specific prey types; one species even has jaws for nipping the scales off of one side of another fish (Hori 1993). Yet, most of the time, these same species feed on algae and zooplankton (reviewed in Liem 1980; Robinson & Wilson 1998). Labroid fishes also exhibit jaw morphologies that range from aggressive suction feeders to algal scrapers, yet these morphologies do not appear to limit species to strict diets (Bellwood *et al.* 2006). Current research in stomatopods is beginning to show a similar pattern. Although selection pressure for specialized feeding morphology is thought to have yielded narrow diets (Caldwell & Dingle 1976, Dingle & Caldwell 1978), some stomatopod species have been observed consuming everything from gastropods to soft-bodied, elusive fish (Caldwell & Dingle 1976, Caldwell, Roderick & Shuster 1989). Further research may reveal that morphological specialization actually corresponds to a broad diet, allowing stomatopods to both capture evasive prey and to break hard-shelled prey.

The key to advancing this new window into the evolutionary and ecological correlations between prey consumption and feeding morphology rests on two key factors: a solid definition of diet specialization and accurate diet reconstruction both within and across species, and across a range of spatial and temporal scales (Irschick & Sherry 2005, Ferry-Graham, Bolnick & Wainwright 2002, Futuyma & Moreno 1988). Thus, the goals of this dissertation are:

1) to understand how feeding mechanics and behavior relate to diet breadth
2) to construct a foundation for quantitatively analyzing, defining, and comparing diet specialization across taxa.

Defining diet specialization

In evolutionary biology and ecology, "specialization" and "generalization" have become common terms for describing how organisms use resources. These terms are inherently relative, because specialists and generalists are defined as organisms with limited or broad resource use, respectively. The definitions are based on Hutchinson's (1957) "n-dimensional" hypervolume, where each dimension, or niche axis, is a different resource that an organism needs to survive. Examples of resources include food, habitat, sunlight, and water. Together, these niche axes

comprise the overall ecological space of an organism (Hutchinson 1957). Thus, an organism can be a specialist on one niche axis but a generalist on another, which is why researchers define and measure each niche axis independently. In this dissertation, the focal niche axis will be the food resources that comprise an organism's diet.

Despite this framework for defining an organism's total niche breath, the terms specialization and generalization remain context dependent, because there is no common metric with which to compare the degree of diet specialization between taxa (Ferry-Graham, Bolnick & Wainwright 2002; Irschick & Sherry 2005). For example, is the scale-eating African cichlid a diet specialist even though the majority of its diet contains algae that is consumable without specialized morphology? This question demonstrates the challenges associated with determining a common set of characteristics that define a specialist and with creating a standard metric of diet specialization that can be used to measure degree of diet specialization across taxa (Bearhop *et al.* 2004).

Most of the current methods for determining diet specialization use diversity indices, such as the Shannon-Weaver Diversity Index, to measure diet specialization on a scale of prey diversity (reviewed in Bearhop *et al.* 2004). These indices provide a foundation on which to develop metrics of specialization, because they take into account the richness and evenness of the prey represented in the diet (Bearhop *et al.* 2004). The problem with this approach, however, is that the methods used to collect data for the index are not standardized. For example, counting the number of prey found in the gut is a common method for examining diet, even though this method is widely known to only document a short time window of a predator's diet (Hyslop 1980; Bearhop *et al.* 2004; Newsome *et al.* 2007). Prey preference studies in the laboratory have also been used to determine important dietary components (Underwood, Chapman & Crowe 2004 and references therein), but these experiments have a limited capacity to accurately reflect natural diets, because laboratory conditions do not account for spatial and temporal variation in prey availability (Stephens & Krebs 1986; Blackwell, O' Hara & Christy 1998). These differences between how diet data are gathered make it difficult to determine which organisms are specialists and which are generalists, because the methods are known to miss key dietary components (Hyslop 1980; Stephens & Krebs 1986; Blackwell, O' Hara & Christy 1998). Additionally, it is challenging to establish what the "cut-off" on a continuum for a specialist or a generalist should be when the scale is not based on the same data collection methodology.

The first step toward developing a comparable metric across taxa is therefore to use a standard method that measures diet breadth in the same way across consumers. Stable isotope analysis, specifically of stable carbon and nitrogen isotope ratios (i.e. $^{13}C/^{12}C$ and $^{15}N/^{14}N$), has been proposed as a novel method for comparing intra- and interspecific patterns of diet breadth (Bolnick *et al.* 2002; Bearhop *et al.* 2004; Layman *et al.* 2007; Newsome *et al.* 2007; Martínez del Rio *et al.* 2009; Boecklen *et al.* 2011). The central principle of stable isotope analysis is that the isotopic compositions of different prey items record a predator's diet with reliable fidelity when prey are consumed, metabolized, and assimilated into a consumer's tissues (reviewed in Fry 2006). Given that all organisms have naturally occurring stable isotopes that reflect their nutrient sources, stable isotope analysis can be used to measure diet specialization across taxa (Bearhop *et al.* 2004; Newsome *et al.* 2007; Martínez del Rio *et al.* 2009). A distinct advantage of using stable isotopes is that they allow for examining spatial and temporal shifts in diet (reviewed in Boecklen *et al.* 2011), which helps to ensure that at least a good portion of organism's diet is described. Stable isotope analysis can also begin to establish a standard diet breadth continuum that can be used to determine degree of diet specialization across taxa. Once

the diet breadth of many species has been measured with this analysis, it may be possible to distinguish between specialists and generalists, because all species will be evaluated directly in terms of their stable isotope variation (Bearhop *et al.* 2004).

Approach

Mantis shrimp provide an excellent group for addressing the two goals mentioned above. Mantis shrimp raptorial appendages are diverse in both form and function (Ahyong 2001), ranging from hammer-shaped appendages ("*smashers*") that are used to crush hard-shelled molluscan and crustacean prey to elongate, streamlined appendages ("*spearers*") that capture evasive prey (Caldwell & Dingle 1975; Caldwell & Dingle 1976; Dingle & Caldwell 1978). This framework remains central to the current understanding of mantis shrimp feeding ecology and behavior (Caldwell & Dingle 1975; Caldwell & Dingle 1976; Caldwell, Roderick & Shuster 1989; Patek & Caldwell 2005), because it explains how appendage morphology influences strategies for capturing and consuming prey (Caldwell & Dingle 1975; Caldwell & Dingle 1976). Although mantis shrimp appendage morphology is well understood (Ahyong 2001), the feeding behavior and mechanics of spearing remain understudied (except see Hamano & Matsuura 1986; Dingle & Caldwell 1978) and most information on both spearer and smasher diets is from anecdotal observations and limited gut content analyses (Camp 1973; Dingle & Caldwell 1978; Caldwell, Roderick & Shuster 1989; Pihl *et al.* 1992; Hamano *et al.* 1996; Maynou, Abello & Sartor 2005).

To attempt to bring the level of understanding of spearing mechanics to that of smashing mechanics, I first performed a kinematic and behavioral analysis of the spearing strike. While a body of literature exists on the kinematics of smashing (Patek, Korff & Caldwell 2004; Burrows 1969; McNeill, Burrows & Hoyle 1972; Patek & Caldwell 2005), the research presented in Chapter I provides the first in depth analysis of the mechanics of the spearing strike. I compare the strike mechanics of the spearer to that of a smasher to provide insight into whether, like smashers, spears produce high speeds and accelerations.

In order to transform anecdotal observations of diet into a foundation for comparing degree of diet specialization across mantis shrimp, I used stable isotope analysis to determine the diet breadth of a smashing mantis shrimp species, *Neogonodactylus bredini*. This group of studies laid the groundwork for using stable isotope analysis across mantis shrimp taxa. Different tissues incorporate new material, and thus its stable isotope composition, at different rates (reviewed in Martínez del Rio *et al.* 2009; Dalerum & Angerbjörn 2005). These rates can be harnessed to analyze diet over both short and long periods of time. To address these temporal changes in diet, Chapter II presents a study of isotopic incorporation rates in *N. bredini*.

Stable isotopes also provide information about spatial variation in diet (France 1995). Marine primary producers use different photosynthetic pathways, which generate variation in $\delta^{13}C$ values (Fry *et al.* 1982; Hemminga & Mateo 1996; Vaslet *et al.* 2011). Once ingested, these distinct $\delta^{13}C$ values are assimilated into the consumer's tissues without much change to the $\delta^{13}C$ ratio (France 1995). Thus, the $\delta^{13}C$ values can be measured in consumers and then used to determine the habitat in which the prey was found (France 1995). $\delta^{15}N$, however, provides information about the trophic level of the consumer (Minagawa & Wada 1984), because there are standard differences between predator and prey $\delta^{15}N$ values that are a result of the predator metabolizing the prey (reviewed in Boecklen *et al.* 2011). When $\delta^{15}N$ is coupled with habitat information provided by $\delta^{13}C$, researchers can trace natural variation in diet that occurs as animals move between habitats, as habitats change seasonally, or as the abundance of prey

changes between habitats and seasons. To determine the complete diet breadth of *N. bredini* over space and time, Chapter III analyzes the $\delta^{13}C$ and $\delta^{15}N$ values of two tissue types with different incorporation rates from animals collected in different seasons and habitats.

Despite the advantages of stable isotope analysis, one challenge is that stable isotope mixing models, which determine the percent contribution of different prey items to the diet, are difficult to solve when the analysis has more potential prey items than the number of isotopes + 1 (Phillips & Gregg 2003 and references therein). The development of mixing models based on Bayesian statistics has made great strides in overcoming the problem of having too many sources and not enough stable isotopes (Moore & Semmens 2008; Parnell *et al.* 2010; Jackson *et al.* 2011). These methods have been tested on animals with diverse diets, such as coral reef fishes (Nagelkerken *et al.* 2009; Greenwood, Sweeting & Polunin 2010; Layman & Allgeier 2012). However, further stable isotope studies in animals with broad diets will greatly aid in determining the extent to which stable isotope analysis can be applied to predators with broad diets. The research presented in Chapter III builds on these studies by combining stable isotope analyses of diet with field observations of feeding behavior, a feeding experiment, and abundance counts of available prey in the habitat.

Broad conclusions

Together, these findings yield insights into the relationship between appendage morphology and diet specialization in mantis shrimp. The kinematic analysis of spearing showed that, even though spearer appendages move much more slowly than smashing appendages, they are fast enough to capture evasive, soft-bodied prey. The analysis of a smasher's diet helped to develop the use of stable isotopes to measure diet breadth. Although stable isotopes were used to measure diet specialization in only one mantis shrimp species, this one species can now be examined on the diet specialization continuum relative to other animals that have undergone similar stable isotope analyses. The results of these studies revealed that, counter to my initial predictions, morphological specialization for speed and acceleration is associated with a diverse diet. These discoveries in mantis shrimp, coupled with novel methods in stable isotope ecology, may yield a fundamental shift in the current understanding of the classic form-function relationships central to modern organismal biology.

References

Ahyong, S.T. (2001) Revision of the Australian stomatopod Crustacea. *Records of the Australian Museum Supplement 26*, 1-326.

Barnett, A., Bellwood, D.R. & Hoey, A.S. (2006) Trophic ecomorphology of cardinalfish. *Marine Ecology Progress Series,* 322, 249-257.

Bearhop, S., Adams, C.E., Waldrons, S., Fuller, R.A. & Macleod, H. (2004) Determining trophic niche width: a novel approach using stable isotope analysis. *Journal of Animal Ecology,* 73, 1007-1012.

Bellwood, D.R., Wainwright, P.C., Fulton, C.J. & Hoey, A.S. (2006) Functional versatility supports coral reef biodiversity. *Proceedings of the Royal Society B-Biological Sciences,* 273, 101-107.

Blackwell, P.R.Y., O' Hara, P.D. & Christy, J.H. (1998) Prey availability and selective foraging in shorebirds. *Animal Behavior,* 55.

Boecklen, W.J., Yarnes, C.T., Cook, B.A. & James, A.C. (2011) On the use of stable isotopes in trophic ecology. *Annual Review of Ecology, Evolution, and Systematics,* 42, 411-440.

Bolnick, D.I., Yang, L.H., Fordyce, J.A., Davis, J.M. & Svanback, R. (2002) Measuring individual-level resource specialization. *Ecology,* 83, 2936-2941.

Burrows, M. (1969) The mechanics and neural control of the prey capture strike in the mantid shrimps *Squilla* and *Hemisquilla*. *Zeitschrift fur vergleichende Physiologie,* 62, 361-381.

Caldwell, R.L. & Dingle, H. (1975) Ecology and evolution of agonistic behavior in Stomatopods. *Naturwissenschaften,* 62, 214-222.

Caldwell, R.L. & Dingle, H. (1976) Stomatopods. *Scientific American*, 81-89.

Caldwell, R.L., Roderick, G.K. & Shuster, S.M. (1989) Studies of predation by *Gonodactylus bredini*. *Biology of Stomatopods* (ed. E.A. Ferrero), pp. 117-131. Mucchi, Modena.

Camp, D.K. (1973) Stomatopod Crustacea. *Memoirs of the Hourglass Cruises*, pp. 1-100. Florida Department of Natural Resources, St. Petersburg, FL.

Dalerum, F. & Angerbjörn, A. (2005) Resolving temporal variation in vertebrate diets using naturally occurring stable isotopes. *Oecologia,* 144, 647-658.

Darwin, C. (1859) *The Origin of Species*. Oxford University Press, Oxford.

Darwin, C. (1862) *The Various Contrivances by which Orchids are Fertilised by Insects*. John Murray, London.

Dingle, H. & Caldwell, R.L. (1978) Ecology and morphology of feeding and agonistic behavior in mudflat stomatopods (Squillidae). *Biological Bulletin,* 155, 134-149.

Ferry-Graham, L.A., Bolnick, D.I. & Wainwright, P.C. (2002) Using functional morphology to examine the ecology and evolution of specialization. *Integrative and Comparative Biology,* 42, 265-277.

France, R.L. (1995) C-13 enrichment in benthic compared to planktonic algae - foodweb implications. *Marine Ecology Progress Series,* 124, 307-312.

Fry, B. (2006) *Stable Isotope Ecology*. Springer Science + Business Media, New York, NY.

Fry, B., Lutes, R., Northam, M. & Parker, P.L. (1982) A $^{13}C/^{12}C$ comparison of food webs in Caribbean seagrass meadows and coral reefs. *Aquatic Botany,* 14, 389-398.

Futuyma, D.J. & Moreno, G. (1988) The Evolution of Ecological Specialization. *Annual Review of Ecology and Systematics,* 19, 207-233.

Grant, B.R. & Grant, P.R. (1993) Evolution of Darwin's finches caused by a rare climatic event. *Proceedings of the Royal Society B-Biological Sciences,* 251, 111-117.

Greenwood, N.D.W., Sweeting, C.J. & Polunin, N.V.C. (2010) Elucidating the trophodynamics of four coral reef fishes of the Solomon Islands using $\delta^{15}N$ and $\delta^{13}C$. *Coral Reefs,* 29, 785-792.

Hamano, T., Hayashi, K.-I., Katsuhiko, K., Matsushita, H. & Tabuchi, K. (1996) Population structure and feeding behavior of the stomatopod crustacean *Kempina mikado* (Kemp and Chopra, 1921) in East China. *Fisheries Science,* 62, 397-399.

Hamano, T. & Matsuura, S. (1986) Optimal prey size for the Japanese mantis shrimp from structure of the raptorial claw. *Bulletin of the Japanese Society of Scientific Fisheries,* 52, 1-10.

Hemminga, M.A. & Mateo, M.A. (1996) Stable carbon isotopes in seagrasses: variability in ratios and use in ecological studies. *Marine Ecology Progress Series,* 140, 285-298.

Hori, M. (1993) Frequency-dependent natural selection in the handedness of scale-eating fish. *Science,* 260.

Hutchinson, G.E. (1957) Concluding Remarks. *Cold Spring Harbour Symposia on Quantitative Biology*, pp. 415-427.

Hyslop, E.J. (1980) Stomach contents analysis--a review of methods and their application. *Journal of Fish Biology,* 17, 411-430.

Irschick, D.J. & Sherry, T.W. (2005) Phylogenetic methodology for studying specialization. *Oikos,* 110, 404-408.

Jackson, A.L., Inger, R., Parnell, A.C. & Bearhop, S. (2011) Comparing isotopic niche widths among and within communities: SIBER – Stable Isotope Bayesian Ellipses in R. *Journal of Animal Ecology,* 80, 595-602.

Layman, C.A. & Allgeier, J.E. (2012) Characterizing trophic ecology of generalist consumers: a case study of the invasive lionfish in The Bahamas. *Marine Ecology Progress Series,* 448.

Layman, C.A., Arrington, D., Montana, C.G. & Post, D.M. (2007) Can stable isotope ratios provide for community-wide measures of trophic structure? *Ecology,* 88, 42-48.

Liem, K.F. (1980) Adaptive significance of intra- and interspecific differences in the feeding repertoires of cichlid fishes. *American Zoologist,* 20, 295-314.

Martínez del Rio, C., Anderson-Sprecher, R., Gonzalez, P. & Sabat, P. (2009) Dietary and isotopic specialization: the niche of three Cinclodes ovenbirds. *Oecologia,* 161, 149-159.

Maynou, F., Abello, P. & Sartor, P. (2005) A review of the fisheries biology of the mantis shrimp, *Squilla mantis* (L., 1758) (Stomatopoda, Squillidae) in the Mediterranean. *Crustaceana,* 77, 1081-1099.

McNeill, P., Burrows, M. & Hoyle, G. (1972) Fine structures of muscles controlling the strike of the mantis shrimp, *Hemisquilla*. *Journal of Experimental Zoology,* 179, 395-416.

Minagawa, M. & Wada, E. (1984) Stepwise enrichment of ^{15}N along food-chain--further evidence and the relation between $\delta^{15}N$ and animal age. *Geochimica Et Cosmochimica Acta,* 48, 1135-1140.

Moore, J. & Semmens, B. (2008) Incorporating uncertainty and prior information into stable isotope mixing models. *Ecology Letters,* 11, 470-480.

Nagelkerken, I., Van der Velde, G., Wartenbergh, S.L.J., Nugues, M.M. & Pratchett, M.S. (2009) Cryptic dietary components reduce dietary overlap among sympatric butterflyfishes (Chaetodontidae). *Journal of Fish Biology,* 75, 1123-1143.

Newsome, S.D., Martínez del Rio, C., Bearhop, S. & Phillips, D.L. (2007) A niche for isotope ecology. *Frontiers in Ecology and the Environment,* 5, 429-439.

Parnell, A., Inger, R., Bearhop, S. & Jackson, A. (2010) Source partitioning using stable isotopes: coping with too much variation. *PLoS Biology,* 5, e9672.

Patek, S.N. & Caldwell, R.L. (2005) Extreme impact and cavitation forces of a biological hammer: strike forces of the peacock mantis shrimp (*Odontodactylus scyllarus*). *Journal of Experimental Biology,* 208, 3655-3664.

Patek, S.N., Korff, W.L. & Caldwell, R.L. (2004) Deadly strike mechanism of a mantis shrimp. *Nature,* 428, 819-820.

Phillips, D.L. & Gregg, J.W. (2003) Source partitioning using stable isotopes: coping with too many sources. *Oecologia,* 136, 261-269.

Pihl, L., Baden, S.P., Diaz, R.J. & Schaffner, L.C. (1992) Hypoxia-induced structural changes in the diet of bottom-feeding fish and Crustacea. *Marine Biology,* 112, 349-361.

Robinson, B.W. & Wilson, D.S. (1998) Optimal foraging, specialization, and a solution to Liem's paradox. *American Naturalist,* 151, 223-235.

Stephens, D.W. & Krebs, J.R. (1986) *Foraging Theory*. Princeton University Press, Princeton, NJ.

Underwood, A.J., Chapman, M.G. & Crowe, T.P. (2004) Identifying and understanding ecological preferences for habitat or prey. *Journal of Experimental Marine Biology and Ecology,* 300, 161-187.

Vaslet, A., France, C., Phillips, D.L., Feller, I.C. & Baldwin, C.C. (2011) Stable-isotope analyses reveal the importance of seagrass beds as feeding areas for juveniles of the speckled worm eel *Myrophis punctatus* (Teleostei: Ophichthidae) in Florida. *Journal of Fish Biology,* 79, 692-706.

Wainwright, P.C. & Reilly, S.M. (1994) *Ecological Morphology: Integrative Organismal Biology.* The U. of Chicago Press, Chicago.

Chapter I

Sit-and-wait predation in the sea: prey capture in mantis shrimp

Key words: foraging strategy, raptorial appendage, Crustacea, kinematics, morphology

Abstract

Sit-and-wait predation strategies rely on an array of key morphological features, predatory kinematics, and behaviors. Many mantis shrimp species (Stomatopoda, Crustacea) hide in sandy burrows and rapidly capture prey swimming overhead. Through computed tomography of raptorial appendages, high-speed image analysis of spearing kinematics, and analysis of feeding behavior in the field and laboratory, I examined the elongated, streamlined appendage of the spearing stomatopod, *Lysiosquillina maculata*. Field videos documenting behavior showed that *L. maculata* strikes at passing prey from its burrow where it also spends the majority of its time. *L. maculata*'s laboratory strikes began with the rotation of the dactyl segment at an average peak speed of 0.76 m s^{-1}. Then, the propodus opened with a mean peak speed of 2.29 m s^{-1} and average duration of 24.98 ms. Both propodus and dactyl rotation were equally variable, indicating that *L. maculata* exerted similar behavioral control throughout the strike. While *L. maculata's* appendage has the exoskeletal structures known to store elastic energy in other stomatopods, movement of these structures was undetectable during *L. maculata's* laboratory strikes, suggesting that the recorded strikes were not spring-loaded. Laboratory behavioral analyses showed that *L. maculata* either speared prey with the tip of the dactyl segment (15% of strikes) or grabbed prey between the propodal and dactyl segments of the appendage (89% of strikes). Field videos revealed similar results as laboratory videos. Overall, this study offers insights into sit-and-wait predation and the diversity of predatory strategies in mantis shrimp.

Introduction

Sit-and-wait, or ambush, predation is a unique mode of prey capture that requires the predator to minimize the distance between itself and its prey over very short timescales (Pianka 1966; reviewed in McBrayer and Wylie 2009; Miles *et al*. 2007). It is defined as a behavior in which a predator motionlessly scans its habitat and then attacks when a prey item presents itself (Pianka 1966; Schoener 1971). Sit-and-wait predation has been shown to profoundly influence the evolution of morphology and behavior in terrestrial animals, namely lizards (Casatti and Castro 2006; Miles *et al*. 2007; Wilga *et al*. 2007; McBrayer and Wylie 2009), frogs (reviewed in van Leeuwen *et al*. 2000), and some insects (Bauer and Pfeiffer 1991; Masuko 2009; reviewed in Betz and Kolsch 2004). Sit-and-wait lizards sprint to ambush prey, which has led to increased sprint speed, decreased endurance, and longer limbs compared to actively foraging lizards (reviewed in Miles *et al*. 2007; McBrayer and Wylie 2009). Some frogs and beetles that exhibit sit-and-wait predation use another mechanism whereby a ballistic tongue extends out of the mouth to capture prey over very short timescales (Bauer and Pfeiffer 1991; van Leeuwen *et al*.

2000). Surprisingly few studies have thoroughly examined sit-and-wait predation in aquatic animals and the existing studies are based on limited laboratory observations (Burrows 1969; Burrows and Hoyle 1972; McNeill *et al*. 1972; Dingle and Caldwell 1978; Hamano and Matsuura 1986b; Lawton 1989). Yet, aquatic sit-and-wait predation may be more difficult, because the high viscosity of water may impose additional challenges to rapidly closing the distance between predator and prey. Here, I focus on the predatory mechanics and behavior of the mantis shrimp, *Lysiosquillina maculata* (Fabricius 1793) (Crustacea: Stomatopoda: Lysiosquillidae) (Fig. 1.1) to determine how prey capture kinematics and morphology relate to aquatic sit-and-wait predation.

Mantis shrimp have classically been categorized along a sit-and-wait to active forager continuum based on their raptorial appendages. These modified maxillipeds are diverse in both form and function (Ahyong 2001), ranging from hammer-shaped appendages ("*smashers*") to elongate, streamlined appendages ("*spearers*") (Caldwell and Dingle 1976). Spearers are generally considered to be sit-and-wait predators that hunt for soft-bodied, evasive fish and crustaceans (Fig. 1.1), while smashers are categorized as active foragers that search for hard-shelled molluscs and crustaceans (Caldwell and Dingle 1976; Dingle and Caldwell 1978).

Despite this general classification, the roles of feeding morphology, kinematics, and behavior in determining foraging mode remain unknown. Gut content analyses suggest that most mantis shrimp have diets consisting of a variety of prey that would likely require different foraging and raptorial strike behaviors to consume. Of the eighteen spearer species for which gut content data exist, sixteen of these species (all in the family Squillidae) consume annelids, crabs, hermit crabs, hydroids, molluscs, pelecypods, and polychaetes in addition to evasive prey such as alpheid shrimp and fish (Camp 1973; Dingle and Caldwell 1975; Dingle and Caldwell 1978; Froglia and Giannini 1989; Hamano and Matsuura 1986a; Hamano and Matsuura 1986b; Maynou *et al.* 2005; Pihl *et al*. 1992). These studies indicate that spearers do not solely exhibit a sit-and-wait predation strategy, because most species also consume prey that requires active foraging. Only two spearers studied have mostly evasive fish and squid prey in their diets, indicating that they are sit-and-wait predators (Dingle and Caldwell 1978; Hamano *et al*. 1996). Similarly, although no smasher species has yet to be documented as a true sit-and-wait predator, three species have been observed capturing evasive thalassid shrimp, amphipods, and soft-bodied worms (Dominguez and Reaka 1988; Caldwell *et al*. 1989), suggesting that smashers do not necessarily actively forage for only hard-shelled prey. However, all of these inferences are based solely on gut content analyses and have yet to be verified with observations of feeding behavior. Thus, the relationship between foraging mode and feeding morphology, behavior, and kinematics has yet to be formally tested in mantis shrimp.

While much recent attention has focused on smashers (Caldwell and Dingle 1975; Caldwell and Dingle 1976; Dominguez and Reaka 1988; Caldwell *et al.* 1989; Full *et al*. 1989; Patek *et al*. 2004; Patek and Caldwell 2005; Patek et al. 2007; Zack et al. 2009), to my knowledge no studies have thoroughly examined spearer kinematics and few have examined spearer feeding behavior (Burrows 1969; Dingle and Caldwell 1978). Analyses of behaviors leading to raptorial strikes in the spearers *Squilla empusa* and *S. mantis* (Squillidae) showed visual tracking of prey with highly mobile eyes and chemical tracking with antennule sweeps (Burrows 1969; Mead 2002; Cronin and Marshall 2004). Once the antennules aligned towards the prey, abdominal pleopods were used to propel the body forward while the raptorial appendages rapidly extended toward the prey (Burrows 1969; Caldwell and Dingle 1975).

In comparison, current knowledge of stomatopod kinematics mostly comes from the smashing mantis shrimp, *Odontodactylus scyllarus* (Odontodactylidae), which has highly calcified merus and dactyl segments (Patek *et al*. 2007). This species hammered hard-shelled prey with strikes speeds of 14-23 m s^{-1}, peak angular speeds of 670-990 rad s^{-1}, peak accelerations of 65-104 km s^{-2}, and strike durations of 1.8-2.7 ms (Patek *et al.* 2004; Patek *et al*. 2007). The slowest appendage movement reported in the literature was documented in *Hemisquilla californiensis* (Hemisquillidae), an active forager with generalized raptorial appendages that lack the elongated spears or bulbous hammers of most other mantis shrimp species (Ahyong 2001; Ahyong and Jarman 2009; Basch and Engle 1989; Basch and Engle 1993; Burrows 1969). Kinematic analyses of the dactyl heel (Fig. 1.1) revealed speeds of 10 m s^{-1}, angular speeds of 350 radians s^{-1}, and strike durations of 4-8 ms (Burrows 1969).

To achieve fast strikes, mantis shrimp rely on a network of structures that enhance the rate of movement beyond what could be generated by muscle alone. Together, these structures constitute a power amplification system (Fig. 1) (Burrows, 1969; Patek et al., 2004; Patek et al., 2007; Claverie et al., 2011; Patek et al., 2011). Preparation for the strike begins with simultaneous contractions of extensor and flexor muscles in the merus (McNeill et al., 1972). Extensor muscles proximally rotate an elastic spring (the "meral-V") and lever system, while compressing a secondary elastic, saddle-shaped structure (the "saddle") (Patek et al., 2004; Patek et al., 2007; Zack et al., 2009). At the same time, flexor muscles engage a pair of sclerites that act as a latch to prevent the propodus from rotating forward (Burrows, 1969; Burrows and Hoyle, 1972; McNeill et al., 1972; Patek et al., 2007). When the sclerites are released, the carpus rotates and causes the propodus to slide along the merus. The propodus and dactyl then suddenly transition from sliding to rotating outward toward the prey. Both smashers and spearers have the requisite structures for generating spring-loaded strikes (Burrows, 1969); however, it is not known whether or how spearers use the power amplification system.

L. maculata's strike kinematics and feeding behaviors have yet to be studied, but its lifestyle of rarely leaving its burrow built in shallow sand and mud flats (Caldwell 1991) makes this species an excellent candidate for being a sit-and-wait predator. *L. maculata* scans for prey from its burrow using a specialized visual system that adjusts to both high and low light conditions (Schiff *et al*. 2002; Schiff *et al*. 2007). It captures prey with elongated, streamlined spearing appendages, which are equipped with moveable spines on the propodus that aid in impaling prey (Fig. 1.1) (Ahyong 2001). As one of the largest mantis shrimp species, adults range in size from 8.5-33.5 cm (Ahyong 2001). The specific aims of this study are to 1) determine if this species is a sit-and-wait predator based on field video observations of behavior, 2) characterize raptorial appendage morphology and mineralization patterns using computed tomography, 3) perform kinematic analyses of raptorial strikes in the laboratory using high speed videography, 4) describe and categorize raptorial strike behavior in the laboratory and the field, and 5) compare the feeding behavior, morphology, and kinematics of *L. maculata* to other stomatopod species.

Methods

Animal acquisition and care

Ten *Lysiosquillina maculata* (Crustacea; Stomatopoda; Lysiosquillidae) specimens (4 females, 6 males) were collected at Lizard Island, Australia (Permit # PRM01599G to J. Marshall and R. L. Caldwell) and purchased from local aquarium stores in the San Francisco Bay

Area. Specimens were keyed to the species level using Ahyong (2001). Body lengths ranged from 13-17 cm measured from rostrum to telson. Animals were maintained at 25˚C, 34-36 parts per thousand artificial saltwater, in individual recirculating tanks (32 cm height x 52 cm width x 26 cm depth). All animals built their own burrows in 20-27 cm depth fine sediment (Sugar-sized Oolite, Aragonite, CaribSea, White City, FL, USA) and were fed frozen and freeze-dried shrimp twice weekly.

Appendage morphology

Micro-computed tomography (micro-CT) scans were used to reconstruct the three-dimensional morphology of the raptorial appendage. A freshly frozen specimen was scanned by the High-Resolution X-ray Computed Tomography Facility (ACTIS, Bio-Imaging Research, Inc.) at the University of Texas, Austin (slice thickness = 0.1078 mm; resolution = 1024x1024 pixels; field of view = 50 mm). Surface volume rendering (Phong algorithm) and mineralization patterns (sum along ray algorithm) were used to visualize the component structures of the raptorial appendage (VGStudio Max v 2.0, Heidelberg, Germany).

High-speed videography of strike kinematics

Raptorial strikes were filmed laterally at 3000 frames s^{-1} (0.2 ms shutter duration, 1024x1024 pixel resolution, APX-RS, Photron USA Inc., San Diego, CA, USA). Two 250-Watt floodlights were used to illuminate tanks during filming and animals were acclimated to lighting conditions for several weeks prior to high speed video data collection. Raptorial strikes were elicited by presenting food items on the end of a stick positioned next to or directly over the burrow entrance. Individuals were lured out of their burrows with the food item and I actively moved the stick away from the individuals to try to keep them away from the food during filming. However, individuals did contact the food in some of strikes.

Correction of off-axis movements

Two methods for correcting off-axis movements were compared, because the strikes were performed at variable angles relative to the video camera's plane of view. First, for 18 sequences from 3 individuals (3-8 strikes per individual), a second video camera (500 frames s^{-1}, 2 ms shutter duration, 720x480 pixel resolution, MotionMeter, Redlake, Tucson, AZ, USA) was positioned above the tank to measure off-axis movements relative to the lateral view camera. Pixel dimensions were converted to SI units by using a ruler placed in the plane of view of the strike. Both dorsal and lateral video sequences were digitized with a custom digital image analysis program (Matlab v. R2006a - R2008b, The Mathworks, Natick, MA, USA) and an off-axis correction was applied to the kinematic measurements based on the angle of the strike relative to the plane of the laterally positioned camera.

For the second off-axis correction method, actual lengths of the appendage segments were measured and then used to correct the lengths measured from the lateral video images. Specifically, animals were removed from their burrows shortly after filming and total body length, carapace length, and appendage length were measured with digital calipers (Absolute Coolant Proof Caliper Series 500, Mitutoyo Corporation, Takatsu, Japan). The lateral side of each appendage was then photographed (D70 digital SLR camera, Nikon Corporation, Tokyo, Japan) with a scale bar next to the appendage and a circular disc on the appendage to confirm that the specimen was perpendicular to the camera's plane of view. Appendage segment lengths were measured in photographs using a custom digital image analysis program (Matlab v. R2006a

- R2008b, The Mathworks, Natick, MA, USA). To determine off-axis correction angles relative to the lateral view videos, the cosine of the length measured from the videos was divided by the known length. This off-axis correction angle was then applied to the kinematic measurements. Both the dorsal-video and digital photograph methods generated similar off-axis correction angles; thus, to be concise, only results calculated from the photograph correction method are reported.

Digital image analysis of strike kinematics

Strike kinematics were measured using dactyl and propodus displacement, speed, and acceleration relative to the merus and then examined as a function of size and distance to the prey item. Five landmarks were digitized on the raptorial appendage in the lateral view videos to calculate raptorial appendage kinematics (Matlab v. R2006a - R2008b, The Mathworks, Natick, MA, USA). Speed and acceleration of the propodus and dactyl were measured from three digitized landmarks: the anterior-distal tip of the carpus, the distal trailing edge of the propodus, and the tip of the distal, leading edge of the dactyl (Fig. 1.2, Points 3-5; for definitions of anatomy, refer to Fig. 1.1). To determine the amount of appendage movement that was not solely due to propodus and dactyl rotation, merus movement was measured by digitizing two landmarks: the proximal end of the meral-V and the distal tip of the meral-V (Fig. 1.2, Points 1-2). Digitizing began at the onset of the strike when the dactyl first began to rotate away from the propodus. All video sequences were digitized 2-5 times so that the mean pixel location of each landmark could be calculated for each frame. Points were digitized only if they were visible in all frames for the duration of the strike. Measurement error for these analyses was estimated by digitizing 5 sequences 3-5 times; percent error ranged from 0-7 % and averaged 5 ± 4 % for each point.

Speed and acceleration of the distal ends of the merus, propodus, and dactyl were measured in 29 sequences from 5 individuals (4-8 sequences per individual). All of these sequences were less than 30° off-axis, based on the off-axis angles (as calculated above). To measure kinematics, I first calculated the cumulative displacement of the distal edges of the merus, propodus, and dactyl. Following the data smoothing recommendations of Walker (1998), raw cumulative displacement data were filtered with a 200 Hz Butterworth and curve-fit with a 10^{th} order polynomial and an interpolated spline (Matlab v. R2006a - R2008b, The Mathworks, Natick, MA, USA). Each method calculated a curve that closely fit the raw cumulative displacement data (Fig. 1.3). Speeds were calculated by taking the derivative of the raw cumulative displacement data and the three curve-fits. Speeds were then curve-fit using the same smoothing equations described above. The 10^{th} order polynomial yielded the best curve-fitting performance for the speed calculations (Fig. 1.3) and thus accelerations were calculated by taking the derivative of this curve-fit.

Statistical analysis of strike kinematics

Peak speeds and accelerations achieved during the strike were determined for each video sequence. Means (± 1 standard deviation) were calculated for peak speeds and accelerations of the dactyl before propodus rotation and peak speeds and accelerations of the merus, propodus, and dactyl after propodus rotation. Mean peak propodus speeds of the 3 fastest strikes for each individual were also calculated in order to evaluate the maximum propodus speeds achieved during the study.

Mean peak angular speeds and accelerations of the propodus and dactyl were estimated for each individual as well. Specifically, angular displacement was estimated by dividing the propodus and dactyl displacements by their respective appendage segment lengths, yielding the change in angle between frames. Angular speeds and accelerations were then calculated from the 10^{th} order polynomial curve-fits of the cumulative displacement and speed data respectively, following the methodology described previously. Mean (± 1 standard deviation) peak angular speeds and accelerations were calculated for propodus and dactyl rotation from the curve-fit data.

To understand the effects of body size on strike kinematics, I examined the relationship between body size and propodus speed. Specifically, I tested whether carapace length, as a measure of body size, correlated with mean propodus speed and mean maximum propodus speed using a least-squares linear regression model (R v. 2.7.1, The R Foundation for Statistical Computing, Vienna, Austria; JMP v. 7.0, SAS Institute Inc., Cary, NC, USA).

I also tested whether the distance between an individual and its prey was positively correlated with strike speed. At the onset of dactyl rotation, I measured the distance between the center of the prey item and the center edge of *L. maculata's* eye that was closest to the prey item (Matlab v. R2008a-b, The Mathworks, Natick, MA, USA). Each distance measurement was repeated three times to estimate percent digitizing error, which ranged from 0.04 – 1.0 % and averaged 0.4 ± 0.3 %. Average distance was then divided by body length to account for body size differences between individuals. Correlations between distance and linear and angular speeds of the propodus and dactyl were tested with a least-squares linear regression model (R v. 2.7.1, The R Foundation for Statistical Computing, Vienna, Austria; JMP v. 7.0, SAS Institute Inc., Cary, NC, USA).

Following recommendations of Wainwright, *et al.* (2008), stereotypy was calculated for strike kinematics before and after propodus rotation with the coefficient of variation (CV). Propodus rotation was expected to be more stereotypic compared to dactyl rotation, because propodus rotation is driven by the merus' spring-latch system in other stomatopods (Burrows 1969; Patek *et al*. 2007; Zack *et al.* 2009). Thus, the hypothesis that speed and acceleration are more variable before propodus rotation compared to after propodus rotation was tested. Specifically, the CVs for dactyl speed and acceleration before the onset of propodus rotation were compared to the CVs of dactyl and propodus speed and acceleration after the propodus started to rotate using t-tests (JMP v. 7.0, SAS Institute Inc., Cary, NC, USA). For angular kinematics, the CV of initial dactyl rotation was compared only to the CV of propodus rotation using a t-test with a significance level of $\alpha = 0.05$ (JMP v. 7.0, SAS Institute Inc., Cary, NC, USA).

Mean strike duration was calculated in 87 video sequences from 9 individuals (3-19 strikes per individual) by multiplying the frame rate by the number of frames between the onset of dactyl movement and either the onset of propodus retraction or initial contact with the prey item. In order to test whether strikes that made contact with the prey exhibited shorter durations than strikes that did not contact the prey, I compared the durations of strikes that ended with propodus retraction to those that ended by contacting the prey item (T-test; R v. 2.7.1, The R Foundation for Statistical Computing, Vienna, Austria; JMP v. 7.0, SAS Institute Inc., Cary, NC, USA). Only individuals that had at least 3 strikes in each category were included in this analysis.

Spring-loading kinematics

I measured meral-V rotation during the strike, because of its role in spring-loading in other mantis shrimp species (Patek *et al.* 2007; Zack *et al.* 2009). Displacement and rotation of the meral-V was measured in 16 sequences from 5 individuals (3-4 strikes per individual). Specifically, I digitized the following points on the merus [described as MP (merus points) 1-3 to avoid confusion with the points digitized for appendage kinematics]: MP 1 – the distal tip of the meral-V, MP 2 – the proximal end of the meral-V, and MP 3 – the dorsal tip of the distal edge of the merus exoskeleton proximal to the meral-V (see Fig. 1.1 for definitions of the anatomy). I then used these points to calculate meral-V length (distance between points MP 1-2), the length of the distal edge of the merus proximal to the meral-V (distance between points MP 2-3), and the distance between the distal tip of the meral-V and the distal edge of the merus proximal to the meral-V (distance between points MP 1-3) (Matlab v. R2008a-b, The Mathworks, Natick, MA, USA). The third length (distance between points MP 1-3) is important, because it is the assumed maximal distance of meral-V contraction based on previous research in a smashing species (Zack et al., 2009). The angle between the meral-V and adjacent edge of the merus was calculated with the Law of Cosines. Absolute and percent changes in angle were calculated by subtracting the meral-V angle before the propodus started to rotate from the angle at maximum propodus velocity. These absolute and percent change calculations were repeated using the length between MP 1-3 to measure meral-V displacement and percent change in displacement.

Measurement error was calculated by digitizing each sequence 5 times. Percent error for the change in angle measurements ranged from 33-57 % and averaged 43 ± 31 %. For the displacement measurements, the range was 24-43 % and averaged 35 ± 33 %. Given the high digitizing error, I also estimated the smallest movement that I was able to resolve with this digitizing method. I compared the highest resolution video, which was the video recorded closest to the animal, to my lowest resolution video, which was the video recorded farthest from the animal. Each of the three meral-V points were digitized 30 times in both sequences (Matlab v. R2009a Student, The Mathworks, Natick, MA, USA). Standard deviations of each point's x and y components were used as a measure of movement resolution and ranged from 0.10-0.25 mm or approximately 1-3 pixels for the closest and farthest videos, respectively, for all three points. Thus, even when the animal was farthest from the camera, I should have been able to resolve meral-V movements that were greater than 0.25 mm or 3 pixels.

Laboratory behavior

To understand raptorial strike behavior, I documented body and appendage movements in 76 video sequences from 6 individuals (8-19 strikes per individual). First, I described how far each individual emerged from the burrow during a strike based on whether all, half, or none of the carapace was outside of the burrow when individuals initially contacted the prey. Second, I documented whether one or both appendages were used to strike the prey. Third, I described the mode of prey capture based on which dactyl spines made initial contact with the prey. Finally, all strikes in which individuals fully raised their movable propodal spines (Fig. 1.1) to approximately 90° relative to the long axis of the propodus were documented.

Field behavior

L. maculata activity was filmed at 17 burrows in the sand flats and mangroves of Lizard Island, Australia (14°40′08″S 145°27′34″E) everyday for three weeks in May, 2009 (Permit # G07/23354.1 to M. S. deVries). Twelve burrows total that were within 26 m from each other

were filmed at Station Beach during the day from 06:00-08:30 H (2 burrows, each filmed for 2 hours), 9:00-13:20 H (4 burrows, each filmed for 2-4 hours), and 15:00-18:00 H (2 burrows, each filmed for 2 hours), and during the late afternoon through night from 17:00-22:30 H (12 burrows, each filmed for 2-4 hours). Five burrows that were within 10 m from each other were filmed at Mangrove Beach from 11:20-14:30 H (2 burrows, each filmed for 2 hours) and from 17:00-20:00 H (3 burrows, each filmed for 2-4 hours). All videos were approximately 2 hours in duration resulting in about 72 hours of nighttime video recordings and 20 hours of daytime recordings (92 hours total). The majority of the burrows were recorded at Station beach at night, because it became apparent early in the observations that most feeding activity occurred at this location at night. Note that while I recorded from unique burrows, I could not verify that different individuals were recorded, because burrows could have been connected below-ground and individuals could have switched burrows during the experiments.

Feeding activity was filmed with 2 low-light underwater cameras (Submergible Submersible Under-Water CCD 480TVL Bullet Color Camera, Sony Corporation, NY, USA) connected to Hi-8 video recorders (30 frames s^{-1}, Sony GV-A500 Hi8 Video Walkman, Sony Corporation, NY, USA). One small dive light per camera was fitted with red filters and placed at an approximately 45° angle relative to the camera. The camera set-ups were placed next to 2 different *L. maculata* burrows during each filming session. Once recorded, videos were converted to digital format (ADVC55 Advanced Digital Video Converter, Tomson Grass Valley, Boulogne Cedex, France and iMovie, Apple Inc., CA, USA).

Thirty-four strikes were recorded from 7 burrows (1-22 strikes per burrow). Strike durations were calculated by multiplying the frame rate by the number of video frames in which the propodus and dactyl rotated forward. Other feeding behaviors including number of appendages used to strike, lunges from the burrow, and grabs with the maxillipeds were documented. Using the maxillipeds to throw sand out of burrows and swimming exits from burrows were also documented. Finally, the number of strike sequences in which a prey item was visible was counted.

Results are presented as mean ± 1 standard deviation.

Results

Micro-CT scans

The ventral surface of the merus exoskeleton has two mineralized strips that begin at the center of the merus and splay laterally toward the distal end (Fig. 1.4 C). The lateral mineralized strip extends ventrally to the meral-V and forms a connection with the mineralized regions of the meral-V (Fig. 1.4 C). The sclerite and mineralized apodeme of the medial flexor muscle are apparent in the micro-CT scans, as are the apodemes of the medial and lateral extensor muscles (Fig. 1.4 A, D). In general, there is greater mineralization along the distal edges (Fig. 1.4 A) and ventral bars of the merus (Fig. 1.4 C) as well as in the sclerite (Fig. 1.4 C, D) compared to the rest of the merus.

Strike kinematics

Raptorial strikes proceeded in two distinct phases defined by dactyl rotation in Phase I and propodus rotation in Phase II (Fig. 1.5). First, in Phase I, the individual emerged from the burrow while the dactyl rotated distally (Table 1.1; Fig. 1.5). Phase II began when the carpus rotated, causing the propodus to slide distally relative to the merus in 84 ± 17 % of the strikes.

The propodus then rotated distally with peak speeds and accelerations that were at least four times greater than those of the dactyl movement in the first strike phase (Table 1.1; Fig. 1.5). During this second phase, the merus moved with a mean speed of 0.34 ± 0.08 m s^{-1} and acceleration of 0.09 ± 0.05 m s^{-2}. However, in 25 ± 28 % of the strikes, Phase II began while Phase I was still in progress and the propodus swung forward without sliding relative to the merus in 4 ± 3 % strikes.

Statistics of strike kinematics

Carapace length was not correlated with peak propodus speed [least-squares linear regression (LSR): R^2=0.21, n=28, individual df=4, carapace length df=1, F= 1.53, P= 0.22], or the peak propodus speeds of the three fastest strikes per individual (LSR: R^2=0.38, n=15, individual df=4, carapace length df=1, F=1.54, P=0.26; Fig. 1.6).

The least-squares linear regression model relating the size corrected distance to the prey item and propodus angular speed was significant (R^2=0.56, n=5, individual df=4, distance df=1, individual x distance df=4, F=2.56, P=0.04). However, none of the parameters of interest (distance to the prey, individual, or the interaction term) were significantly correlated with propodus angular speed when evaluated with effect tests (all p-values greater than 0.17); thus, these parameters could not explain the significant correlation between distance to the prey and propodus angular speed. Additionally, there were no correlations between distance to the prey item and propodus speed (LSR: R^2=0.46, n=5, individual df=4, distance df=1, individual x distance df=4, F=1.70, P=0.16), dactyl speed (LSR: R^2=0.32, n=5, individual df=4, distance df=1, individual x distance df=4, F=1.02, P=0.46), and angular dactyl speed (LSR: R^2=0.39, n=5, individual df=4, distance df=1, individual x distance df=4, F=1.36, P=0.27).

None of the comparisons of kinematic stereotypy between Phase I and II were significant (t-tests, all p-values greater than 0.35; Table 1.2), except for the comparison of the dactyl acceleration CVs (t-test: n=5, df=8, t=-3.00, p=0.017; Table 1.2). Thus, I could not reject the null hypothesis that the two strike phases were equally variable.

There were also no significant differences between mean durations of strikes that did and did not make contact with the prey item for the propodus, dactyl, and entire strike (Table 1.3). Thus, Table 1.3 only shows the results for the entire strike, as the analysis of propodus and dactyl durations yielded similar results. T-tests were performed on each individual separately, because the complete datasets that included all individuals were not normally distributed (Shapiro-Wilk normality test; total duration: n=61, W=0.93, P=0.002; propodus duration: n=60, W=0.91, P< 0.001; dactyl duration: n=59, W=0.83, P<0.001) and, except for the propodus data set (Bartlett test of homogeneity; n=60, K^2=8.69, df = 5, P=0.07), the variances were not equal (Bartlett test of homogeneity; total duration: n=61, K^2=30.46, df = 5, P<0.001; dactyl: n=59, K^2=31.85, df = 5, P<0.001). However, within individuals, almost all data were normally distributed and had equal variances. Overall, given that contacting the prey did not significantly influence strike duration, mean durations reported in Table 1.1 were calculated by pooling all strike durations for each individual regardless of whether contact with the prey item was achieved.

Spring-loading kinematics

I was unable to differentiate between no movement of the meral-V and movements that were too small to detect with my digitizing technique. The average absolute change in angle and displacement were 0.10 ± 0.07 rad and 0.5 ± 0.32 mm respectively. The average percent change in angle and displacement were 9.94 ± 5.99 % and 8.05 ± 5.01 % respectively. Given that the

mean ± SD absolute change in angle was about equal to the calculated movement resolution of ± 3 pixels, or 0.25 mm, and the digitizing errors for both measurements were so high, it is likely that I was unable to resolve meral-V movement with this digitizing technique. If the meral-V moved at all, then both the percent change in displacement and angle calculations showed that meral-V movements were consistently less than 16 % of the assumed full contracting distance when the standard deviations around the means are taken into account.

Laboratory behavior

Emergence from the burrow and the number of appendages used to strike were relatively consistent across strike sequences. In 88 ± 9 % of the recorded strikes in which both the burrow and animals were visible (76 strikes, 6 individuals, 8-19 strikes per individual), individuals emerged from the burrow so that at least half of the carapace was exposed upon initial contact with the prey item. In 55 ± 28 % of these strikes, the carapace was fully exposed. In 83 ± 22 % of the strike events, individuals used both appendages to capture prey, while in 15 ± 14 % of the strikes either the right or the left appendage was used (76 strikes, 6 individuals, 8-19 strikes per individual).

Mode of prey capture was categorized as either a stab or a grab, based on which dactyl spines made initial contact with the prey item. Of the strikes in which contact was made (55 strikes, 6 individuals, 5-17 strikes per individual), 89 ±16 % were classified as grabs, because the prey was impaled with the inner dactyl spines, whereas only 15 ±16 % were classified as stabs, because the individual contacted the prey with the tip of the dactyl. As the propodus rotated forward, the dactyl remained open at a fixed angle and movable propodal spines were raised to approximately 90° relative to the long axis of the propodus in 56 ± 25 % of the prey capture sequences (76 strikes, 6 individuals, 8-19 strikes per individual). Movable spines were used to impale prey in both the grab and stab behaviors.

Field behavior

To accurately quantify durations of field strikes given the 30 frames s^{-1} recording rate of the video camera, means are presented in terms of the number of frames (± 1 frame) over which strikes occurred. The low frame rate did not allow for accurately assessing whether the animal was striking with an open or closed dactyl for 9 of the 34 recorded strikes. Thus, I present results from the whole data set and a subset of the data that includes only confirmed predatory strikes with an open dactyl. For all strikes (34 strikes from 7 burrows, 1-17 strikes per burrow), the mean number of frames in which the strike occurred was 1 ± 1 frame or 33 ± 33 ms. Of these strikes, 26 (from 7 burrows, 1-17 strikes per burrow) occurred in 1 frame (≤ 33 ms), while 8 (from 3 burrows, 1-5 strikes per burrow) occurred over 2 frames (≤ 66 ms). For confirmed predatory strikes with an open dactyl, the mean number of frames in which the strike occurred was also 1 ± 1 frame with 19 strikes (from 7 burrows, 1-12 strikes per burrow) proceeding in 1 frame (≤ 33 ms) and 6 strikes (from 3 burrows, 1-3 strikes per burrow) proceeding over 2 frames (≤ 66ms).

Two appendages were seen striking in 24 strike sequences from 3 burrows, but only 21 of these were strikes with open dactyls. I was unable to determine whether one or both appendages were used in the remaining strikes.

Finally, I quantified the frequency and time of day of visible behaviors. All raptorial strikes occurred at Station Beach at night from 18:30-21:00 H (Fig. 1.7). Individuals were recorded striking at small prey items rapidly swimming through the water column in 24 strike

sequences. However, prey items were not identifiable due to low resolution of the recording equipment. All 26 lunges (from 7 burrows, 1-8 lunges per burrow) that were documented at Station Beach occurred from 18:00-22:00 H, while only 2 lunges (1 individual, 1 burrow) were documented at Mangrove Beach between 11:20-13:30 H. An average of 18 ± 26 sand throwing events (from 4 burrows, 1-48 events per burrow, 66 events total) occurred from 06:00-08:30 H and 18:40-22:00 H at Station Beach. Other than two ambiguous behavior sequences, which may have actually been sand throwing events, none of the behaviors appeared to be grabs with the maxillipeds. The data were also sparse for swimming exits from the burrow. There were only 2 confirmed sequences (2 individuals, 2 burrows) during which the individuals swam from their burrows, out of the frame of view, and then returned to their burrows about 1 second later. Both sequences occurred at night between 18:40-20:40 H.

Discussion

Given the limited understanding of sit-and-wait predation in aquatic predators and especially in crustaceans (except see Dingle and Caldwell 1978; Hamano and Matsuura 1986b; Lawton 1989; Mascaro *et al*. 2003), my goal was to explore whether *L. maculata* exhibits sit-and-wait predation, active foraging, or a mix of both strategies. The field videos provided convincing evidence supporting the hypothesis that *L. maculata* is a sit-and-wait predator, because the videos documented *L. maculata* spending the majority of its time in its burrow and striking only when prey passed by. To my knowledge, this is the first in-depth analysis of the behavior, morphology, and kinematics associated with sit-and-wait predation in crustaceans. To better understand the mechanics of the strike, I studied raptorial appendage kinematics in a laboratory setting. Strikes proceeded more slowly compared to speeds reported in previous studies of stomatopod strike kinematics. These findings suggest that *L. maculata* was not producing spring-loaded strikes in the laboratory and that, even though *L. maculata* has elastic energy storage structures, it was able to consistently strike without engaging the spring. Below, I present detailed answers to the following questions raised during this study. 1) Is *L. maculata* a sit-and-wait or active predator? 2) Why were strike speeds and accelerations relatively slow? 3) Does *L. maculata* have appendage morphology consistent with a spring apparatus? 4) How does *L. maculata*'s prey capture strategy compare to that of other stomatopod species?

Is L. maculata *a sit-and-wait or active predator?*

By definition, sit-and-wait predators motionlessly scan for prey and then attack when prey items present themselves (Pianka 1966). Field recordings of burrow activity showed that *L. maculata's* predatory behaviors are in line with the definition of sit-and-wait predation, because individuals searched for prey from their burrows and attacked when prey swam overhead. Before the strikes occurred, individuals were seen using antennal sweeps and visual scans to locate prey. All strikes occurred by rapidly lunging from the burrows and unfurling one or both of the dactyls, followed by the propodi, towards passing prey. In addition, I only saw two individuals exit completely from their burrows, but both returned seconds later, which implies that *L. maculata* individuals do not leave their burrows often nor for long periods of time. In contrast, actively foraging stomatopod species rarely attack prey from their burrows. Instead they leave their burrows often and for long durations to search for prey (Basch and Engle 1989; Caldwell *et al*. 1989; Hamano and Matsuura 1986b); some have been documented leaving and returning to their burrows up to nine times in one day (Caldwell *et al*. 1989).

The field videos revealed further information about *L. maculata's* hunting patterns and strike behaviors. All raptorial strikes were documented during night recordings from 18:00-22:00 H (Fig. 1.7), suggesting that *L. maculata* is a nocturnal predator. All but two lunges also occurred between 18:00-22:00 H, indicating that they were associated with the feeding events. Although the quality of the recording equipment precluded my ability to identify prey types, all prey items were small and swam rapidly through the water column before being captured, suggesting that they were small, evasive fish and crustaceans. Most of the confirmed predatory strikes ended in one frame or 33 ms. However, I could not determine if and how much shorter in duration these strikes were than 33 ms, because the videos lacked the temporal resolution required for determining strike kinematics. Yet, even with low temporal resolution, I could determine that all field recorded strikes ended in 2 frames at most, which means that no strike duration was greater than 66 ms and most occurred in less than 33 ms.

While I successfully documented field predatory strikes, I cannot be certain that strike behaviors and frequencies accurately reflect feeding behavior under normal lighting conditions and throughout the year. It is possible that the small dive lights placed by the underwater video cameras attracted more prey to the burrows being filmed than would have been present under normal nighttime light conditions, even though these lights were covered with red filters. Attracting more prey with the lights could have artificially increased feeding activity during the nighttime recordings. In addition, because burrows were only filmed at certain times (Fig. 1.7) for approximately one month, *L. maculata* may exhibit different foraging strategies depending on seasonal variation or on variation in prey availability that I could not document in this study.

Why were strike speeds and accelerations relatively slow?

Although propodus kinematics in Phase II were faster than dactyl kinematics in Phase I (Table 1.1), the propodus moved slowly compared to reports from other stomatopods. For example, the slowest propodus speed reported previously was 10 m s^{-1} and the angular speed was 350 radians s^{-1} in *Hemisquilla californiensis* (Burrows 1969), while in this study, I estimated speeds of approximately 2 m s^{-1} and angular speeds of 0.07 radians s^{-1} (Table 1.1).

Comparing stereotypy between speed and acceleration calculations and between the two strike phases may elucidate why *L. maculata*'s strike kinematics are relatively slow. The speed variables had a higher degree of stereotypy compared to acceleration variables (Table 1.2). However, calculating acceleration requires taking the second derivative of the original displacement data, which inflates the error associated with the acceleration estimates (Walker 1998). Thus, the coefficients of variation for acceleration were higher than the coefficients of variation for speed simply due to the derivative calculation and cannot explain strike kinematics differences in *L. maculata*.

When I examined kinematic variation between Phase I and II, Phase I appeared to exhibit higher variation, because *L. maculata* adjusted the position of their appendages in order to align them with the prey item during this strike phase. During strike Phase II, the propodus swung forward with markedly higher speeds and accelerations in one direction, and the variation between strikes appeared to decrease. Based on the observations of appendage adjustments in Phase I and the assumption that propodus rotation is driven by the merus' spring-latch system (Patek *et al*. 2007; Zack *et al*. 2009), I expected Phase II to be more stereotypic compared to Phase I.

However, comparing stereotypy between dactyl movement during Phase I to both propodus and dactyl movement in Phase II revealed no significant differences between the

average coefficients of variation for dactyl speed in Phase I, which was 0.36, and the average coefficients of variation for propodus speed and dactyl speed in Phase II, which were 0.35 and 0.31 respectively (Table 1.2). This result counters the prediction that propodus rotation is driven by elastic energy stored in the merus, because if the strike depended on a spring-loaded mechanism, then strike Phase II would likely have exhibited significantly less variation between strikes and thus a higher degree of stereotypy (Wainwright *et al.* 2008; for kinematic data on spring-loaded strikes, see Patek *et al*. 2004; Patek *et al*. 2007). If the strikes were not spring-loaded, then appendage movements were likely a result of extensor muscle contraction in both Phase I and Phase II. The advantage of producing strikes solely by muscular contraction is that the animal is able to behaviorally modulate strike kinematics using fine-scale motor control in the merus (Burrows 1969; Burrows and Hoyle 1972; McNeill *et al*. 1972). In fact, no significant difference in stereotypy between the strike phases provides evidence for equal behavioral control over both strike phases (Wainwright *et al*. 2008).

The possibility that I did not elicit spring-loaded strikes, even though *L. maculata* may be capable of producing such strikes, raises an important issue surrounding the interpretation of these results. As with most kinematic studies, I was unable to definitively confirm whether or not maximal effort strikes were elicited from the study individuals. Given the experimental design of initiating strikes with non-evasive prey, I cannot rule out the possibility that *L. maculata* would have produced fast, spring-loaded strikes if I had presented alternative evasive prey items during the kinematic study. However, the frozen shrimp prey items were placed on a stick that allowed us to control the direction of the strike from outside of the tank and to keep prey items away from the striking individuals, which motivated the individuals to strike quickly.

Additionally, finding no relationship between carapace length and propodus speed was surprising considering the expectation that kinematics scale with body size (Fig. 1.6) (reviewed in Vogel 2003). One possible reason why kinematics did not scale with body size could be that individuals were not sufficiently challenged by the frozen shrimp (Wainwright and Friel 2000) and therefore did not produce maximal-effort, spring-loaded strikes. However, the individuals used in this study did not span a wide range of body sizes, which suggests that I was unable to detect a correlation between body size and kinematics. Repeating this study with a greater size range and evasive prey would better address whether scaling patterns exist for strike speed and acceleration.

Despite the possibility that I did not elicit spring-loaded strikes, there is precedence for the interpretation that slow strikes were not spring-loaded. *H. californiensis* is believed to modulate between strikes that do engage the meral sclerites and strikes that do not (Burrows 1969). Strike durations can last between 5 ms to several hundred ms in *H. californiensis*, which Burrows (1969) suggests reflects the difference in duration between strikes that engaged the meral sclerites and muscle-powered strikes, respectively. Thus, while *H. californiensis* may have the capacity to latch the appendage in place, it does not always do so. This example demonstrates the ability of stomatopods to produce slower muscle-powered strikes, despite having morphology that could increase appendage speed.

Although using non-evasive prey likely affected laboratory strike kinematics, it is interesting to note that average propodus duration is comparable to or faster than the durations of a range of aquatic predators that do not use elastic energy storage to capture prey. Teleosts such as the largemouth bass, blue gill sunfish, midas cichlids, and eels reach peak gape in approximately 22-38 ms (deVries and Wainwright 2006; Higham *et al*. 2006), 32 ms (Higham *et al*. 2005), 30 ms (Mehta and Wainwright 2007), and even 347 ms (Mehta and Wainwright 2007)

respectively. *L. maculata*'s strike durations are also similar to the protraction of squid tentacles, which occurs in 20-50 ms (reviewed in van Leeuwen *et al*. 2000). Unlike *L. maculata*, these other aquatic predators swim towards their prey (ram feeding), which contributes to successful prey capture (Higham *et al*. 2005). However, some of the durations listed above were collected from stationary and successful prey capture events (Higham *et al*. 2005; Mehta and Wainwright, 2007), indicating that these individuals were able to capture prey even though there was no contribution of ram feeding to prey capture kinematics (Higham *et al*. 2005). Thus, while the mechanics of a stomatopod strike differ dramatically from fish and squid prey capture mechanics, this comparison illustrates the fact that high speeds generated from spring-loaded strikes are not necessarily required for capturing evasive prey in an aquatic environment. As long as *L. maculata* can reach a considerable distance, it may only need to attain certain minimum speeds and accelerations to capture prey.

Does* L. maculata *have appendage morphology consistent with a spring apparatus?

Micro-CT scans confirmed that *L. maculata's* raptorial appendage has the major structures required for elastic energy storage. The mineralized ventral bar in the merus connects to the proximal end of the meral-V, forming the appendage's main unit of elastic storage (Fig. 1.4 B, C) (Patek *et al*. 2007; Zack *et al*. 2009). A non-mineralized membrane layer attached to the proximal edge of the meral-V provides space for the meral-V to flex against the distal portion of the merus (Fig. 1.4 B). The sclerite latches that are used for performing antagonistic contractions prior to a strike are also present (Fig. 1.4 C, D). The saddle structure, which is thought to help the merus deal with conformational changes that occur when elastic energy is stored (Zack *et al*. 2009), is also well-defined in the merus. However, *L. maculata's* meral-V is considerably thinner and curves distally, compared to the meral-V's of other species that have been analyzed for raptorial appendage mechanics (Burrows 1969; McNeill *et al*. 1972; Patek *et al*. 2007; Zack *et al*. 2009; Claverie *et al*. 2011). The saddle is also in a different location on the merus compared to other species (Burrows 1969; Zack *et al*. 2009; Claverie *et al*. 2011).

While *L. maculata* has the required elements for elastic energy storage (Patek *et al*. 2007; Zack *et al*. 2009; Claverie *et al*. 2011), the capacity of these structures to behave as springs remains unknown. I could not detect relaxation of the meral-V upon propodus rotation. If the meral-V moved at all, then it only moved at most 16 % of the full contracting distance. Thus, it is likely that little to no elastic energy was being stored in the meral-V and that elastic energy was not driving propodus movement in the laboratory strikes. I also could not determine whether the sclerites were holding the propodus against the merus, which would have allowed for antagonistic muscle contraction of the extensor and flexor muscles in the merus. There are three possible explanations for these results that should be addressed in future studies. Either *L. maculata* controls spring and sclerite engagement, elastic energy storage structures in the merus are stiff and do not compress enough to affect propodus rotation, or *L. maculata*'s merus structures do not actually store elastic energy.

How does* L. maculata*'s prey capture strategy compare to that of other stomatopod species?

Different strike behaviors documented in the laboratory study reinforce the notion that while categorizing stomatopods as spearers and smashers provides a helpful distinction, these categories may not reflect the full range of prey capture behaviors that each species is capable of producing. In the high-speed laboratory videos, the majority of strikes were grabs with the inner-most dactyl spines, not spears with the distal dactyl spines. The different prey capture

behaviors exhibited during this study demonstrate that there is variation in the way that stomatopods use their appendages. Other stomatopods with mixed diets of hard- and soft-bodied prey have been shown to use a variety of feeding behaviors, regardless of appendage morphology, to consume different prey types, including hammering prey with a closed dactyl and grabbing prey with an open dactyl (Caldwell and Dingle 1975; Dingle and Caldwell 1975; Dingle and Caldwell 1978; Hamano and Matsuura 1986a; Hamano and Matsuura 1986b). Future studies should consider how the variation in prey capture behavior relates to raptorial appendage morphology and kinematics.

In the field, however, low contrast and resolution of the videos precluded my ability to determine which dactyl spines contacted the prey, or even if the prey was captured at all. With the current data, I cannot determine whether grabbing prey is a behavior that is only seen in the laboratory and not in the field. Future studies using high resolution field videos would help to resolve whether spearing behavior and kinematics in the laboratory reflect field strikes.

In general, comparing *L. maculata* to other stomatopod species reveals an interesting pattern: as speed and acceleration decrease from smashing to spearing stomatopods, appendage reach increases. The kinematics of *L. maculata*'s strike are much slower than the 10 m s^{-1} strike of *H. californiensis* (Burrows 1969) and the 23 m s^{-1} strike of *O. scyllarus* (Patek *et al*. 2004; Patek *et al*. 2007). Strike behaviors differ considerably between these species. While *L. maculata* almost always rotates its dactyls distally to strike with an open appendage, *H. californiensis* and *O. scyllarus* strike primarily with closed dactyls (Burrows 1969; Caldwell and Dingle 1976; Basch and Engle 1989; Patek *et al*. 2004; Patek *et al*. 2007). Raptorial appendage morphology also exhibits variation. *L. maculata* has elongated, streamlined appendages that extend far outside of the burrow to grasp prey. Fixed spines on the dactyl and moveable spines on the propodus are also elongated and sharp, so that *L. maculata* can impale evasive prey between its propodus and dactyl. In contrast, *O. scyllarus* has short, bulky appendages, and *H. californiensis* has appendages that are in between the spearing and smashing morphology in terms of length and amount of calcification of the dactyl heel (Burrows 1969; Ahyong 2001). Taken together, the kinematics, behavior, and morphology across these three species suggest a functional trade-off between strike kinematic output and appendage reach.

Further research may reveal that this trade-off corresponds to a change in foraging mode from sit-and-wait predation to a mixed strategy, which includes active foraging as well. For example, sit-and-wait predators have elongated, slow appendages used to capture evasive, soft-bodied prey and active foragers have short, fast appendages used to consume a wide diversity of prey. If this trade-off exists, then the morphology, kinematics, and behavior associated with *L. maculata*'s extended reach may actually limit its diet breadth to only soft-bodied prey, because this species cannot generate the high accelerations and forces required for crushing hard-shelled prey. However, this potential trade-off should be tested in a phylogenetic context in future research.

To my knowledge, this study is the first comprehensive analysis of the morphology, kinematics, and behavior associated with sit-and-wait predation in stomatopods. Capturing evasive prey requires the predator to minimize the distance between itself and its prey rapidly (Huey *et al*. 1984; Garland Jr. and Losos 1994; Miles *et al*. 2007; McBrayer and Wylie 2009). Most sit-and-wait predators meet this requirement by having fast-moving prey capture mechanisms and structures that can extend considerable distances, such as long lizard limbs with fast muscles or ballistic frog and beetle tongues (Bauer and Pfeiffer 1991; Miles *et al*. 2007; McBrayer and Wylie 2009; van Leeuwen *et al*. 2000). *L. maculata*'s strategy is similar to that of

the frog and beetle, which involves rapidly extending the prey capture mechanism away from the body towards the prey item (Bauer and Pfeiffer 1991; van Leeuwen *et al*. 2000). Yet, when compared to other stomatopods that likely use a mix of both sit-and-wait and active foraging based on gut content analyses (Dingle and Caldwell 1975; Dingle and Caldwell, 1978; Hamano and Matsuura 1986a; Hamano and Matsuura 1986b; Dominguez and Reaka 1988; Basch and Engle 1989; Caldwell *et al*. 1989; Pihl *et al*. 1992; Basch and Engle 1993), *L. maculata's* strikes are slow, probably because this species has a longer reach. Thus, for this sit-and-wait spearing stomatopod, reach may be more important for catching evasive prey than speed, as long as minimum speeds and accelerations are attained. Comparing three stomatopod species further suggested that stomatopods likely exhibit a continuum of sit-and-wait to active foraging across species, with *L. maculata* at the sit-and-wait end of the foraging spectrum. Future studies should test whether this potential correlation between morphology, kinematics, and behavior holds with a wider range of taxa and in a phylogenetic comparative context.

References

Ahyong, S. (2001). Revision of the Australian stomatopod Crustacea. *Records of the Australian Museum Supplement 26*, 1-326.

Ahyong, S. and Jarman, S. (2009). Stomatopod interrelationships: preliminary results based on analysis of three molecular loci. *Arthropod Systematics & Phylogeny* 67, 91-98.

Basch, L. V. and Engle, J. M. (1989). Aspects of the ecology and behavior of the stomatopod *Hemisquilla ensigera californiensis* (Gonodactyloidea: Hemisquillidae). In *Biology of Stomatopods*, vol. 3 (ed. E. A. Ferrero), pp. 199-212. Mucchi, Modena.

Basch, L. V. and Engle, J. M. (1993). Biogeography of *Hemisquilla ensigera californiensis* (Crustacea: Stomatopoda) with emphasis on Southern California bight populations. In *Third California Islands Symposium*, (ed. F. G. Hochberg), pp. 211-220. Santa Barbara: Santa Barbara Museum of Natural History.

Bauer, T. and Pfeiffer, M. (1991). 'Shooting' springtails with a sticky rod: the flexible hunting behaviour of *Stenus comma* (Coleoptera; Staphylinidae) and the counter strategies of its prey. *Animal Behavior* 41, 819-828.

Betz, O. and Kolsch, G. (2004). The role of adhesion in prey capture and predator defense in arthropods. *Arthropod Structure & Development* 33, 3.

Burrows, M. (1969). The mechanics and neural control of the prey capture strike in the mantid shrimps *Squilla* and *Hemisquilla*. *Zeitschrift fur vergleichende Physiologie* 62, 361-381.

Burrows, M. and Hoyle, G. (1972). Neuromuscular physiology of the strike mechanism of the mantis shrimp, *Hemisquilla*. *Journal of Experimental Zoology* 179, 379-394.

Caldwell, R. L. (1991). Variation in reproductive behavior in stomatopod Crustacea. In *Crustacean Sexual Biology*, eds. R. Bauer and J. Martin), pp. 67-90: Columbia University Press.

Caldwell, R. L. and Dingle, H. (1975). Ecology and evolution of agonistic behavior in Stomatopods. *Naturwissenschaften* 62, 214-222.

Caldwell, R. L. and Dingle, H. (1976). Stomatopods. *Scientific American*, 81-89.

Caldwell, R. L., Roderick, G. K. and Shuster, S. M. (1989). Studies of predation by *Gonodactylus bredini*. In *Biology of Stomatopods*, vol. 3 (ed. E. A. Ferrero), pp. 117-131. Modena: Mucchi.

Camp, D. K. (1973). Stomatopod Crustacea. In *Memoirs of the Hourglass Cruises*, vol. 3, pp. 1-100. St. Petersburg, FL: Florida Department of Natural Resources.

Casatti, L. and Castro, R. M. C. (2006). Testing the ecomorphological hypothesis in a headwater riffles fish assemblage of the Rio Sao Francisco, southeastern Brazil. *Neotropical Ichthyologist* 4, 203-214.

Claverie, T., Chan, E. and Patek, S. N. (2010). Modularity and scaling in fast movements: power amplification in mantis shrimp. *Evolution* 65, 443-461.

Cronin, T. W. and Marshall, J. (2004). The unique visual world of mantis shrimps. In *Complex Worlds from Simpler Nervous Systems*, (ed. F. R. Prette), pp. 239-268. Cambridge, MA: The MIT Press.

deVries, M. S. and Wainwright, P. C. (2006). The effects of acute temperature change on prey capture kinematics in largemouth bass, *Micropterus salmoides*. *Copeia* 3, 437-444.

Dingle, H. and Caldwell, R. L. (1975). Distribution, abundance, and interspecific agonisitic behavior of two mudflat stomatopods. *Oecologia* 20, 167-178.

Dingle, H. and Caldwell, R. L. (1978). Ecology and morphology of feeding and agonistic behavior in mudflat stomatopods (Squillidae). *Biology Bulletin* 155, 134-149.

Dominguez, J. H. and Reaka, M. L. (1988). Temporal activity patterns in reef-dwelling stomatopods: a test of alternative hypotheses. *Journal of Experimental Marine Biology and Ecology* 117, 47-69.

Froglia, C. and Giannini, S. (1989). Field observations on diel rhythms in catchability and feeding in *Squilla mantis* (L.) (Crustacea, Stomatopoda) in the Adriatic Sea. In *Biology of Stomatopods*, vol. 3 (ed. E. A. Ferrero), pp. 221-228. Modena: Mucchi.

Full, R. J., Caldwell, R. L. and Chow, S. W. (1989). Smashing energetics: prey selection and feeding efficiency of the stomatopod, *Gonodactylus bredini*. *Ethology* 81, 134-147.

Garland Jr., T. and Losos, J. B. (1994). Ecological morphology of locomotor performance in squamate reptiles. In *Ecological Morphology: An Integrative Approach to Organismal Biology*, (ed. P. C. Wainwright), pp. 240-302. Chicago: University of Chicago.

Hamano, T., Hayashi, K.-I., Katsuhiko, K., Matsushita, H. and Tabuchi, K. (1996). Population structure and feeding behavior of the stomatopod crustacean *Kempina mikado* (Kemp and Chopra, 1921) in East China. *Fisheries Science* 62, 397-399.

Hamano, T. and Matsuura, S. (1986a). Food habits of the Japanese mantis shrimp in the benthic community of Hakata Bay. *Bulletin of the Japanese Society of Scientific Fisheries* 52, 787-794.

Hamano, T. and Matsuura, S. (1986b). Optimal prey size for the Japanese mantis shrimp from structure of the raptorial claw. *Bulletin of the Japanese Society of Scientific Fisheries* 52, 1-10.

Higham, T. E., Day, S. W. and Wainwright, P. C. (2005). Sucking while swimming: evaluating the effects of ram speed on suction generation in bluegill sunfish *Lepomis macrochirus* using digital particle image velocimetry. *Journal of Experimental Biology* 208, 2653-2660.

Higham, T. E., Day, S. W. and Wainwright, P. C. (2006). Multidimensional analysis of suction feeding performance in fishes: fluid speed, acceleration, strike accuracy and ingested volume of water. *Journal of Experimental Biology* 209, 2713-2725.

Huey, R. B., Bennett, A. F., John-Alder, H. B. and Nagy, K. A. (1984). Locomotor capacity and foraging behavior of Kalahari lacertid lizards. *Animal Behavior* 32, 41-50.

Lawton, P. (1989). Predatory interaction between the brachyuran crab *Cancer pagurus* and decapod crustacean prey. *Marine Ecology Progress Series* 52, 169-179.

Mascaro, M., Hidalgo, L. E., Chiappa-Carrara, X. and Simoes, N. (2003). Size-selective foraging behavior of blue crabs, *Callinectes sapidus* (Rathbun), when feeding on mobile prey: active and passive components of predation. *Marine and Freshwater Behaviour and Physiology* 36, 143-159.

Masuko, K. (2009). Studies on the predatory biology of Oriental dacetine ants (Hymenoptera: Formicidae) II. Novel prey specialization in *Pyramica benten*. *Journal of Natural History* 43, 825-841.

Maynou, F., Abello, P. and Sartor, P. (2005). A review of the fisheries biology of the mantis shrimp, *Squilla mantis* (L., 1758) (Stomatopoda, Squillidae) in the Mediterranean. *Crustaceana* 77, 1081-1099.

McBrayer, L. D. and Wylie, J. E. (2009). Concordance between locomotor morphology and foraging mode in lacertid lizards. *Zoology* 112, 370-378.

McNeill, P., Burrows, M. and Hoyle, G. (1972). Fine structures of muscles controlling the strike of the mantis shrimp, *Hemisquilla*. *Journal of Experimental Zoology* 179, 395-416.

Mead, K. S. (2002). From odor molecules to plume tracking: an interdisciplinary, multilevel approach to olfaction in stomatopods. *Integrative and Comparative Biology* 42, 258.

Mehta, R. S. and Wainwright, P. C. (2007). Biting releases constraints on moray eel feeding kinematics. *Journal of Experimental Biology* 210, 495-504.

Miles, D. B., Losos, J. B. and Irschick, D. (2007). Morphology, performance, and foraging mode. In *Lizard Ecology: The Evolutionary Consequences of Foraging Mode*, eds. S. M. Reilly L. D. McBrayer and D. B. Miles), pp. 49-93. Cambridge: Cambridge University Press.

Patek, S. N. and Caldwell, R. L. (2005). Extreme impact and cavitation forces of a biological hammer: strike forces of the peacock mantis shrimp (*Odontodactylus scyllarus*). *Journal of Experimental Biology* 208, 3655-3664.

Patek, S. N., Korff, W. L. and Caldwell, R. L. (2004). Deadly strike mechanism of a mantis shrimp. *Nature* 428, 819-820.

Patek, S. N., Nowroozi, B. N., Baio, J. E., Caldwell, R. L. and Summers, A. P. (2007). Linkage mechanics and power amplification of the mantis shrimp's strike. *Journal of Experimental Biology* 210, 3677-3688.

Patek, S. N., Dudek, D. M. and Rosario, M. V. (2011). From bouncy legs to poisoned arrows: elastic movements in invertebrates. *J. Exp. Biol.* 214, 1973-1980.

Pianka, E. R. (1966). Convexity, desert lizards, and spatial heterogeneity. *Ecology* 47, 1055-1059.

Pihl, L., Baden, S. P., Diaz, R. J. and Schaffner, L. C. (1992). Hypoxia-induced structural changes in the diet of bottom-feeding fish and Crustacea. *Marine Biology* 112, 349-361.

Schiff, H., Dore, B. and Boido, M. (2007). Morphology of adaptation and morphogenesis in stomatopod eye. *Italian Journal of Zoology* 74, 123-134.

Schiff, H., Dore, B. and Donna, D. (2002). A mantis shrimp wearing sun-glasses. *Italian Journal of Zoology* 69, 205-214.

Schoener, T. W. (1971). Theory of feeding strategies. *Annual Review of Ecology and Systematics* 2, 369-404.

van Leeuwen, J. L., De Groot, J. H. and Kier, W. M. (2000). Evolutionary mechanics of protrusible tentacles and tongues. *Netherlands Journal of Zoology* 50, 113-139.

Vogel, S. (2003). Comparative Biomechanics: Life's Physical World, pp. 1-580. Princeton, NJ: Princeton University Press.

Wainwright, P. C. and Friel, J. P. (2000). Effects of prey type on motor pattern variance in Tetraodontiform fishes. *Journal of Experimental Zoology* 286, 563-571.

Wainwright, P. C., Mehta, R. S. and Higham, T. E. (2008). Stereotypy, flexibility and coordination: key concepts in behavioral functional morphology. *The Journal of Experimental Biology* 211, 3523-3528.

Walker, J. A. (1998). Estimating velocities and accelerations of animal locomotion: a simulation experiment comparing numerical differentiation algorithms. *Journal of Experimental Biology* 201, 981-995.

Wilga, C. D., Motta, P. J. and Sanford, C. P. (2007). Evolution and ecology of feeding in elasmobranchs. *Integrative and Comparative Biology* 47, 55-69.

Zack, T. I., Claverie, T. and Patek, S. N. (2009). Elastic energy storage in the mantis shrimp's fast predatory strike. *The Journal of Experimental Biology* 212, 4002-4009.

Tables

Table 1.1. The kinematics of *L. maculata*'s strikes. Acceleration and speed were measured at the distal end of the propodus. Time is the chronological location of maximum speed relative to the onset of propodus rotation. Duration is the amount of time between the onset of propodus rotation and full extension.

Individual	Speed ($m\ s^{-1}$)	Acceleration ($m\ s^{-2}$)	Angular speed ($x10\ rad\ s^{-1}$)	Angular acceleration ($rad\ s^{-2}$)	Duration (ms)	Time of max speed (ms)
1	2.00±0.90 (n=6)	0.40±0.69 (n=6)	5.44±2.90 (n=6)	11.68±20.36 (n=6)	28.56±6.15 (n=6)	15.39±5.70 (n=6)
2	1.94±0.37 (n=6)	0.13±0.04 (n=6)	5.76±0.90 (n=6)	3.43±1.12 (n=6)	49.27±0.15.39 (n=7)	15.17±2.84 (n=6)
3	3.06 ± 1.52 (n=3)	0.48 ± 0.27 (n=3)	8.33±4.12 (n=3)	13.81±7.85 (n=3)	31.89±3.34 (n=15)	12.78±6.26 (n=3)
4	2.36±0.87 (n=7)	0.21±0.25 (n=7)	5.25±1.93 (n=7)	4.74±5.57 (n=7)	36.5±10.32 (n=6)	24.57± 9.40 (n=7)
5	2.14±0.60 (n=3)	0.26 ± 0.26 (n=3)	7.57±2.54 (n=3)	7.78±1.90 (n=3)	24.0±5.7 (n=6)	8.89±2.55 (n=3)
Means of all *L. maculata*	2.30±0.85 (N=5)	0.30±0.28 (N=5)	6.47±2.48 (N=5)	4.43±7.77 (N=5)	34.04±4.75 (N=5)	15.36±5.78(N=5)

Values are mean ± s.d. *n*, number of strikes for each individual; *N*, number of individuals.

Table 1.2. T-tests comparing stereotypy of propodus and dactyl movements between strike phases. Mean coefficients of variation (CV) calculated for each strike phase and segment movement are presented along with associated significance values from the t-test comparisons. Significant differences ($p < 0.05$) either between dactyl movement in Phase I and propodus movement in Phase II (Dactyl I / Propodus II) or between dactyl movement in Phase I and II (Dactyl I / Dactyl II) were determined. N=5 individuals for each kinematic variable.

	Phase I CVs	**Phase II CVs**		***p*-values**	
	Dactyl	**Propodus**	**Dactyl**	**Dactyl I / Propodus II**	**Dactyl I / Dactyl II**
Speed	0.36	0.36	0.31	0.98	0.36
Acceleration	0.85	0.84	0.50	0.98	0.02 *
Angular speed	0.54	0.38	NA	0.36	NA
Angular acceleration	0.67	0.86	NA	0.63	NA

Table 1.3. A comparison of durations between strikes that did (contact) and did not (no contact) end in contact with the prey item. Statistical differences ($p < 0.05$) between mean durations of contact and no contact strikes are evaluated with t-tests for each individual. # strikes = the total number of strikes used in the comparison.

	Total time durations (ms)		t-test results	
Individual (# strikes)	**Contact**	**No contact**	**t-statistic**	***p***
1 (14)	80.75 ± 27.94	80.27 ± 10.90	<0.01	0.97
2 (6)	97.27 ± 20.71	124.67 ± 19.15	0.52	0.09
3 (10)	143.00 ± 26.96	157.89 ± 24.68	3.79	0.52
4 (17)	73.44 ± 15.18	79.33 ± 6.98	0.42	0.53
5 (12)	135.72 ± 39.78	148.77 ± 76.52	0.14	0.72

* Note that the mean durations presented here are greater than the mean durations presented in Table 1.1. When the durations of each strike phase are added together, the means presented in Table 1.1 are lower than the Table 1.3 means because, by chance, all but one of the individuals included only in Table 1.1 had faster durations, which brought down the means in Table 1.1. Faster individuals were excluded from this comparison in Table 1.3, because they did not have at least three strikes in either or both of the contact/no contact categories.

Figure Legends

Figure 1.1. The behaviors and key structures associated with the raptorial strike of *Lysiosquillina maculata*. (A) A depiction of *L. maculata* rapidly emerging from its sandy burrow to capture evasive prey with the two most distal spines of the dactyl. Structures on (A) lateral and (B) medial sides of the left raptorial appendage highlight the primary anatomical features involved in prey capture and are labeled as follows: merus (m), meral-V (v), saddle (s), carpus (c), propodus (p), moveable propodal spines (ms), dactyl (d). Other structures in (A) that are important for prey capture are labeled as follows: eyes (e), antennules (a). Scale bars = 10 mm.

Figure 1.2. A high speed video image shows *L. maculata* in lateral view with the configuration of the digitized points. Numbers represent anatomical locations of the points where (1) is the proximal end of the meral-V, (2) is the tip of the distal edge of the meral-V, (3) is the anterior-distal edge of the carpus, (4) is the distal, trailing edge of the propodus, and (5) is the tip of the dactyl's distal, leading edge.

Figure 1.3. Raw and smoothed dactyl data from a typical strike sequence showing dactyl movement over time. Raw cumulative displacement and velocity data (red line) were fit with a Butterworth filter (black line), an interpolated spline (blue line), and a 10^{th} order polynomial curve fit (green line). The 10^{th} order polynomial yielded the best curve-fit of the raw data.

Figure 1.4. Computed Tomography images of *L. maculata's* raptorial appendage show four different views of the appendage: (A) lateral, (B) medial, (C) ventral, and (D) dorsal. Within each frame, the upper images show surface conformations of the entire appendage and lower images show relative mineralization of only the merus segment, where bright white areas indicate greater mineralization. Anatomical features are labeled as follows: merus (m), meral-V (v), saddle (s), apodeme (a), ventral bar (Vb), carpus (c), sclerites (Sc), propodus (p), and dactyl (d). Scale bar = 10 mm.

Figure 1.5. A kinematic analysis of a typical raptorial strike reveals faster propodus speeds than dactyl speeds. (A) A composite of high speed images documents *L. maculata* rotating its dactyl and extending its propodus to impale prey with the distal dactyl spines. (B) A cumulative displacement profile, which was smoothed with a 10^{th} order polynomial curve-fit, shows movement of the distal ends of the propodus and dactyl. (C) Speed profile of the distal ends of the propodus and dactyl, which was also smoothed using a 10^{th} order polynomial curve-fit, shows strike velocity. Solid lines represent the 10^{th} order polynomial curve-fits of the raw displacement and speed data. The blue diamonds, white triangles, and green squares represent the raw data of the merus, propodus, and dactyl respectively. Numbers 1-5 on panels A-C represent corresponding time points during the strike. Points 1 and 2 represent dactyl rotation occurring during strike Phase I. Points 3-5 represent propodus rotation during strike Phase II.

Figure 1.6. The relationship between carapace length and the mean ± 1 standard deviation of the three fastest peak propodus speeds for each of the five individuals.

Figure 1.7. Strike activity of all seventeen *L. maculata* burrows filmed at Lizard Island, Australia. Black bars on the x-axis mark the hours of video observation. Gray bars represent the number of strikes that occurred per hour of observation.

Figures

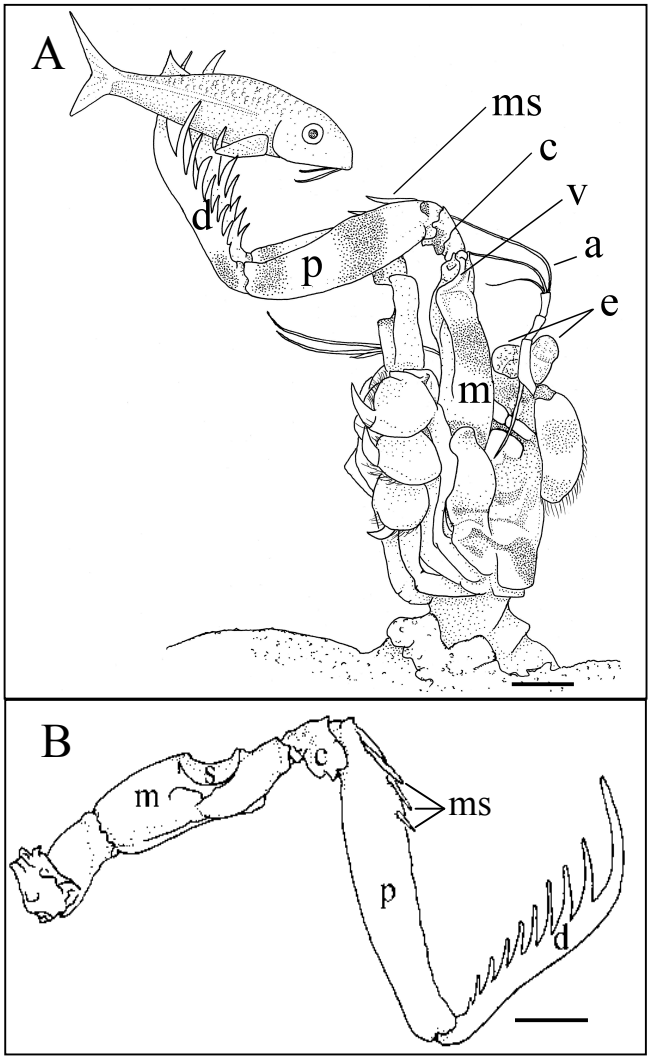

Figure 1.1. The behaviors and key structures associated with the raptorial strike of *Lysiosquillina maculata*. (A) A depiction of *L. maculata* rapidly emerging from its sandy burrow to capture evasive prey with the two most distal spines of the dactyl. Structures on (A) lateral and (B) medial sides of the left raptorial appendage highlight the primary anatomical features involved in prey capture and are labeled as follows: merus (m), meral-V (v), saddle (s), carpus (c), propodus (p), moveable propodal spines (ms), dactyl (d). Other structures in (A) that are important for prey capture are labeled as follows: eyes (e), antennules (a). Scale bars = 10 mm.

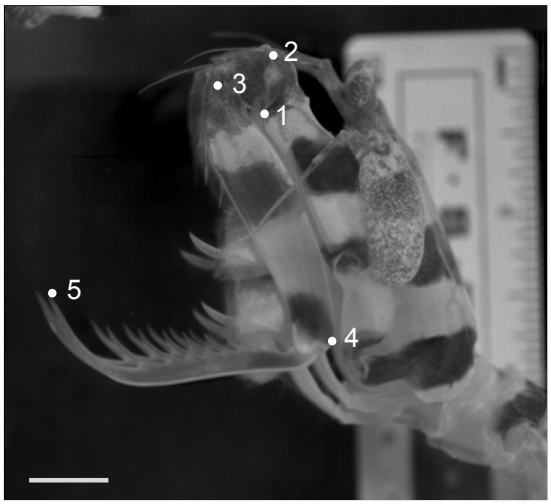

Figure 1.2. A high speed video image shows *L. maculata* in lateral view with the configuration of the digitized points. Numbers represent anatomical locations of the points where (1) is the proximal end of the meral-V, (2) is the tip of the distal edge of the meral-V, (3) is the anterior-distal edge of the carpus, (4) is the distal, trailing edge of the propodus, and (5) is the tip of the dactyl's distal, leading edge.

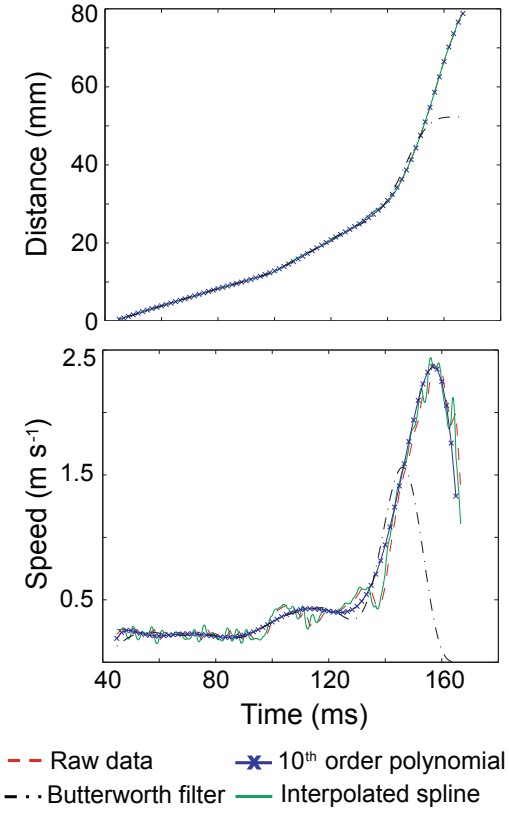

Figure 1.3. Raw and smoothed dactyl data from a typical strike sequence showing dactyl movement over time. Raw cumulative displacement and velocity data (red line) were fit with a Butterworth filter (black line), an interpolated spline (blue line), and a 10^{th} order polynomial curve fit (green line). The 10^{th} order polynomial yielded the best curve-fit of the raw data.

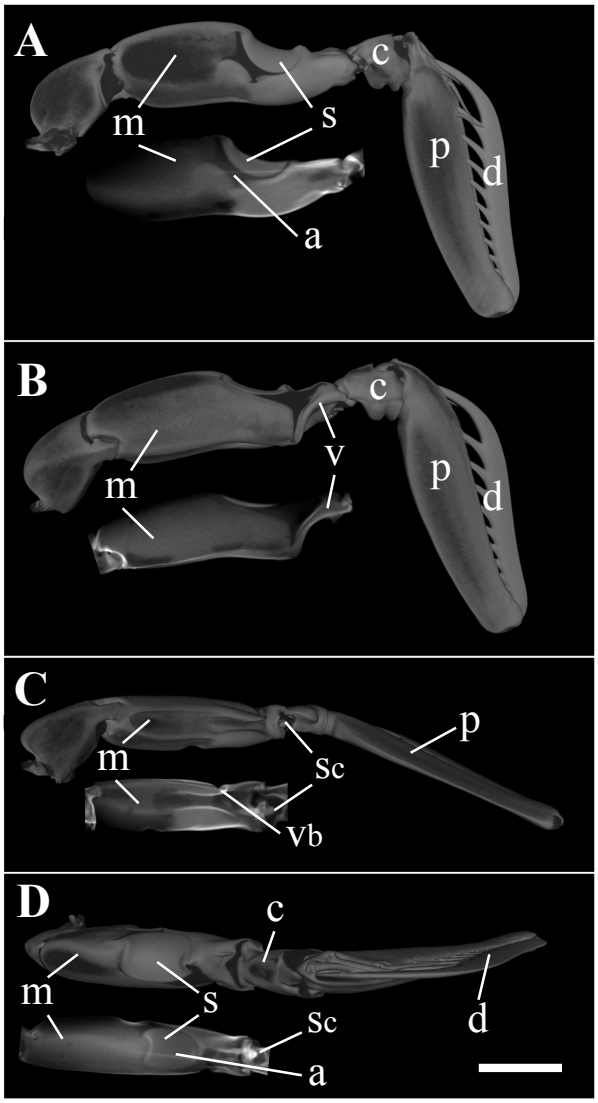

Figure 1.4. Computed Tomography images of *L. maculata's* raptorial appendage show four different views of the appendage: (A) lateral, (B) medial, (C) ventral, and (D) dorsal. Within each frame, the upper images show surface conformations of the entire appendage and lower images show relative mineralization of only the merus segment, where bright white areas indicate greater mineralization. Anatomical features are labeled as follows: merus (m), meral-V (v), saddle (s), apodeme (a), ventral bar (Vb), carpus (c), sclerites (Sc), propodus (p), and dactyl (d). Scale bar = 10 mm.

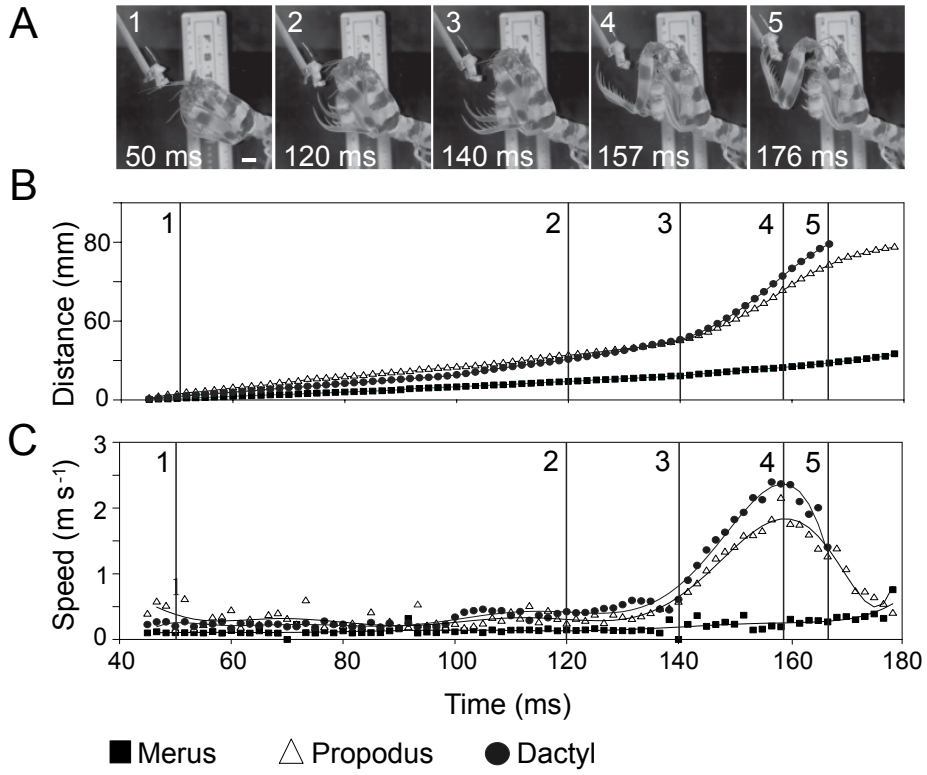

Figure 1.5. A kinematic analysis of a typical raptorial strike reveals faster propodus speeds than dactyl speeds. (A) A composite of high speed images documents *L. maculata* rotating its dactyl and extending its propodus to impale prey with the distal dactyl spines. (B) A cumulative displacement profile, which was smoothed with a 10th order polynomial curve-fit, shows movement of the distal ends of the propodus and dactyl. (C) Speed profile of the distal ends of the propodus and dactyl, which was also smoothed using a 10th order polynomial curve-fit, shows strike velocity. Solid lines represent the 10th order polynomial curve-fits of the raw displacement and speed data. The blue diamonds, white triangles, and green squares represent the raw data of the merus, propodus, and dactyl respectively. Numbers 1-5 on panels A-C represent corresponding time points during the strike. Points 1 and 2 represent dactyl rotation occurring during strike Phase I. Points 3-5 represent propodus rotation during strike Phase II.

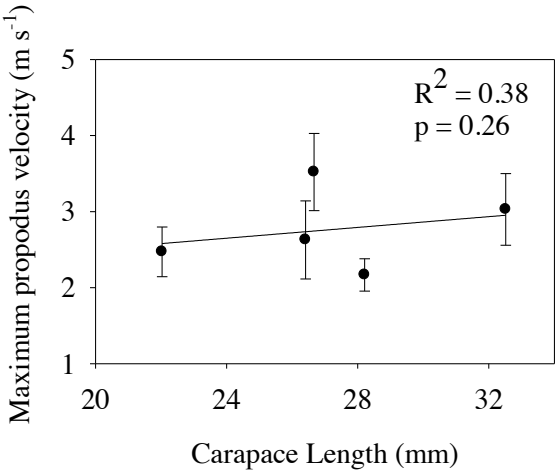

Figure 1.6. The relationship between carapace length and the mean ± 1 standard deviation of the three fastest peak propodus speeds for each of the five individuals.

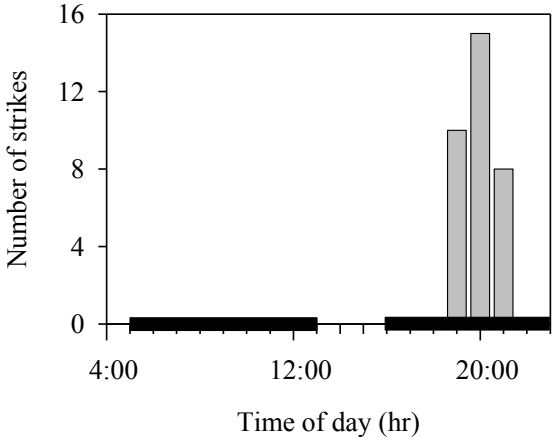

Figure 1.7. Strike activity of all seventeen *L. maculata* burrows filmed at Lizard Island, Australia. Black bars on the x-axis mark the hours of video observation. Gray bars represent the number of strikes that occurred per hour of observation.

Chapter II

Isotopic incorporation rates and discrimination factors in mantis shrimp: insights into crustacean physiology and life history

Key words: Stomatopoda, stable isotope, tissue turnover, molting, catabolism

Abstract

Stable isotope analysis has provided insights into the trophic ecology of a wide diversity of animals. Tissue incorporation rate and isotopic discrimination are essential for correctly interpreting stable isotope data, but these parameters remain relatively understudied in aquatic invertebrates. My goal was to expand upon previous investigations primarily conducted in vertebrates, by measuring the carbon and nitrogen incorporation rates and discrimination factors in the mantis shrimp, *Neogonodactylus bredini*. I performed a 292-day diet-switch experiment on 92 individuals. I periodically measured individual growth and sampled muscle and hemolymph tissues. Discrimination factors between mantis shrimp muscle and the new diet were 3.0 ± 0.6‰ for the carbon isotope ($\delta^{13}C$) and 0.9 ± 0.3‰ for the nitrogen isotope ($\delta^{15}N$), which were much different than the conventional values of 3‰ for $\delta^{15}N$ and 0-1‰ for $\delta^{13}C$. A first order kinetic, single-compartment model showed that both $\delta^{13}C$ and $\delta^{15}N$ incorporated faster into hemolymph tissue than into muscle. Variation in incorporation rates between tissues and unexpected discrimination factors likely stemmed from distinct nutritional requirements for biological compounds containing $\delta^{15}N$ or $\delta^{13}C$. Although there was variation in $\delta^{15}N$ and $\delta^{13}C$ incorporation, the rate of carbon incorporation into muscle was consistent with rates predicted by an allometric equation correlating incorporation rate to body mass that was developed by Weidel *et al.* (2011) for teleost fishes and expanded upon by Kim *et al*. (2012) for sharks.

Introduction

It is now firmly established that stable carbon and nitrogen isotope ratios (i.e., $^{13}C/^{12}C$ and $^{15}N/^{14}N$) can provide new insights into the trophic ecology of animals (Boecklen *et al.* 2011). Variation in the isotope ratio of each element can reveal individual diet and thereby show the hierarchy of predator-prey dependency. One central principle of stable isotope analysis that underlies trophic investigations is that the isotopic compositions of different prey items "record" a predator's diet with reliable fidelity when prey are consumed and assimilated into predator tissues (reviewed in Fry 2006). A major advantage of stable isotope analysis is that stable

isotopes provide much more information about an animal's biology in addition to just its diet. For example, stable isotopes integrate information about physiological processes associated with an animal's metabolism and nutritional requirements, which in turn are tightly linked to general traits such as body size, ontogeny, and gender (Boecklen *et al.* 2011). Therefore, stable isotopes provide diet information within the context of the life history properties and strategies of the animal (Boecklen *et al.* 2011).

Moreover, unlike traditional methods of diet analysis that can only document finite snap-shots in time of a predator's diet, stable isotope analysis has the added capability of reconstructing diet assimilated over various windows of time (Tieszen *et al.* 1993; Bearhop *et al.* 2004; Martinez del Rio *et al.* 2009). Stable isotope analysis has this capacity because different tissues incorporate new material, and thus their stable isotope composition, at different rates (Dalerum & Angerbjörn 2005; reviewed in Martínez del Rio *et al.* 2009). This time window depends on a tissue's incorporation or turnover rate. Despite the known influences of certain life history properties on stable isotope variation, there is still a paucity of information about whether there are general patterns in the stable isotope variation that relate to life history properties (Martinez del Rio *et al.* 2009; Wyatt, Waite & Humphries 2010 and references therein; Boecklen *et al.* 2011; Lecomte *et al.* 2011). With these factors in mind, I determined the incorporation rates of multiple tissues in mantis shrimp (Crustacea: Stomatopoda), a ubiquitous coral reef predator.

To estimate the incorporation rates of different tissues, the consumer is switched to a new diet that is isotopically distinct from its former diet and tissues are sampled over time to measure the time required for the predator's tissue to equilibrate with the new diet. Most of these studies have been conducted in vertebrates on a variety of different tissue types (Martínez del Rio *et al.* 2009 and references therein; Sponheimer *et al.* 2003; Dalerum & Angerbjörn 2005; Passey *et al.* 2005; Podlesak, McWilliams & Hatch 2005; Cerling *et al.* 2007; Murray & Wolf 2012). A common finding is that there are tissues with slower incorporation rates, such as muscle, which show dietary inputs assimilating into tissues over as few as 20 days in quail (mass range 14 -18 g) to 555 days in whitefish (mass range 5 - 325 g) (Hobson & Clark 1992; Hesslein, Hallard & Ramlal 1993). Other tissues incorporate diet much faster, such as blood plasma, which have incorporation rates that range from 4 days in American crows (mass range 400-430 g) to 50 days in leopard sharks (mass range 1000-4000 g) (Hobson & Clark 1993; Kim *et al.* 2012).

Incorporation rates are mostly governed by the addition of new material to tissues via growth and anabolism (Fry & Arnold 1982; reviewed in Martínez del Rio *et al.* 2009). However, tissue replacement, resulting from catabolic processes that export material from tissues, also contributes to incorporation rates (Fry & Arnold 1982; Hesslein, Hallard & Ramlal 1993; reviewed in Martínez del Rio *et al.* 2009). Most studies on ectothermic vertebrates, including fish, tortoises, and lizards, have shown that the contribution of growth to turnover spans a wide range of 10-100% (Suzuki *et al.* 2005; Martinez del Rio *et al.* 2009 and references therein; Graham *et al.* 2010; Warne, Gilman & Wolf 2010; Murray & Wolf 2012). This variation likely stems from metabolic differences between animals at varying developmental stages (Martínez del Rio *et al.* 2009; Warne, Gilman & Wolf 2010), between aquatic and terrestrial ectotherms (Warne, Gilman & Wolf 2010; Murray & Wolf 2012), and between different tissue types (Martinez del Rio *et al.* 2009; Buchheister & Latour 2010; Warne, Gilman & Wolf 2010; Murray & Wolf 2012).

Martínez del Rio et al. (2009) proposed body size as another related factor that could explain variation in incorporation rates. Given that incorporation rates are intimately linked to

metabolic processes, it is logical to predict that incorporation rates, like many biological rates, would decrease as a function of body size (Martinez del Rio *et al.* 2009). Conversely, the residence time of an isotope in a tissue should increase predictably with body size (Martinez del Rio *et al.* 2009). Recent studies in birds, fish, and sharks have tested this correlation and are finding it to be accurate (Carleton & Martínez del Rio 2005; Weidel *et al.* 2011; Kim *et al.* 2012).

Another important parameter of interest that can be measured in turnover studies is the isotopic discrimination factor (also known as the fractionation factor), which is the difference between the stable isotope ratios of the predator and the prey (Martínez del Rio & Wolf 2005). Accurate measurements of discrimination are integral to correctly interpreting diet reconstruction models, because even a slight change in discrimination can significantly alter estimates of the percent contributions of different prey items to the diet (Vander Zaden & Rasmussen 2001; McCutchan *et al.* 2003; Caut, Angulo & Courchamp 2009 McCutchan *et al.* 2003; Newsome *et al.* 2007; Bond & Diamond 2011). The conventional discrimination factors for $\delta^{15}N$ and $\delta^{13}C$ were once considered to be 3‰ and 0-1‰, respectively, across animal taxa (DeNiro & Epstein 1978; Minagawa & Wada 1984). However, recent literature reviews of discrimination factors have reported values ranging between 0-5‰ for both $\delta^{15}N$ and $\delta^{13}C$, which casts doubt on the universality of the convention that $\delta^{15}N$ discrimination is 3‰ and $\delta^{13}C$ discrimination is 0-1‰ (Vander Zaden & Rasmussen 2001; McCutchan *et al.* 2003; Caut, Angulo & Courchamp 2009).

As with incorporation rates, aspects of animal biology, from growth and body size, to ontogeny and males vs. females are thought to contribute to intraspecific variation in discrimination factors (Caut, Angulo & Courchamp 2009; Martinez del Rio *et al.* 2009; Wyatt, Waite & Humphries 2010 and references therein; Lecomte *et al.* 2011; Weidel *et al.* 2011; Kim *et al.* 2012). Administering different diets in laboratory-based investigations has also been shown to alter turnover times and discrimination factors (McCutchan *et al.* 2003; Olive *et al.* 2003; Passey *et al.* 2005; Caut, Angulo & Courchamp 2009; Fisk *et al.* 2009; Suring & Wing 2009; Lecomte *et al.* 2011; Kim *et al.* 2012) especially for $\delta^{15}N$ (Hobson, Alisauskas & Clark 1993; Robbins, Felicetti & Sponheimer 2005; Tsahar *et al.* 2008).

Although differences between individuals are known to affect incorporation rates and discrimination factors, studies historically group all individuals together to measure these parameters. This approach could mask novel interactions between isotopic incorporation and an animal's unique biological characteristics. Furthermore, to my knowledge, only one study in crustaceans has measured incorporation and discrimination in more than one tissue type (Suring & Wing 2009), even though measuring multiple tissues is known to reveal intraspecific variation related to body size, ontogeny, and differences between males and females (Lecomte *et al.* 2011).

My goal, therefore, was to expand upon previous investigations largely focused on vertebrates by measuring the carbon and nitrogen incorporation rates and discrimination factors of muscle and hemolymph in mantis shrimp. To estimate these parameters, I performed a 292-day diet-switch experiment on the intertidal, coral reef species, *Neogonodactylus bredini* (Manning 1969). This species is relatively small, with a maximum size of 65 mm (measured from rostrum to telson), and can live up to three years in the laboratory (Caldwell & Steger 1987). *Neogonodactylus bredini* is a ubiquitous coral reef predator that produces one of the fastest movements in the animal kingdom with its predatory appendages (Patek, Korff & Caldwell 2004; Patek & Caldwell 2005), which it uses to hammer hard-shelled prey items (Caldwell, Roderick & Shuster 1989). Like many tropical mantis shrimp, *N. bredini* molts

indeterminately (Reaka 1975) and mates year round with mating patterns that exhibit lunar periodicity (Caldwell 1991). Given this species' patterns of molting and mating, I expected differences between individuals to impact estimates of incorporation rate. However, overall, I expected the residence time of muscle to be slower than that of hemolymph, but that these rates would be similar to residence times measured in other aquatic ectotherms (Fry & Arnold 1982; Trueman, McGill & Guyard 2005; Guelinckx *et al.* 2007; Suring & Wing 2009; Buchheister & Latour 2010; Weidel *et al.* 2011). I also expected discrimination factors to be similar to the conventional values of 3 ‰ and 0 to 1 ‰ for $\delta^{15}N$ and $\delta^{13}C$, respectively (DeNiro & Epstein 1978; Minagawa & Wada 1984; McCutchan *et al.* 2003; Caut, Angulo & Courchamp 2009).

Given that this study provides the first in depth stable isotope analysis in mantis shrimp (except see Risk & Erdmann 2000), a secondary goal was to test sample treatment methods for mantis shrimp tissues. Researchers often remove lipids or carbonates from tissues, because these compounds have more negative $\delta^{13}C$ values relative to the proteins used in metabolism (DeNiro & Epstein 1978; reviewed in Boecklen *et al.* 2011). Yet, sample preparation recommendations for marine invertebrates differ widely (Mateo *et al.* 2008). With the goal of standardizing sample preparation methods for mantis shrimp, I compared the stable isotope ratios of delipidified and untreated tissue samples.

Methods

Captive feeding experiment

One-hundred *Neogonodactylus bredini* (Crustacea: Stomatopoda: Gonodactylidae) were captured at Punta Galeta, Colón, Panama between December 6-12, 2008 (Permit No. SEX/A-133-08). Body sizes, measured from rostrum to telson, ranged from 33-49mm. Animals were held at the Naos Marine Laboratory (Smithsonian Tropical Research Institute) and transported to the Department of Integrative Biology at the University of California (UC) Berkeley on December 30, 2008. At UC Berkeley, animals were maintained at 25˚C in individual plastic cups with 0.2L of 34-36 parts per thousand artificial saltwater. From the time of capture until the start of the diet-switch experiment, animals were fed Western Atlantic, intertidal, sea grass snail, *Cerithium eburneum* (mean ± SD: $\delta^{13}C$ = -8.72 ± 0.84 ‰, $\delta^{15}N$ = 4.58 ± 0.34 ‰). One day prior to switching *N. bredini* to the new diet, the sex of each individual was determined. Carapace length and body length (from rostrum to telson) were measured with digital calipers to the nearest mm (Absolute Coolant Proof Caliper Series 500, Mitutoyo Corporation, Takatsu, Japan). Animals were weighed three times at 15-second intervals to account for mass changes that occurred when water evaporated from the animals while out of water.

After 43 days in the laboratory, animals were switched to a diet of the Pacific, temperate, rocky intertidal snail, *Tegula funebralis*. The diet switch occurred after this relatively short amount of time, because the turnover time of mantis shrimp tissues was predicted to be fast due to their small body size (Martinez del Rio *et al.* 2009; Weidel *et al.* 2011). Nine individuals were randomly selected to be sexed, measured, weighed, and euthanized. Hemolymph was then removed with a 27-gauge needle and 1ml syringe by inserting the needle above the fifth abdominal somite from the anterior-most abdominal somite (abdominal somite 5). Muscle from abdominal somites 2-6 was also dissected. Both tissues were stored frozen at -20°C until preparation for stable isotope analysis.

All other *N. bredini* individuals began receiving a diet of one whole snail every three days for the duration of the experiment. Before feeding, a small tissue sample was removed

from each *T. funebralis* individual and stored for isotopic analyses. *N. bredini* were given six hours to feed. Leftover snail shells were then removed from the cups and the seawater was changed. Deaths and molts were recorded daily. On days 1, 2, 4, 7, 13, 19, 25, 31, 40, 64, 97, 127, 160, 193, 223, and 292 of the experiment, 3 to 6 animals were randomly selected and euthanized, yielding a total of 92 individuals sampled throughout the experiment. Individuals were then sexed, measured, and weighed before their tissues were dissected and stored.

Sample preparation

Ninety-two muscle and 63 hemolymph samples from *N. bredini* were freeze-dried (FreezeZone 12 Liter Freeze Dry System, Labconco, Kansas City, MO, USA) for 48 hours along with ten *T. funebralis* muscle samples. The sample sizes for muscle and hemolymph are different, because in some cases, the hemolymph sample was too small for isotopic analysis. In an attempt to preserve hemolymph, these samples were placed in coin envelopes and deeply frozen at -80°C for 12 hours before being freeze-dried. Once dry, muscle and hemolymph samples were homogenized (Mini-WIG-L-BUG Mixer Amalgamator, Dentsply, Surrey, United Kingdom). Lipids were extracted with petroleum ether (Mateo et al. 2008) from a subsample of 44 *N. bredini* muscle tissues and from ten *T. funebralis* muscle samples by rinsing the sample twice in 0.2ml of solution. Treated samples were then placed on the freeze-drier for twelve hours. Washing tissues with hydrochloric acid and deionized water are other common preparation techniques for arthropod samples, but they were not performed here, because they are known to increase variation in the stable isotope measurements of crustacean muscle (Yokoyama *et al.* 2005; Mateo *et al.* 2008).

All samples were placed in 5 x 9 mm tin capsules and weighed (Costech Analytical Technologies, Valencia, CA, USA; 180 ± 50 µg for *N. bredini* and *T. funebralis* muscle and 220 ± 50 µg for *N. bredini* hemolymph). $\delta^{13}C$ and $\delta^{15}N$ stable isotope ratios were analyzed with elemental analyzer/continuous flow isotope ratio mass spectrometry at the Center for Stable Isotope Biogeochemistry at UC Berkeley using a CHNOS Elemental Analyzer (vario ISOTOPE cube, Elementar, Hanau, Germany) coupled with an IsoPrime100 Isotope Ratio Mass Spectrometer (Isoprime, Cheadle, UK). Isotope ratios are expressed using δ notation as:

$$\delta^{h}X = (R_{sample}/R_{standard}-1) \times 1000 \qquad \text{(Equation 1)}$$

where X is the element, h is the high mass number, R is the high mass-to-low mass isotope ratio, and $R_{standard}$ is Vienna Pee Dee belemnite (VPDB) for carbon and AIR for nitrogen. Units are parts per thousand (per mil, ‰). I used both peach leaves ($\delta^{13}C$ and $\delta^{15}N$ = x and y, respectively, Standard Reference Material [SRM] No. 1547, n= 105, standard deviation [SD] of both $\delta^{13}C$ and $\delta^{15}N$ was =0.1‰) and bovine liver ($\delta^{13}C$ and $\delta^{15}N$ = x and y, respectively, SRM No. 1577, n=38, SD of both $\delta^{13}C$ and $\delta^{15}N$ was =0.1‰) as references and standards and to correct the stable isotope ratios for drift and linearly of the mass spectrometer.

Analysis

The $\delta^{13}C$ and $\delta^{15}N$ values of lipid-extracted samples were compared to those of untreated samples with paired t-tests to determine whether lipid extraction had the expected effect of making $\delta^{13}C$ less negative and $\delta^{15}N$ more variable.

The time course of isotopic incorporation after the diet shift was modeled with a one-compartment, first-order kinetics model:

$$\delta^h X_t = \delta^h X_\infty - (\delta^h X_\infty - \delta^h X_0)\, e^{(-t/\tau)}, \qquad \text{(Equation 2)}$$

where $\delta^h X_t$ is the stable isotope value at time (t), $\delta^h X_\infty$ is the estimate of the final stable isotope value when the predator tissue is in equilibrium with the new diet, $\delta^h X_0$ is the initial isotopic value, and τ is the average residence time or the time to equilibrate to the new diet (JMP v. 9.0, SAS Institute Inc., Cary, NC, USA). I chose a one-compartment incorporation model after first analyzing the data with the reaction progress model (Cerling *et al.* 2007), which determined that both muscle and hemolymph only exhibited one turnover compartment.

Many studies report average residence time (τ) as the fractional turnover rate or λ, where $\lambda = 1/\tau$. I report both λ and τ, but the model was calculated with τ because this parameter provides a measure of residence time in days (Carleton *et al.* 2008; Martínez del Rio & Anderson-Sprecher 2008). From τ, the isotopic half-life was calculated as $\ln(2)\tau$ (or $\ln(2)/\lambda$) for both muscle and hemolymph.

To determine whether aspects of mantis shrimp biology, such as sex and molting, significantly affected estimates of turnover time, I modified a random effects model presented in Lecompte *et al*. (2011), which treated intraspecific differences as random effects (R v. 2.15.0, R Development Core Team, The R Foundation for Statistical Computing, Vienna, Austria). Model fits were compared with AIC. These comparisons were made on the muscle data only, because the hemolymph dataset was too small for the model to converge on an answer. To illustrate how biological differences between individuals can impact model results, I also estimated the parameter values for all individuals and subsets of the data including just males, just females, and excluding individuals that molted at least once during the course of the study (R v. 2.11.0 and v. 2.15.0, R Development Core Team, The R Foundation for Statistical Computing, Vienna, Austria ; JMP v. 9.0, SAS Institute Inc., Cary, NC, USA).

Another biological parameter of interest that can be calculated from the turnover model is the diet-to-tissue discrimination factor. Discrimination factors were calculated for both isotopes from both muscle and hemolymph as:

$$\Delta^h = \delta^h X_{\infty\ stomatopod} - \delta^h X_{\ prey} \qquad \text{(Equation 3)}$$

where Δ^h is the discrimination factor for h stable isotope, $\delta^h X_{\infty\ stomatopod}$ is the estimated isotopic value of a stomatopod tissue in equilibrium with the prey and $\delta^h X_{\ prey}$ is the isotopic value of prey. Discrimination factors were also calculated for all individuals together, just males, and just females, and all animals excluding individuals that molted at least once during the course of the study.

Growth over the course of the experiment was measured by examining the change in mass and the change in carapace length. Significant changes in mass and carapace length were evaluated using a linear regression model (R v. 2.11.0 and v. 2.15.0, R Development Core Team, The R Foundation for Statistical Computing, Vienna, Austria). Following Hesslein et al. (1993), I also attempted to calculate the percent contributions of turnover to growth and metabolism for the individuals at the end of the experiment (day 292).

Results

Delipidification treatment

There were no significant differences between untreated and treated muscle tissue for either isotope in all *N. bredini* individuals ($\delta^{13}C$: mean difference = 0.1 ± 0.3 ‰, p=0.3, t_{43}=0.49, n=44; $\delta^{15}N$: mean difference = 0.1 ± 0.3 ‰, p = 0.75, t_{42}= 0.32, n = 43) and $\delta^{13}C$ in *T. funebralis* (mean difference: -0.0 ± 0.1 ‰, paired t-test: p=0.7, t_9=-0.40, n=10). However, significant differences were found in *N. bredini* individuals that had equilibrated with the new diet for $\delta^{13}C$ (mean difference = 0.4 ± 0.1 ‰, p=0.04, t_3=2.56, n=4) and in *T. funebralis* for $\delta^{15}N$ (mean difference: 0.2 ± 0.1 ‰, paired t-test: p=0.01, t_9=3.04, n=10).

***Discrimination* (Δ)**

Isotopic discrimination (**Δ**) between the new diet and *N. bredini's* tissues were much greater for $\delta^{13}C$ than for $\delta^{15}N$ (Fig. 2.1). This pattern was especially pronounced for $\delta^{13}C$ in muscle with **Δ** being 3.0 ± 0.6 ‰ (Table 2.1). None of the predators' isotope ratios overlapped with the mean ratio of the new diet (Fig 2.1). The $\delta^{13}C$ for hemolymph overlapped slightly with the mean prey ratio but **Δ** was still 1.7 ± 0.3 ‰ (Table 2.1, Fig 2.1). In contrast, $\delta^{15}N$ of muscle showed a small **Δ** (0.9 ± 0.3 ‰) and hemolymph showed no considerable **Δ** (0.1 ± 0.2 ‰; Table 2.1, Fig. 2.1). Even though both tissues appeared to equilibrate with the new diet (Fig 2.1), *N. bredini's* $\delta^{13}C$ values for both muscle and hemolymph never became more negative than the new diet (Fig 2.1). $\delta^{15}N$ in muscle surpassed the stable isotope value of the new diet and then showed slight **Δ** with the new diet (Fig. 2.1).

Differences between individuals within initial and final groups

At the beginning of the experiment, the individuals spanned a wide range of values (range: $\delta^{13}C$=-12.5 to -7.6 ‰, $\delta^{14}N$=6.9 to 8.7‰; Fig. 2.1) compared to the final day of the experiment (range: $\delta^{13}C$=-11.9 to -11.3, $\delta^{14}N$=10.9 to 11.4; Fig. 2.1). Muscle tissues reached relatively constant stable isotope values at around 127 days of the experiment (Fig. 2.1). When muscle tissues were at the asymptotic isotopic value, there were significant differences between individuals that did not molt and individuals that molted at least once throughout the experiment for both $\delta^{13}C$ (mean difference between molted and unmolted individuals ± SE = 1.3 ± 0.4 ‰; t-test: p=0.003, $t_{16.23}$=3.53, n=19) and $\delta^{15}N$ (mean difference ± SE = 1.0 ± 0.4 ‰; t-test: p=0.04, $t_{13.25}$= -2.23, n=19). Comparing initial stable isotope ratios between males and females revealed no significant differences for either stable isotope (mean difference between males and females ± SE for $\delta^{13}C$ and $\delta^{15}N$ = 0.6 ± 0.6 ‰ and 0.3 ± 0.18 ‰, respectively, $p \geq 0.05$, $t<2.43$, n=9). There were also no significant differences between the equilibrium values for females and males (mean difference ± SE for $\delta^{13}C$ and $\delta^{15}N$ = 0.6 ± 0.4 ‰ and -0.2 ± 0.5, respectively, $p \geq 0.05$, $t<1.10$, n=19 and n=9, respectively). These comparisons were only conducted for muscle tissues.

Tissue incorporation

A one-compartment non-linear model for incorporation fit to the untreated stable isotope ratios estimated incorporation rates and equilibrium δ-values for $\delta^{13}C$ and $\delta^{14}N$ (Table 2.1, Fig 2.1). As predicted, the incorporation rate of hemolymph was much faster than the incorporation rate of muscle, but the final equilibrium values were similar (Table 2.1, Fig. 2.1). Except for

$\delta^{14}N$ in hemolymph, the 95% confidence intervals from the models did not overlap with the mean value of the new diet.

Including sex and molting in the random effects model caused no change in the AIC scores for either stable isotope in muscle. However, estimates of average residence times and equilibrium values changed when molted individuals were included in the model and when the model was run on males and females separately (Suppl. Tables 2.1-2.2). Lower average residence times and equilibrium values were estimated when molted individuals were excluded from the model compared to when the model was run with all individuals (Suppl. Table 2.1, Suppl. Fig 2.1). Parameter estimates for males were much higher but lower for females compared to when all individuals were included in the model (Suppl. Fig 2.2). The 95% confidence intervals around the parameter estimates for males were large (Suppl. Fig 2.2). Isotopic half-life values were also different when calculated with all individuals, with just individuals that did not molt, with just males, and just females (Suppl. Table 2.2). Specifically, the half-lives of individuals that did not molt were much shorter for both isotopes in both tissues compared to the half-lives calculated from the whole dataset (Suppl. Table 2.2, Suppl. Fig 2.1). The female half-lives showed a similar pattern (Table 2.2, Suppl. Fig 2.2). However, for $\delta^{15}N$ in males, the half-life estimates were approximately 104 days for both tissues, which are considerably longer than all of other half-life values.

Growth and mortality

Change in carapace length over time was not significantly different from zero (linear regression: R^2=0.03 p=0.06, $F_{1,87}$=3.78, n=89; Fig. 2.2). Change in mass decreased slightly over time (linear regression: R^2=0.06, P=0.01, $F_{1,87}$=6.72, n=89; Fig. 2.2). However, there were no significant differences between mass before and after treatment (pair-wise t-test: mean difference: -0.005, P=0.38, t_{88}=-0.33, n=89). Given that the growth rate was essentially zero, I were unable to apply Hesslein et al.'s (1993) model to this dataset. Eight individuals (9%) did not survive for the duration of the experiment and were therefore not included in final analyses.

Discussion

Turnover rates of different substrates with different chemical composition are intimately linked to metabolic processes, which in turn can connect to many properties of an animal's life history such as body size, gender, age, etc. (Boecklen *et al.* 2011). I found that turnover rates of muscle in *N. bredini* were consistent with predicted values from other aquatic ectotherms based on body size. This finding suggests that for a given tissue type an overarching relationship exists between body size and turnover time across taxa. In addition, as with muscle and blood plasma in ectothermic vertebrates, *N. bredini* incorporated the new diet much more slowly in muscle compared to in hemolymph. Interestingly, a few of my results were contrary to the published findings for ectothermic vertebrates. First, delipidifying samples did not lead to significantly more enriched $\delta^{13}C$ values, which has been show for vertebrate tooth enamel and invertebrate calcium carbonate shells and exoskeleton (Bunn, Loneragan & Kempster 1995; Passey *et al.* 2005; Serrano *et al.* 2008; Kolasinski *et al.* 2011). Second, isotopic discrimination factors for both tissues were not in the usual 0 - 2 ‰ range for $\delta^{13}C$ nor around 3 ‰ for $\delta^{15}N$. Third, I had expected that the turnover rates of $\delta^{13}C$ and $\delta^{15}N$ would be similar within tissue type and were surprised to find the opposite result for hemolymph.

Delipidification treatment

In mantis shrimp, the only significant difference between samples from which lipids were removed and untreated samples was for $\delta^{13}C$ in equilibrated muscle tissue. However, the mean difference between treated and untreated samples was only 0.4 ± 0.1 ‰. Such a small difference is likely not biologically relevant, because the variation between initial and final stable isotope ratios is much greater (≥ 3 ‰; Fig 2.1). $\delta^{15}N$ values from delipidified *T. funebralis* muscle were significantly more enriched than treated samples. However, delipidification treatments should alter $\delta^{13}C$ ratios in tissues with high lipid contents (Mateo *et al.* 2008). This result suggests that the delipidification treatment may have damaged the proteins, instead of removing lipids from *T. funebralis* tissue (Mateo *et al.* 2008). Furthermore, I calculated the carbon to nitrogen elemental ratio (C:N) for both tissues, which was 3.5 (± 0.3 muscle, ± 0.4 hemolymph). This ratio corresponds to a tissue with a low lipid content, and therefore lipid removal was unlikely to effect isotopic values (see Post *et al.* 2007). Based on these results, I excluded the treated data from turnover analyses.

Differences in discrimination between $\delta^{13}C$ and $\delta^{15}N$

The current understanding of discrimination factors follows the convention that $\Delta^{13}C$ ranges from 0 to 1 ‰ and $\Delta^{15}N$ is about 3 ‰ (DeNiro & Epstein 1978; Minagawa & Wada 1984). The $\Delta^{13}C$ of 2 - 4 ‰ and $\Delta^{15}N$ of 0 - 1 ‰ measured here clearly counter this convention (Fig 2.3). Other animals show similar deviations from conventional discrimination values, and the idea that $\delta^{15}N$ bioaccumulates but $\delta^{13}C$ does not, is breaking down. For example, I compared the mantis shrimp discrimination factors to average literature values of 0.5 ± 0.1 for $\Delta^{13}C$ and 2.3 ± 0.2 for $\Delta^{15}N$ (Fig 2.3), which were calculated in McCutchan *et al.* (2003) from 111 taxa. Mantis shrimp had similar discrimination factors as the shrimp species, *Paneus vannemai*, for both isotopes, as pigs (*Sus scofra)* and locusts (*Locusta migritoria)* for the carbon isotope, which have $\Delta^{13}C$ between 2.6 and 2.8‰, and to blue crabs (*Callinecies sapidus*), red drum fish (*Sciaenops ocellatus),* and quail (*Corturnix japonica*) for the nitrogen isotope, which have $\Delta^{15}N$ between 0.9 and 1.0‰ (McCutchan *et al.* 2003 and referenced therein). Most of these literature values changed, however, depending on the food sources provided during experimentation (McCutchan *et al.* 2003). When fed zooplankton, *P. vannemai* exhibited discrimination factors that were similar to conventional values of discrimination (Dittel *et al.* 1997). Leopard sharks fed tilapia had a $\Delta^{15}N$ of 4 ‰, but when fed squid, this factor changed to one that ranged from 2 to 3 ‰ Kim *et al.* 2012). Similarly, whole body amphipods that consumed different macrophyte diets had discrimination factors ranging from -2 ‰ to -10 ‰ for $\Delta^{13}C$ and -1 ‰ to 3 ‰ for $\Delta^{15}N$ depending on diet (Crawley, Hyndes & Vanderklift 2007).

In light of this evidence, it appears that discrimination values are primarily driven by the type of food consumed rather than any emergent properties of the tissues. For example, the magnitude of difference between the new diet's stable isotope values and the consumer's equilibrium values is thought to influence discrimination values (McCutchan *et al.* 2003; Reich, Bjorndal & Martínez del Rio 2008). In turn, the equilibrium value is thought to be governed by the protein composition of the new diet, whereby high protein diets generally correspond to lower equilibrium values for $\delta^{15}N$ in taxa such as birds and mammals (Hobson, Alisauskas & Clark 1993; Robbins, Felicetti & Sponheimer 2005; Tsahar *et al.* 2008). In my experiment, mantis shrimp were fed snail muscle tissue, which has a high content of essential (and often limiting) amino acids (Zarai *et al.* 2011 and references there). I therefore hypothesize that the

low $\Delta^{15}N$ values found in mantis shrimp are the consequence of the high protein content (= high quality) of their experimental diet and the efficient use of such food.

The consumer's metabolic requirements are also thought to contribute to its equilibrium value (Martínez del Rio & Wolf 2005; Martinez del Rio *et al.* 2009). Large amounts of protein in the mantis shrimp diet may be important for sustaining this animal's active lifestyles of crushing hard shelled prey (Caldwell, Roderick & Shuster 1989), fighting with conspecifics (Caldwell & Dingle 1975), and swimming at high speeds from predators and competitors (Campos, Vilhena & Caldwell 2012). Performing these activities may require mantis shrimp to absorb all available nitrogen in the diet, thus yielding a low $\Delta^{15}N$. An important next step is to perform additional diet switch experiments on *N. bredini* with different prey items to test whether *N. bredini's* discrimination factors change with different quality diets.

The mechanism behind the high $\Delta^{13}C$ values documented here is more difficult to determine. High $\Delta^{13}C$ values can sometimes be attributed to high concentrations of calcium carbonate in invertebrate tissues, which is essentially an issue of contamination by inorganic C sources (Mateo *et al.* 2008). Mantis shrimp are known to sequester the calcium carbonate used to build exoskeleton in their soft tissues during the pre-molt period (Reaka 1975). However, most crustacean tissues, including exoskeleton, have very low carbonate contents, and in fact muscle tissue is thought to not contain any calcium carbonate (Yokoyama *et al.* 2005; Mateo *et al.* 2008). Thus, it is possible that the muscle tissue analyzed here did possess calcium carbonate, but given the lack of evidence for such an affect from other crustaceans, I suggest that further experiments be conduced to compare untreated mantis shrimp muscle to tissue from which carbonates were removed before this issue can be ruled out as underlying the high $\Delta^{13}C$ values I obtained.

Incorporation rates in muscle and hemolymph

The result showing that hemolymph $\delta^{15}N$ turned over in 29 days but $\delta^{13}C$ turned over in only 3 days (Table 2.1) suggests that hemolymph incorporates and releases carbon at faster rates than it incorporates and releases nitrogen. This finding deviates from most other studies, which show that both stable isotopes incorporate into tissues at similar rates (Pearson *et al.* 2003; Ogden, Hobson & Lank 2004; Dalerum & Angerbjörn 2005; Suring & Wing 2009; Lecomte *et al.* 2011; Kim *et al.* 2012). One exception is seen in the $\delta^{13}C$ and $\delta^{15}N$ turnover rates of temperate bass liver, which was very similar to mantis shrimp hemolymph and is also considered a "fast" tissue type (Suzuki *et al.* 2005). Thus, both of these "fast" tissues appear to exhibit differential resource use between carbon and nitrogen in metabolic processes.

The observed differences between turnover rates of $\delta^{13}C$ and $\delta^{15}N$ and the known impacts of intraspecific variation in life history traits (sex, size, age, molting or not) on turnover (Wyatt, Waite & Humphries 2010; Lecomte *et al.* 2011) led us to examine how differences among the animals that were included in this study could have affected parameter estimates from the turnover model. For example, including sex or the presence of molting during the experiment as random effects in the model caused no change in the AIC scores for either stable isotope. However, the parameter estimates from the turnover model did change when they were generated from subsets of the data, which were only males, only females, and only individuals that did not molt during the study (Suppl. Tables 2.1, 2.2; Suppl. Figs. 2.1, 2.2). For example, when the model was run on the whole muscle dataset, the average residence time ± standard error for $\delta^{13}C$ was 89.3 ± 44.4 days. In comparison, when individuals that molted during the study were excluded from the model, the average residence time for muscle $\delta^{13}C$ was 41.6 ± 26.6 days,

which is less than half as many days as when the model was run on the complete muscle dataset (Suppl. Tables 2.1, 2.2, Suppl. Fig 2.1). Thus, although the presence of molting did not significantly affect parameter estimates, running the model on this subset of the data changed the estimate of average residence time in ways that are biologically relevant. Said another way, if none of the individuals in this study had molted, then the average residence time would have been underestimated and my description of the time window that muscle represents would have been inaccurate. This example highlights the importance of running these models in more than one way (including or excluding known subsets of data that may have an affect) as a type of sensitivity analysis.

The physiological changes linked to molting could explain why the turnover model results changed when molted individuals were excluded from the model, because molting is tightly linked to arthropod growth and metabolism (Reaka 1975 and references therein; Reaka 1976). Molting occurs when an arthropod secretes new cuticle under the old exoskeleton, sheds the old exoskeleton, and then expands in size. These processes involve changes in the synthesis and degradation of glycogen and lipids throughout the molt cycle, which may change the overall metabolic replacement rate of tissues (Suring & Wing 2009).

A unique aspect of the mantis shrimp molting process is that mantis shrimp do not have a terminal molt (Reaka 1975). Instead, they continue to molt and grow as they age (Caldwell & Steger 1987). Interestingly, *N. bredini* individuals did not grow in the laboratory but they did continue to molt. *N. bredini* can therefore be used to study the degree to which turnover rates are affected by the aging process without growth as a covariate in the laboratory. Future studies specifically linking molting to estimates of incorporation rates and discrimination factors would greatly improve our understanding of the how ontogeny and molting affect tissue turnover.

The model estimates for males only and for females only were also quite unexpected (Table 2.3, Sup Fig 2.2). Specifically, the turnover model run on males only gave parameter estimates that differed greatly from any of the other models estimates (Table 2.2, 2.3, Sup Fig 2.2), likely because the dataset for males was relatively small (n=19), and because there were fewer males at the end of the experiment. While having fewer data points could have altered the model results for males, the estimates reported here are not too surprising, given known differences in resource allocation between male and female mantis shrimp (Caldwell 1991). Females have a high reproductive cost, because they devote a considerable amount of energy to egg production and maintenance (Caldwell 1991). In this study, females may have absorbed all protein in their diets in order to produce and maintain eggs, resulting in faster incorporation rates and lower discrimination factors for females compared to males (Suppl. Fig 2.2). These results are supported by recent findings in Artic foxes, which also show clear intraspecific differences between males and females for both turnover rate and discrimination factors (Lecomte *et al.* 2011). Together, these studies highlight a growing need for detailed research on differences in incorporation rates and discrimination factors between males and females.

Despite potential intraspecific differences in turnover rates, similarities between the turnover rates of *N. bredini* and other ecothermic vertebrates cannot be ignored. Martinez del Rio, *et al*. (2009) proposed that incorporations rates should correlate with body size, given the tight relationship between body size and metabolism (reviewed in Brown *et al.* 2004). Recent studies in ectothermic aquatic vertebrates have documented an allometric relationship between body size and incorporation rate, whereby tissues in small animals have higher incorporation rates than analogous tissues in large animals (Weidel *et al.* 2011; Kim *et al.* 2012). While *N. bredini's* biology and life history differs from ecothermic vertebrates, *N. bredini*'s incorporation

rates fall within the range of expected values based on the allometric relationship calculated in Weidel *et al*. (2011) (Fig. 2.4). This comparison suggests a relationship between turnover rate and body size that spans both vertebrate and invertebrate aquatic ectotherms and provides a foundation for addressing a general relationship between body size and turnover rate across animal taxa.

References

Bearhop, S., Adams, C.E., Waldrons, S., Fuller, R.A. & Macleod, H. (2004) Determining trophic niche width: a novel approach using stable isotope analysis. *Journal of Animal Ecology,* 73, 1007-1012.

Boecklen, W.J., Yarnes, C.T., Cook, B.A. & James, A.C. (2011) On the use of stable isotopes in trophic ecology. *Annual Review of Ecology, Evolution, and Systematics,* 42, 411-440.

Bond, A.L. & Diamond, A.W. (2011) Recent Bayesian stable-isotope mixing models are highly sensitive to variation in discrimination factors. *Ecological Applications,* 21, 1017-1023.

Brown, J.H., Gillooly, J.F., Allen, A.P., Savage, V.M. & West, G.B. (2004) Toward a metabolic theory of ecology. *Ecology,* 85, 1771-1789.

Buchheister, A. & Latour, R.J. (2010) Turnover and fractionation of carbon and nitrogen stable isotopes in tissues of a migratory coastal predator, summer flounder (Paralichthys dentatus). *Canadian Journal of Fisheries and Aquatic Sciences,* 67, 445-461.

Bunn, S.E., Loneragan, N.R. & Kempster, M.A. (1995) Effects of acid washing on stable isotope ratios of C and N in penaeid shrimp and seagrass: omplications for food-web studies using multiple stable isotopes. *Limnology and Oceanography,* 40, 622-625.

Caldwell, R.L. (1991) Variation in reproductive behavior in stomatopod Crustacea. *Crustacean Sexual Biology* (eds R. Bauer & J. Martin), pp. 67-90. Columbia University Press, New York.

Caldwell, R.L. & Dingle, H. (1975) Ecology and evolution of agonistic behavior in Stomatopods. *Naturwissenschaften,* 62, 214-222.

Caldwell, R.L., Roderick, G.K. & Shuster, S.M. (1989) Studies of predation by *Gonodactylus bredini*. *Biology of Stomatopods* (ed. E.A. Ferrero), pp. 117-131. Mucchi, Modena.

Caldwell, R.L. & Steger, R. (1987) Effects of May, 1986 oil spill on gonodactylid stomatopods near Galeta Point *Short-term assesment of an oil spill at Bahia Las Minas, Panama* (eds J.B.C. Jackson, J.D. Cubit, B.D. Keller, V. Batista, K. Burns, H.M. Caffey, R.L. Caldwell, S.D. Garrity, C.D. Getter, C. Gonzalez, H.M. Guzman, K.W. Kaufmann, A.H. Knap, S.C. Levings, M.J. Marshall, R. Steger, R.C. Thompson & E. Weil), pp. 113. Smithsonian Tropical Research Institute, Panama City

Campos, E.O., Vilhena, D. & Caldwell, R.L. (2012) Pleopod rowing is used to achieve high forward swimming speeds during the escape response of *Odontodactylus havanensis* (Stomatopoda). *Journal of Crustacean Biology,* 32, 171-179.

Carleton, S., Kelly, L., Anderson-Sprecher, R. & Martínez del Rio, C. (2008) Should we use one-, or multi- compartment models to describe ^{13}C incorporation into animal tissues? . *Rapid Communication in Mass Spectrometry,* 22, 3008-3014.

Carleton, S.A. & Martínez del Rio, C. (2005) The effect of cold-induced increased metabolic rate on the rate of and ^{15}N incorporation in house sparrows (*Passer domesticus*). *Oecologia,* 144, 226-232.

Caut, S., Angulo, E. & Courchamp, F. (2009) Variation in discrimination factors ($\Delta^{15}N$ and $\Delta^{13}C$): the effect of diet isotopic values and applications for diet reconstruction. *Journal of Applied Ecology,* 46, 443-453.

Cerling, T., Ayliffe, L., Dearing, M., Ehleringer, J., Passey, B., Podlesak, D., A.Torregrossa & West, A. (2007) Determining biological tissue turnover using stable isotopes: the reaction progress variable *Oecologia,* 151, 175-189.

Crawley, K.R., Hyndes, G.A. & Vanderklift (2007) Variation among diets in discrimination of $\delta^{13}C$ and $\delta^{15}N$ in the amphipod *Allorchestes compressa*. *Journal of Experimental Marine Biology and Ecology,* 349, 370-377.

Dalerum, F. & Angerbjörn, A. (2005) Resolving temporal variation in vertebrate diets using naturally occurring stable isotopes. *Oecologia,* 144, 647-658.

DeNiro, M.J. & Epstein, S. (1978) Influence of diet in the distribution of carbon isotopes in animals. *Geochimica Et Cosmochimica Acta,* 42, 495-506.

Dittel, A.I., Epifanio, C.E., Cifuentes, L.A. & Kirchman, D.L. (1997) Carbon and nitrogen sources for shrimp postlarvae fed natural diets from a tropical mangrove system. *Estuarine, Coastal and Shelf Science,* 45, 629-637.

Fisk, A.T., Sash, K., Maerz, J., Palmer, W., Carroll, J.P. & MacNeil, M.A. (2009) Metabolic turnover rates of carbon and nitrogen stable isotopes in captive juvenile snakes. *Rapid Communications in Mass Spectrometry,* 23, 319-326.

Fry, B. (2006) *Stable Isotope Ecology*. Springer Science + Business Media, New York, NY.

Fry, B. & Arnold, C. (1982) Rapid $^{13}C/^{12}C$Turnover During Growth of Brown Shrimp (*Penaeus aztecus*). *Oecologia,* 54, 200-204.

Graham, B.S., Koch, P.L., Newsome, S.D., McMahon, K.W. & Aurioles, D. (2010) Using isoscapes to trace the movements of and foraging behavior of top predators in oceanic ecosystems. *Isoscapes: Understanding Movement, Pattern, and Process on Earth Through Isoscape Mapping* (eds J.B. West, G.J. Bowen, T.E. Dawson, & K.P. Tu). Springer, New York, NY.

Guelinckx, J., Maes, J., Van Den Driessche, P., Geysen, B., Dehairs, F. & Ollevier, F. (2007) Changes in $\delta^{13}C$ and $\delta^{15}N$ in different tissues of juvenile sand goby *Pomatoschistus minutus*: a laboratory diet-switch experiment. *Marine Ecology Progress Series,* 341, 205-215.

Hesslein, R.H., Hallard, K.A. & Ramlal, P. (1993) Replacement of sulfer, carbon, and nitrogen in tissues of growing broad whitefish (Coregonus asus) in response to a change in diet traced by $\delta^{34}S$, $\delta^{13}C$, and $\delta^{15}N$. *Canadian Journal of Fisheries and Aquatic Science,* 10, 2071-2076.

Hobson, K.A., Alisauskas, R.T. & Clark, R.G. (1993) Stable-nitrogen isotope enrichment in avian tissues due to fasting and nutritional stress: implications for isotopic analyses of diet. *The Condor,* 95, 388-394.

Hobson, K.A. & Clark, R.G. (1992) Assessing avian diets using stable isotope analysis I, turnover of ^{13}C in tissues. *The Condor,* 1, 181-188.

Hobson, K.A. & Clark, R.G. (1993) Turnover of ^{13}C in Cellular and Plasma Fractions of Blood: Implications for Nondestructive Sampling in Avian Dietary Studies. *The Auk,* 110, 638-641.

Kim, S.L., Martínez del Rio, C., Casper, D. & Koch, P.L. (2012) Isotopic incorporation rates for shark tissues from a long-term captive feeding study. *Journal of Experimental Biology,* 215, 2495-2500.

Kolasinski, J., Rogers, K., Cuet, P., Barry, B. & Frouin, P. (2011) Sources of particulate organic matter at the ecosystem scale: stable isotope and trace element study in a tropical coral reef. *Marine Ecology Progress Series,* 443, 77-93.

Lecomte, N., Ahlstrøm, Ø., Ehrich, D., Fuglei, E., Ims, R. & Yoccoz, N. (2011) Intrapopulation variability shaping isotope discrimination and turnover: experimental evidence in Artic foxes. *PloS ONE,* 6, e21357.

Manning, R.B. (1969) *Stomatopod Crustacea of the Western Atlantic*. University of Miami Press, Coral Gables, FL.

Martínez del Rio, C. & Anderson-Sprecher, R. (2008) Beyond the reaction progress variable: the meaning and significance of isotopic incorporation data. *Oecologia,* 156, 765-772.

Martínez del Rio, C., Anderson-Sprecher, R., Gonzalez, P. & Sabat, P. (2009) Dietary and isotopic specialization: the niche of three Cinclodes ovenbirds. *Oecologia,* 161, 149-159.

Martínez del Rio, C. & Wolf, B.O. (2005) Mass balance models for animal isotopic ecology. *Physiological and Ecological Adaptations to Feeding in Vertebrates* (eds M.A. Starck & T. Wang), pp. 141-174. Science Publishers, Enfield, New Hampshire.

Martinez del Rio, C., Wolf, N., Carleton, S. & Gannes, L.Z. (2009) Isotopic ecology ten years after a call for more laboratory experiments. *Biological Review Cambridge Philosophical Society,* 84, 91-111.

Mateo, M.A., Serrano, O., Serrano, L. & Michener, R.H. (2008) Effects of sample preparation on stable isotope ratios of carbon and nitrogen in marine invertebrates: implications for food web studies using stable isotopes. *Oecologia,* 157, 105-115.

McCutchan, J.H., Jr., Lewis, W.M., Jr., Kendall, C. & McGrath, C.C. (2003) Variation in trophic shift for stable isotope ratios of carbon, nitrogen, and sulfur. *Oikos,* 102, 378-390.

Minagawa, M. & Wada, E. (1984) Stepwise enrichment of ^{15}N along food-chains -further evidence and the relation between $\delta^{15}N$ and animal age. *Geochimica Et Cosmochimica Acta,* 48, 1135-1140.

Murray, I.W. & Wolf, B.O. (2012) Tissue Carbon Incorporation Rates and Diet-to-Tissue Discrimination in Ectotherms: Tortoises Are Really Slow. *Physiological and Biochemical Zoology,* 85, 96-105.

Newsome, S.D., Martínez del Rio, C., Bearhop, S. & Phillips, D.L. (2007) A niche for isotope ecology. *Frontiers in Ecology and the Environment,* 5, 429-439.

Ogden, L.E., Hobson, K.A. & Lank, D.B. (2004) Blood isotopic ($\partial^{13}C$ and $\partial^{15}N$) turnover and diet-tissue fractionation factors in captive dunlin (*Calidris alpina pacifica*). *The Auk,* 121, 170-117.

Olive, P.J.W., Pinnegar, J.K., Polunin, N.V.C., Richards, G. & Welch, R. (2003) Isotope trophic-step fractionation: a dynamic equalibrium model. *Journal of Animal Ecology,* 72, 608-617.

Passey, B., Robinson, T.F., Ayliffe, L., Cerling, T., Sponheimer, M., Dearing, M.D., Roeder, B.L. & Ehleringer, J.R. (2005) Carbon isotope fractionation between diet, breath CO_2, and bioapatite in different mammals. *Journal of Archaeological Science,* 32, 1459-1470.

Patek, S.N. & Caldwell, R.L. (2005) Extreme impact and cavitation forces of a biological hammer: strike forces of the peacock mantis shrimp (*Odontodactylus scyllarus*). *Journal of Experimental Biology,* 208, 3655-3664.

Patek, S.N., Korff, W.L. & Caldwell, R.L. (2004) Deadly strike mechanism of a mantis shrimp. *Nature,* 428, 819-820.

Pearson, S.F., Levey, D.J., Greenburg, C.H. & Martínez del Rio, C. (2003) Effects of elemental composition on the incorporation of dietary nitrogen and carbon isotopic signatures in an omnivourous songbird. *Oecologia,* 135, 516-523.

Podlesak, D., McWilliams, S.R. & Hatch, K.A. (2005) Stable isotopes inbreath, blood, feces and feathers can indicate intra-individual changes in the diet of migratory songbirds. *Oecologia,* 142, 501-510.

Post, D.M., Layman, C.A., Arrington, D.A., Takimoto, G., Quattrochi, J. & Montaña, C.G. (2007) Getting to the fat of the matter: models, methods and assumptions for dealing with lipids in stable isotope analyses. *Oecologia,* 152, 179-189.

Reaka, M.L. (1975) Molting in stomatopod crustaceans. 1. Stages of molt cycle, setagenesis, and morphology. *Journal of Morphology,* 146, 50-80.

Reaka, M.L. (1976) Lunar and tidal periodicity of molting and reproduction in stomatopod crustacea: a selfish herd hypothesis. *Biological Bulletin,* 150, 468-490.

Reich, K.J., Bjorndal, K.A. & Martínez del Rio, C. (2008) Effects of growth and tissue type on the kinetics of ^{13}C and ^{15}N incorporation in a rapidly growing ectotherm. *Oecologia,* 155, 651-658.

Risk, M.J. & Erdmann, M.V. (2000) Isotopic composition of nitrogen in stomatopod (Crustacea) tissues as an indicator of human sewage impacts on Indonesian coral reefs. *Marine Pollution Bulletin,* 40, 50-58.

Robbins, C.T., Felicetti, L.A. & Sponheimer, M. (2005) The effect of dietary protien quality on nitrogen isotope discrimination in mammals and birds. *Oecologia,* 144, 534-540.

Serrano, O., Serrano, L., Mateo, M.A., Colombini, I., Chelazzi, L., Gagnarli, E. & Fallaci, M. (2008) Acid washing effect on elemental and isotopic composition of whole beach arthropods: Implications for food web studies using stable isotopes. *Oecologia,* 34, 89-96.

Sponheimer, M., Robinson, T.F., Ayliffe, L., Passey, B., Roeder, B.L., Shipley, L., Lopez, E., Cerling, T., Dearing, M.D. & Ehleringer, J. (2003) An experimental study of carbon-isotope fractionation between diet, hair, and feces of mammalian herbivores. *Canadian Journal of Zoology,* 81, 871-876.

Suring, E. & Wing, S.R. (2009) Isotopic turnover rate and fractionation in multiple tissues of red rock lobster (*Jasus edwardsii)* and blue cod (*Parapercis colias*): Consequences for ecological studies. *Journal of Marine Biology and Ecology,* 370, 56-63.

Suzuki, K., Kasai, A., Nakayama, K. & Tanaka, M. (2005) Differential isotopic enrichment and half-life amoung tissues in Japanese temperate bass (*Lateolabrax japonicus*) juveniles: implications for analyzing migration. *Canadian Journal of Fisheries and Aquatic Science,* 62, 671-678.

Tieszen, L.L., Boutton, T.W., Tesdahl, K.G. & Slade, N.A. (1993) Fractionation and turnover of stable carbon isotopes in animal tissues: implications for $\delta^{13}C$ analysis of diet. *Oecologia,* 57, 32-37.

Trueman, C.N., McGill, R.A.R. & Guyard, P.H. (2005) The effect of growth rate on tissue-diet isotopic spacing in rapidly growing animals. An experimental study with Atlantic salmon (*Salmo salar*). *Rapid Communication in Mass Spectrometry,* 19.

Tsahar, E., Wolf, N., Izhaki, I., Arad, Z. & Martínez del Rio, C. (2008) Dietary protein influences the rate of ^{15}N incorporation in blood cells and plasma of Yellow-vented bulbuls (*Pycnonotus xanthopygos)*. *Journal of Experimental Biology,* 211, 459-465.

Vander Zaden, J.M. & Rasmussen, J.B. (2001) Variation in δ15N and δ13C trophic fractionation: implications for aquatic food web studies. *Limnology and Oceanography,* 46, 2061-2066.

Warne, R.W., Gilman, C.A. & Wolf, B.O. (2010) Tissue-Carbon Incorporation Rates in Lizards: Implications for Ecological Studies Using Stable Isotopes in Terrestrial Ectotherms. *Physiological and Biochemical Zoology,* 83, 608-617.

Weidel, B.C., Carpenter, S.R., Kitchell, J.F. & Vander Zaden, J.M. (2011) Rates and components of carbon turnover in fish and muscle: insights from bioenergetics models and a whole-lake ^{13}C addition. *Canadian Journal of Fish Aquatic Science,* 68, 387-399.

Wyatt, A.S., Waite, A.M. & Humphries, S. (2010) Variability in isotope discrimination factors in coral reef fishes: implications for diet and food web reconstruction. *PloS ONE,* 5, e13682.

Yokoyama, H., Tamaki, A., Harada, K., Shimoda, K., Koyama, K. & Ishihi, Y. (2005) Variability of diet-tissue isotopic fractionation in estuarine macrobenthos. . *Marine Ecology Progress Series,* 296, 115-128.

Zarai, Z., Frikha, F., Balti, R., Miled, N., Gargouri, Y. & Mejdoub, H. (2011) Nutrient composition of the marine snail (*Hexaplex trunculus*) from the Tunisian Mediterranean coasts. *Journal of the Science of Food and Agriculture,* 91, 1265-1270.

Table

Table 2.1. Model parameters (average residence time, final equilibrium isotope value, and the difference between the initial and final isotope values) ± standard error of carbon and nitrogen stables isotope ratios for muscle and hemolymph calculated from Equation 2. Fractional turnover rates ($days^{-1}$) calculated from $\lambda=1/\tau$, half lives (days), and discrimination values are also presented. M=muscle tissue, H= hemolymph tissue, C= the carbon isotope ($\delta^{13}C$), N=the nitrogen isotope ($\delta^{15}N$), n=sample size, * = P< 0.001.

Tissue	Isotope	n	Residence time τ (days)	Equilibrium value δ_∞ (‰)	Initial-final value $\delta_\infty - \delta_0$ (‰)	R^2 for model fit	Fractional turnover rate λ ($days^{-1}$)	Half-life (days)	Discrimination Δ (‰)
M	C	92	89.3 ± 44.4	-12.2 ± 0.6	-2.8 ± 0.5	0.39*	0.011 ± 0.006	61.9 ± 30.8	3.0 ± 0.6
M	N	92	72.8 ± 18.8	10.9 ± 0.3	3.0 ± 0.30	0.67*	0.014 ± 0.004	50.4 ± 13.0	0.9 ± 0.3
H	C	61	3.4 ± 1.4	-13.3 ± 0.2	-3.0 ± 0.6	0.33*	0.293 ± 0.150	2.4 ± 1.2	1.7 ± 0.3
H	N	63	28.9 ± 8.3	9.9 ± 0.2	3.3 ± 0.3	063*	0.035 ± 0.010	20.0 ± 5.7	0.1 ± 0.2

Figure Legends

Figure 2.1. $\delta^{13}C$ (A, B) and $\delta^{15}N$ (C, D) stable isotope ratios for muscle (A, C) and hemolymph (B, D) were fit with a one-compartment model of turnover, where solid lines are the model fits for each tissue and stable isotope, dotted lines are the mean stable isotope ratios of the new diet and grey shaded areas show the 95% confidence intervals for the model fits. To illustrate intraspecific variation in stable isotope values, grey symbols represent individuals that did not molted during the study, black symbols represent individuals that molted at least once during the study, circles represent females, and triangles represent males. For R^2 values of the model fits, see Table 2.1.

Figure 2.2. Growth for the duration of the study was examined by measuring the change in carapace length (A) and the change in mass (B) over time. Changes were calculated by subtracting the carapace length or mass at the beginning of the experiment from the length or mass measured on the day that each individual was sampled. Linear regression models were fit to both the change in length and mass of the individuals over time, but only the regression model for the significant relationship is shown (solid line in B; for detailed statistics, see results section).

Figure 2.3. Discrimination (Δ) factors for *N. bredini* are presented, along with a mean literature Δ factor that was calculated in McCutchan *et al*., 2003 from 111 taxa. Δ factors for *N. bredini* were calculated by subtracting the mean stable isotope ratio of the prey from *N. bredini's* estimated equilibrium value, which was derived from the one-compartment turnover model (see Table 2.1). For both ^{13}C (A) and ^{15}N (B), black bars are the mean Δ factors from the literature, dark grey bars are hemolymph Δ, and light grey bars are muscle Δ. Numeric values for each Δ factor are listed on the frequency bars. Error bars represent standard error.

Figure 2.4. The carbon incorporation rates (represented as fractional turnover rate, λ) for mantis shrimp muscle in this experiment (black circle) are within the 95% confidence intervals (dotted lines) of the allometric relationship (solid line) derived by Weidel *et al*. (2011; open circles) and confirmed by Kim *et al*. (2012; grey circles). Error bars are standard error and are only shown for mantis shrimp, because λ for mantis shrimp was calculated from the turnover model using all individuals together, unlike the shark study in which each data point above is the λ for a different individual. A combination of both means and individual values was used to calculate λ in Weidel, *et al*. (2011) but standard errors are not shown for visual clarity.

Figures

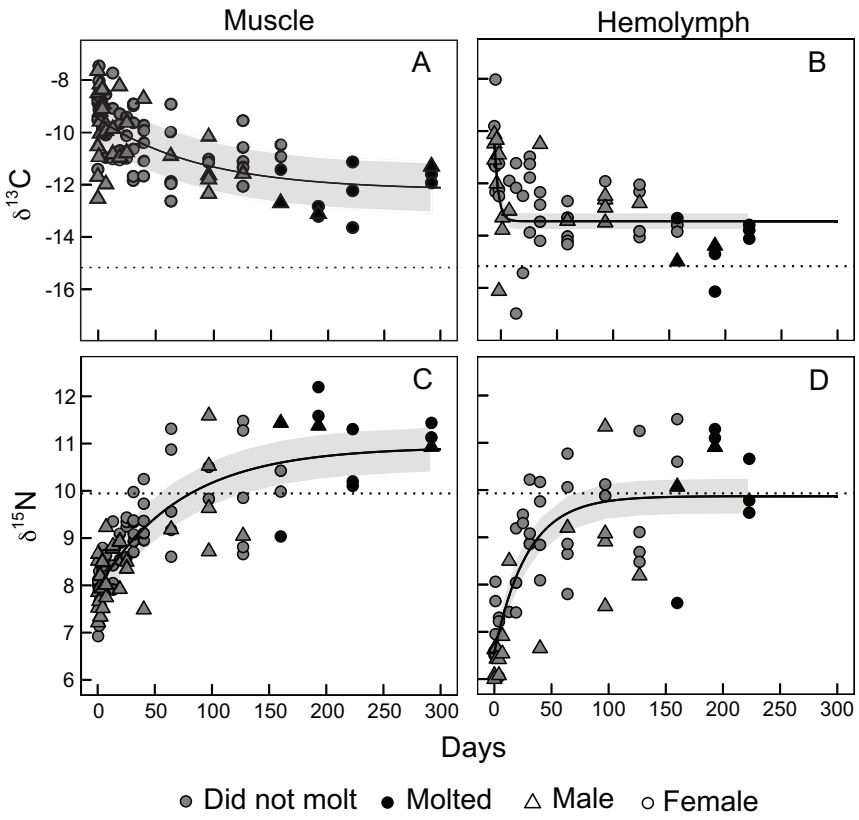

Figure 2.1. $\delta^{13}C$ (A, B) and $\delta^{15}N$ (C, D) stable isotope ratios for muscle (A, C) and hemolymph (B, D) were fit with a one-compartment model of turnover, where solid lines are the model fits for each tissue and stable isotope, dotted lines are the mean stable isotope ratios of the new diet and grey shaded areas show the 95% confidence intervals for the model fits. To illustrate intraspecific variation in stable isotope values, grey symbols represent individuals that did not molted during the study, black symbols represent individuals that molted at least once during the study, circles represent females, and triangles represent males. For R^2 values of the model fits, see Table 2.1.

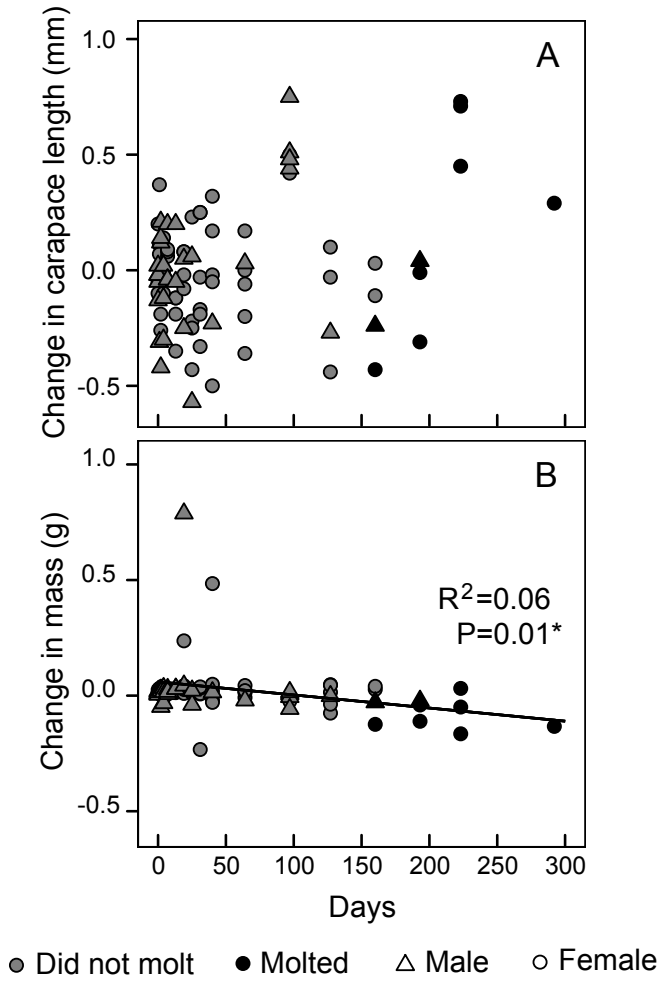

Figure 2.2. Growth for the duration of the study was examined by measuring the change in carapace length (A) and the change in mass (B) over time. Changes were calculated by subtracting the carapace length or mass at the beginning of the experiment from the length or mass measured on the day that each individual was sampled. Linear regression models were fit to both the change in length and mass of the individuals over time, but only the regression model for the significant relationship is shown (solid line in B; for detailed statistics, see results section).

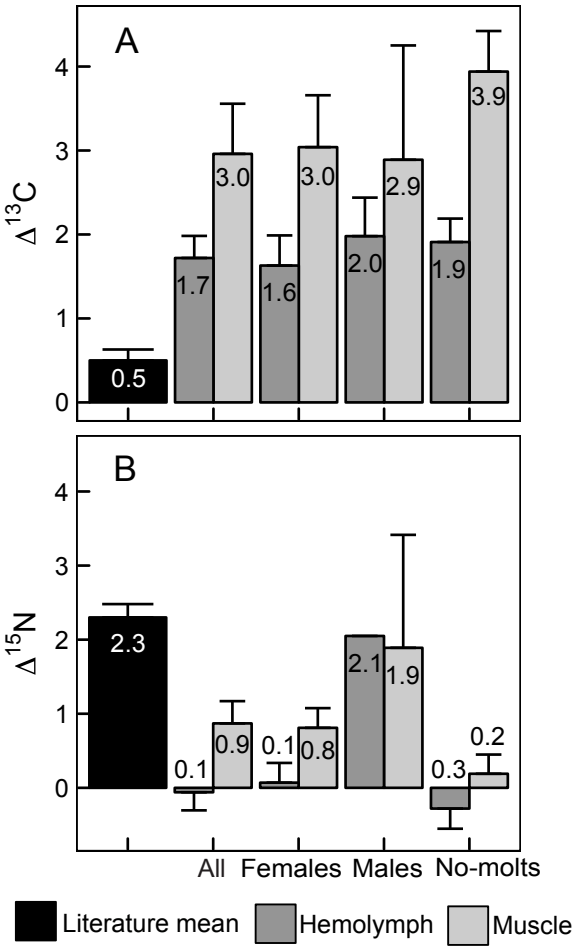

Figure 2.3. Discrimination (Δ) factors for *N. bredini* are presented, along with a mean literature Δ factor that was calculated in McCutchan *et al*., 2003 from 111 taxa. Δ factors for *N. bredini* were calculated by subtracting the mean stable isotope ratio of the prey from *N. bredini's* estimated equilibrium value, which was derived from the one-compartment turnover model (see Table 2.1). For both ^{13}C (A) and ^{15}N (B), black bars are the mean Δ factors from the literature, dark grey bars are hemolymph Δ, and light grey bars are muscle Δ. Numeric values for each Δ factor are listed on the frequency bars. Error bars represent standard error.

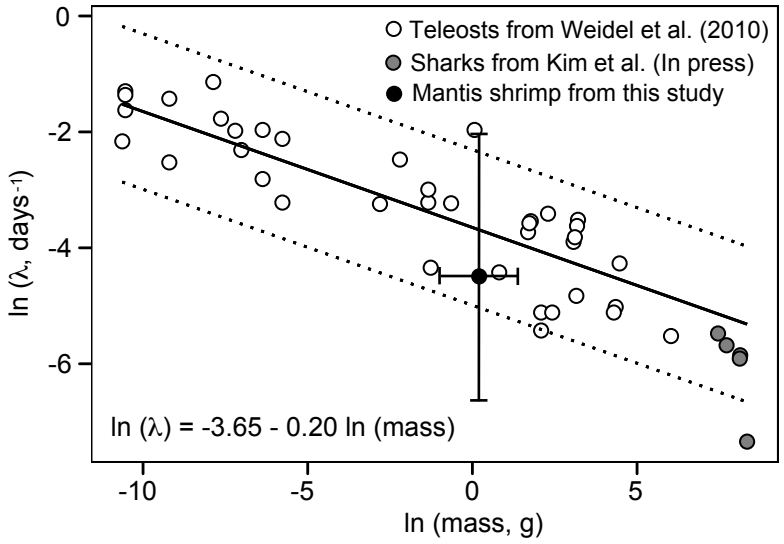

Figure 2.4. The carbon incorporation rates (represented as fractional turnover rate, λ) for mantis shrimp muscle in this experiment (black circle) are within the 95% confidence intervals (dotted lines) of the allometric relationship (solid line) derived by Weidel *et al*. (2011; open circles) and confirmed by Kim *et al*. (2012; grey circles). Error bars are standard error and are only shown for mantis shrimp, because λ for mantis shrimp was calculated from the turnover model using all individuals together, unlike the shark study in which each data point above is the λ for a different individual. A combination of both means and individual values was used to calculate λ in Weidel, *et al*. (2011) but standard errors are not shown for visual clarity.

Supplementary Material

Supplementary Table 2.1. A comparison of model parameters (average residence time, final equilibrium isotope value, and the difference between the initial and final isotope values) ± standard error of carbon and nitrogen stables isotope ratios for muscle and hemolymph with all individuals and model parameters excluding individuals that molted during the study. Columns labeled "All" signify the model parameters calculated with the whole data set including the individuals that molted at least once during the study. The columns labeled "No Molts" signify the model parameters calculated without the individuals that molted. Mean differences between estimates generated in the presence of and in the absence of molting are only given for average residence time because this is the only parameter for which the mean difference seemed biologically relevant. Models for males and females are not shown, because sample sizes for males and females only were small. For limited information on males and females, see Supplementary Table 2.2. M=muscle tissue, H= hemolymph tissue, C= the carbon isotope ($\delta^{13}C$), N=the nitrogen isotope ($\delta^{15}N$), n=sample size, * = P< 0.001.

		Residence time τ (days)			Equilibrium value δ_∞ (‰)		Initial-final value $\delta_\infty - \delta_0$ (‰)	
Tissue	Isotope	All	No molt	Mean difference	All	No Molt	All	No Molt
M	C	89.3 ± 44.4 n=92	41.6 ± 26.6 n=81	47.8 ± 35.6	-12.2 ± 0.6	-11.2 ± 0.5	-2.8 ± 0.5	-1.9 ± 0.5
M	N	72.8 ± 18.8 n=92	37.9 ± 11.1 n=81	34.9 ± 15.1	10.9 ± 0.3	10.1 ± 0.3	3.0 ± 0.3	2.3 ± 0.3
H	C	3.4 ± 1.7 n=61	2.9 ± 1.6 n=53	0.5 ± 0.6	-13.3 ± 0.2	-13.0 ± 0.2	-3.0 ± 0.6	-2.7 ± 0.6
H	N	28.9 ± 8.3 n=63	23.6 ± 7.6 n=55	5.3 ± 3.4	9.9 ± 0.2	9.7 ± 0.3	3.3 ± 0.3	3.1 ± 0.3

Supplementary Table 2.2. Fractional turnover rates ($days^{-1}$) calculated from $\lambda=1/\tau$ and half lives (days) for all individuals (All), individuals excluding individuals that molted during the study (No Molt), males only, and females only. M=muscle, H=hemolymph, C= carbon isotope ($\delta^{13}C$), N= nitrogen isotope ($\delta^{15}N$).

Tissue	Isotope	Fractional turnover rate λ ($days^{-1}$)				Half-life (days)			
		All	No molt	Males*	Females	All	No molt	Males*	Females
M	C	0.01 ± 0.006	0.02 ± 0.015	0.01 ± 0.01, n=31	0.01 ± 0.007, n=61	61.9 ± 30.8	28.8 ± 18.5	68.6 ± 74.5	56.2 ± 30.8
M	N	0.01 ± 0.004	0.03 ± 0.008	0.007 ± 0.005, n=31	0.02 ± 0.005, n=61	50.4 ± 13.0	26.3 ± 7.7	104.8 ± 73.2	38.2 ± 10.2
H	C	0.29 ± 0.150	0.34 ± 0.19	0.44 ± 0.38, n=19	0.45 ± 0.37, n=44	2.4 ± 1.2	2.0 ± 1.1	1.6 ± 1.4	1.5 ± 1.3
H	N	0.04 ± 0.010	0.04 ± 0.01	0.007 ± 0.008, n=19	0.04 ± 0.01, n=44	20.0 ± 5.7	16.3 ± 5.2	104.4 ± 121.4	19.8 ± 6.3

* Estimates may be inaccurate, because only 3 males were sampled at the end of the study.

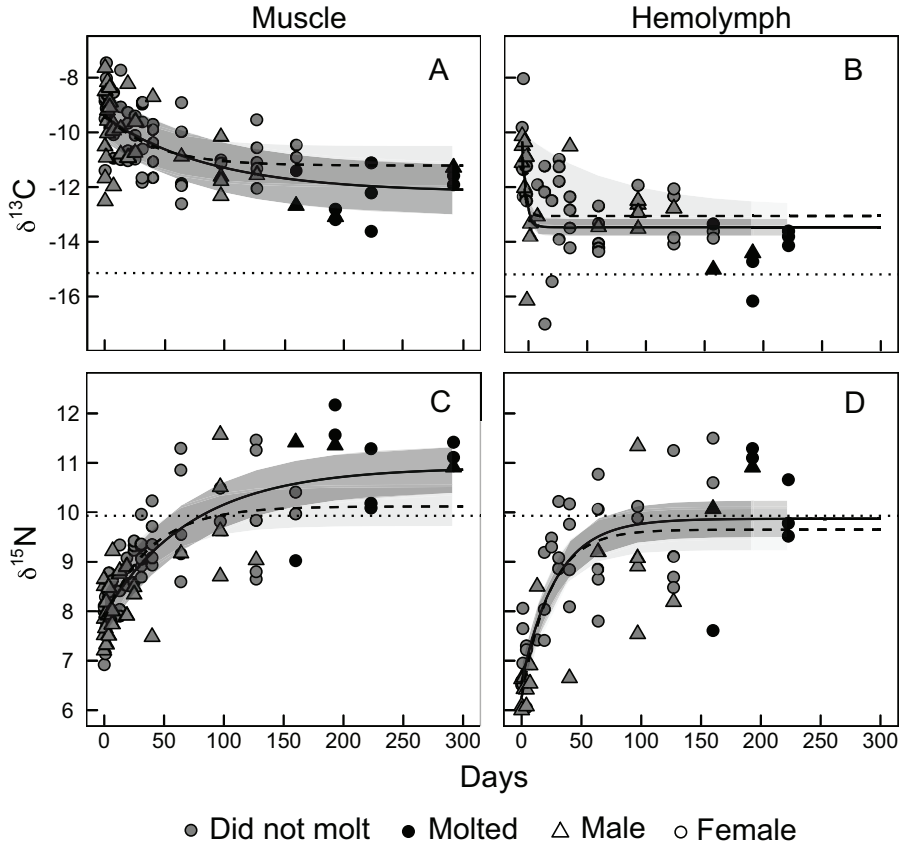

Supplementary Figure 2.1. $\delta^{13}C$ (A, B) and $\delta^{15}N$ (C, D) stable isotope ratios for muscle (A, C) and hemolymph (B, D) were fit with one-compartment models run for all individuals (solid line) and excluding individuals that molted during the study (dashed line). For muscle, the model results changed when molts were excluded from the analysis, as is evident from the 95% confidence intervals, shaded in grey for all individuals and light grey for the molted individuals, which do not show much overlap. The dark grey area shows overlap of the two confidence intervals. The dark grey area is especially small for the $\delta^{15}N$ of muscle, suggesting that the model results are especially different for this tissue and isotope. For hemolymph, the model results were similar when run with and without molted individuals. Specifically, for $\delta^{13}C$, the confidence intervals for the model excluding molted individuals were large; thus, it may not be possible to resolve the differences between these two models for this isotope and tissue. Dotted lines are the mean stable isotope ratios of the new diet.

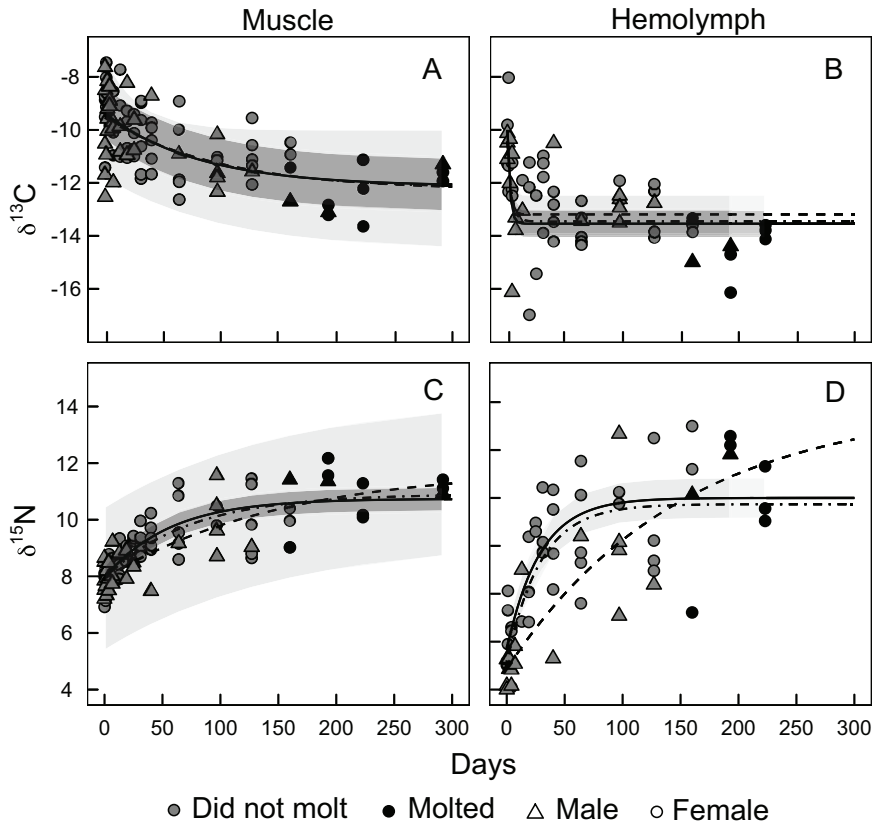

Supplementary Figure 2.2. $\delta^{13}C$ (A, B) and $\delta^{15}N$ (C, D) stable isotope ratios for muscle (A, C) and hemolymph (B, D) were fit with one-compartment models run on females only (solid line, 95% confidence intervals shown as grey shaded area), on males only (dashed line, 95% confidence intervals shown as light grey shaded area). The model fit to all of the data is also shown (dotted-dashed line). Overlap of the confidence intervals is shown in dark grey. For $\delta^{13}C$, the model results are similar. However, for $\delta^{15}N$ in both tissues, males did not appear to equilibrate with the new diet, which is why the predications of average residence time are both very long at approximately 104 days. The 95% confidence intervals for the models run on males are also large (not shown for $\delta^{15}N$ in hemolymph, because they were too large). The result that males may not have equilibrated with the new diet is especially apparent in in the hemolymph results, because the male trend line does not appear to asymptote and it extends far beyond those for females and all individuals. This trend is present in the male muscle data as well; on close inspection, the trend line is beginning to curve upwards, which, if plotted over more days, would likely also extend past the other two lines. Though, it must be noted that the dataset for males is relatively small (n=19), and there were also fewer males at the end of the experiment. The model is known to perform poorly at smaller sample sizes (Martínez del Rio & Anderson-Sprecher 2008). Thus, it is possible that the long half-lives in males are a result of under-sampling. Grey lines are the mean stable isotope ratios of the new diet.

Chapter III

Specialized morphology corresponds to a generalist diet: linking form and function in mantis shrimp crustaceans

Key words: stable isotopes, Bayesian mixing model, sea grass, coral rubble, predation

Abstract

Animals with specialized feeding morphology are generally thought to consume very specific prey types. Mantis shrimp are a group of crustaceans with raptorial appendages that are specialized for generating high forces for hammering hard-shelled prey. However, anecdotal observations suggest that mantis shrimp are not limited to consuming only hard-shelled prey. The goal of this study was to examine the diet of the mantis shrimp, *Neogonodactylus bredini,* to determine if it consumes both hard- and soft-bodied prey. To describe *N. bredini*'s diet, I combined abundance studies of prey items, a laboratory feeding experiment that examined which prey *N. bredini* would consume, a stable isotope analysis of diet, and field observations of feeding behavior. I conducted and compared these studies in a sea grass habitat and a coral rubble habitat in Panama over two different seasons to determine whether diet changed spatially and temporally. The abundance study revealed that prey abundances vary between habitats. The feeding experiment showed that *N. bredini* was capable of consuming both hard- and soft-bodied prey. The stable isotope analysis showed that *N. bredini* consumed a wide range of different prey in the field, including snapping shrimp and worms. The proportional contributions of prey items to the diet changed between habitats in the wet season. In coral rubble, *N. bredini* consumed all prey items in equal proportions, whereas in sea grass, the greatest proportion of the diet was clams (*Arcopsis adamsi)* and alpheid shrimp (*Alpheus spp)*. While more limited, the results from the seasonal comparison suggested that diet was broader in the wet season than in the dry season. In contrast with the hypothesis that specialized feeding morphology should correspond to a specialized diet, this suite of observations and experiments demonstrate that *N. bredini* has a broad diet consisting of both hard- and soft-bodied prey.

Introduction

A foundational tenet in animal ecology is that species with specialized feeding morphology consume very specific prey types (Darwin 1859; Wainwright & Reilly 1994). The powerful seed-crushing beak of the Galapagos finch (Grant & Grant 1993) and the long nectar-sucking proboscis of the hawkmoth (Darwin 1862) provide classic examples of the tight link between feeding morphology and ecology. Understanding this relationship has provided insight into the ecological and evolutionary processes that produced the vast morphological diversity

seen across organisms and that underlie community structure (Van Valen 1965; Futuyma & Moreno 1988; Wainwright & Reilly 1994; Ferry-Graham, Bolnick & Wainwright 2002). For example, the variety of beak forms seen in Galapagos finches directly relates to competition for available food resources (Grant & Grant 1993). Consumers that exhibit this tight link between morphology and diet have been categorized as *functional specialists*, because their morphology limits them to a subset of available resources (Ferry-Graham, Bolnick & Wainwright 2002).

Mantis shrimp (Stomatopoda: Crustacea) are another group of organisms often touted as being functional specialists; their raptorial appendages produce among the fastest and most powerful strikes in the animal kingdom, allowing mantis shrimp to crush hard-shelled prey (Caldwell & Dingle 1976; Patek, Korff & Caldwell 2004; Patek & Caldwell 2005). Mantis shrimp achieve these fast, powerful strikes through a series of springs, latches, and linkages in the raptorial appendage that store elastic energy in the appendage's exoskeleton and then release the energy over very short time windows (Burrows 1969; Patek, Korff & Caldwell 2004; Patek & Caldwell 2005; Zack, Claverie & Patek 2009; Claverie, Chan & Patek 2011; deVries, Murphy & Patek 2012). Mantis shrimp species that produce such impressive strikes are categorized as "*smashers*," because they use hammer-like clubs at the base of their appendages to deliver powerful blows to their prey (Caldwell & Dingle 1976, Patek, Korff & Caldwell 2004; Patek & Caldwell 2005). The ability of smashers to produce high-impact strikes has been hypothesized to correspond to a specialized diet of hard-shelled molluscs, hermit crabs, and crabs (Caldwell & Dingle 1976; Dingle & Caldwell 1978; Caldwell, Roderick & Shuster 1989; Full, Caldwell & Chow 1989). There are, however, observations of some smasher species capturing evasive, soft-bodied prey items such as thalassid shrimp, amphipods, and worms (Dominguez & Reaka 1988; Caldwell, Roderick & Shuster 1989). Although smasher diets still remain largely unknown, these observations indicate that smashers have a more diverse diet than previously considered, suggesting that morphological specialization for speed and acceleration does not necessarily correspond to diet specialization in this group of animals. Here, I study the diet breadth of a smashing species to determine if it is limited to hard-shelled prey. I then relate these findings to raptorial appendage morphology and consider how a smasher's diet influences the trophic ecology of the coral reef communities in which mantis shrimp live.

Investigating correlations between diet breadth and feeding morphology rests on accurate diet reconstruction across a range of spatial and temporal scales (Ferry-Graham, Bolnick & Wainwright 2002; Futuyma & Moreno 1988; Irschick & Sherry 2005). Methods such as gut content analysis have been the historic focus of these studies, even though these methods are widely known to only document a short time window of a predator's diet (Hyslop 1980; Bearhop *et al.* 2004; Newsome *et al.* 2007). Mantis shrimp, in particular, digest their prey in a matter of hours rendering gut content analysis very difficult to perform (Dingle & Caldwell 1978; Kunze 1981; Caldwell, Roderick & Shuster 1989). Prey preference studies in the laboratory have also been used to determine important dietary components (Underwood, Chapman & Crowe 2004 and references therein), but these experiments have a limited capacity to accurately reflect natural diets, because laboratory conditions do not account for spatial and temporal variation in prey availability (Stephens & Krebs 1986; Blackwell, O' Hara & Christy 1998).

Stable isotope analysis, specifically of stable carbon and nitrogen isotope ratios (i.e. $^{13}C/^{12}C$ and $^{15}N/^{14}N$), has become a common alternative method for the *in situ* study of intra- and interspecific diet specialization (Bolnick *et al.* 2003; Layman *et al.* 2007; Newsome *et al.* 2007; Martínez del Rio *et al.* 2009; Araújo, Bolnick & Layman 2011; Layman *et al.* 2011). The central principle of stable isotope analysis is that the isotopic compositions of different prey items record

a predator's diet with reliable fidelity when prey are consumed, metabolized, and assimilated into a consumer's tissues (reviewed in Fry 2006). Given that all organisms have naturally occurring stable isotopes that reflect their nutrient sources, stable isotope analysis can be used to measure diet specialization across taxa (Bearhop *et al.* 2004; Newsome *et al.* 2007; Martínez del Rio *et al.* 2009). Another advantage of this approach is that stable isotopes allow for examining spatial (Fry *et al.* 1982; France 1995; Hemminga & Mateo 1996; Vaslet *et al.* 2011) and temporal (Tieszen *et al.* 1993; Bearhop *et al.* 2004; Dalerum & Angerbjörn 2005; Martinez del Rio *et al.* 2009) shifts in diet. These methods have been tested on animals with diverse diets, such as coral reef fishes, in conjunction with the traditional methods of diet analysis, which help to narrow the range of possible prey items in the diet (de la Moriniere *et al.* 2003; Nagelkerken *et al.* 2009; Frédérich *et al.* 2010; Vaslet *et al.* 2011; Layman & Allgeier 2012).

By coupling stable isotope analyses of diet with studies of prey abundance and feeding behavior in the field, I examined the diet of *Neogonodactylus bredini* (Manning 1969), an ubiquitous intertidal predator that inhabits Caribbean coral reef flats and sea grass beds. Most of the information on smasher diets comes from *N. bredini*; therefore, there was a foundation on which to build a more complete analysis of smasher diets (Caldwell, Roderick & Shuster 1989; Full, Caldwell & Chow 1989; Caldwell & Childress 1990). In addition, there exist accurate measurements of isotopic turnover rate (the rate at which new material is incorporated into tissues) and isotopic discrimination factors (the differences between predator and prey stable isotope values), which aid in measuring temporal shifts in diet and increase the accuracy of stable isotope diet reconstruction methods (deVries *et al.* In review).

This study specifically examined whether the diet of *N. bredini* included both hard- and soft-bodied prey items. I then compared *N. bredini's* diet between the coral reef and sea grass beds, as well as between the wet and dry seasons to describe spatial and temporal diet variation. I predicted that *N. bredini* would consume both hard-shelled and soft-bodied prey items, because its smashing appendage should allow it to process different kinds of prey. If *N. bredini* is able to consume different kinds of prey without difficulty, then the resulting diet should reflect the differences in prey abundance that occur among habitats and seasons. The outcome of this dual experimental and field-based approach informed the diet breadth of smashers while also providing insights into tropical marine intertidal food web dynamics.

Methods

Study site and sampling

This study was conducted in the intertidal zone at the Galeta Point Marine Laboratory (GPML) of the Smithsonian Tropical Research Institute, Colón, Panama (9° 24' 18" N, 79° 51' 48.5" W), where *N. bredini* are exceptionally abundant (Caldwell & Steger 1987). The intertidal zone consists of shallow flats that alternate between being dominated by either coral rubble or sea grass beds (*Thalassia testudinum*) and stretch from the shore to the reef crest. *N. bredini* are found in high densities in coralline algae nodules and coral rubble crevices in both habitats from the low-intertidal to the reef crest (Caldwell & Steger 1987). There are two distinct seasons at GPML. In the dry season (December to May), the reef flat experiences high winds and extreme low tides during the day, which expose the sea grass beds and leads to high sea grass mortality. During the wet season (June to November), the extreme low tides occur at night leaving the sea grass beds intact, but there may be increased fresh water input from ≤30 cm of rainfall day^{-1} (reviewed in Caldwell & Steger 1987).

Initial collections for stable isotope analysis occurred in April 2008 and included only the hard-shelled prey items. I returned to GPML in October 2008 to collect additional potential prey items and to examine whether diet was changing seasonally. To define additional potential prey items, I quantified the abundance of prey in both habitats, performed a feeding experiment to determine which prey *N. bredini* was capable of consuming, and observed feeding behavior in the field. Thus, there are stable isotope datasets for both the wet and dry seasons, but data from the abundance counts, the experiment, and the field observations only exist for the wet season.

Percent cover and relative abundance

To explore which prey items were available to *N. bredini* in the two habitats, abundance surveys of potential prey items were conducted in both habitats in October 2008. A sea grass habitat and a coral rubble habitat that neighbored each other in front of GPML were chosen and a 200 m^2 plot was established in each habitat. Although the two habitats were adjacent, the plots were 600 m apart, because they were placed approximately in the center of each habitat. Abundance counts of all potential prey items were made in 30 randomly selected 0.25 m^2 quadrats within each plot. Potential prey items were surveyed by counting all visible species in each quadrat. Coral rubble and rocks were also broken with a rock hammer to ensure that crevice-dwelling organisms were counted. Potential prey items were defined as any animal <70 mm in length. Body lengths were measured with digital calipers to the nearest mm (Absolute Coolant Proof Caliper Series 500, Mitutoyo Corporation, Takatsu, Japan). This size criterion assumed that *N. bredini* would not capture organisms much larger than its maximum body length of 65 mm. In each quadrat, percent cover of sea grass, sand, coral rubble, and rocks was visually assessed on snorkel to confirm the observed differences between habitats. Mean (± standard deviation) relative abundances were calculated for all animals in each habitat and Welch Two Sample t-tests were used to compare habitat features and organism abundances between the sea grass and coral rubble. These, and all additional statistical tests described below, were performed in R 2.15.0 (The R Foundation for Statistical Computing, Vienna, Austria).

Feeding experiment

To determine which of the available prey items *N. bredini* was capable of consuming, regardless of habitat and natural diets *in situ,* a feeding experiment was performed. Potential prey items were selected based on the abundance counts described above, as well as previous research on *N. bredini* diet (Caldwell, Roderick & Shuster 1989; Full, Caldwell & Chow 1989). The seven animal groups included crabs (*Xanthius spp*.), snapping shrimp (*Alpheus spp*.), brittle stars (*Ophiothrix angulata*), clams (*Arcopsis adamsi*), snails (*Cerithium atratum*), hermit crabs (*Clibanarius tricolor*), and worms (*Pontodrilus bermudensis*). Experimental animals were collected opportunistically from a habitat that had both sea grass and coral rubble (Permit No.'s: spring SEX/A-88-08, fall SEX/A-133-08). Sea grass (50 mm^2 pieces) was also included as a potential prey item in case *N. bredini* was supplementing its diet with plant material. All animals were measured as described above. *N. bredini* body sizes, measured from rostrum to telson, ranged from 31-55 mm (mean ± standard deviation = 41 ± 4 mm). Prey item body sizes ranged from 6 mm measured from the hinge joint to anterior end of a clam to 112 mm measured from the anterior to posterior ends of a worm.

The feeding experiment was conducted at GPML in an aquarium system with sixteen 15 cm^3 aquaria and filtered seawater. Sixteen 7.4 cc artificial cavities made of cement (Rockite Expansion Cement, Hartline Products Co., Cleveland, OH, USA) were constructed based on

methods described in Caldwell *et al*. (1989). A cavity was placed in each aquarium so that *N. bredini* individuals could hunt from a place of hiding. A layer of beach sand soaked in freshwater and subsequently dried in the sun for 24 hrs was also placed at the bottom of each tank. One mantis shrimp was released in each aquarium and given 24 hrs to acclimate. Each aquarium was then stocked with one of the eight potential prey items. Ten feeding trials per prey item were conducted with a different mantis shrimp individual and a different prey individual for each trial. *N. bredini* was documented as having consumed the prey item when it was either observed consuming the prey, or if the prey item was dead with evidence of consumption (e.g. missing tissue and marks where *N. bredini* had hammered the prey). Trials were terminated after four days if the prey item had not yet been consumed. If mantis shrimp molted (11 individuals), laid eggs (2 individuals), or died (one individual) during a trial, then the trial was repeated with a new mantis shrimp and prey item. Between trials, aquaria were drained, rinsed with freshwater, and given a new layer of sand.

In addition to determining which prey *N. bredini* would consume, I observed when and how prey were captured and consumed. I made approximate estimates of search and handling times by monitoring each trial for 1 min every hour from 06:00 to 18:00 for the duration of the experiment. When a prey item was placed in the aquarium with the *N. bredini* individual, I began recording search time and I monitored each trial for 1 minute to determine whether the prey was consumed immediately. Search time ended when the individual captured the prey. If a capture event occurred immediately, then the search time was recorded as 0 hr. Handling time was defined as the total time between capture and the completion of consumption. Captures were often visible, but the handing and consumption of the prey usually occurred in the cavities, especially for less mobile species, such as hermit crabs and snails. For these hard-shelled prey items, *N. bredini* individuals would deposit the shell remains outside of their cavities once they had finished processing the prey; therefore these acts were used to mark the end of handling time. Given that tanks were monitored every hour, the precise start and end of a search or handling event could often not be documented precisely. Instead, search and handling times were estimated to the nearest hour. Additional observations were made between the set hourly observations when possible, but all times are rounded to the nearest hour to be consistent with the set observation periods. For example, if a capture event was observed between the set hourly observations, then the search period was terminated and search time was estimated to the nearest hour.

Field observations of feeding behavior

To document feeding activity, I filmed *N. bredini* individuals in a 45 m^2 mixed sea grass, rock habitat plot during the transition from the wet to dry season (November 2010 to February 2011; Permit No. SEX/A-63-11). Behavior was filmed with 2 underwater cameras (Submergible Submersible Under-Water CCD 480TVL Bullet Color Camera, Sony Corporation, NY, USA) connected to Hi-8 video recorders (30 frames s^{-1}, Sony GV-A500 Hi8 Video Walkman, Sony Corporation, NY, USA). The cameras were placed in front of *N. bredini* cavities during each filming session and videos were later converted to digital format (Memorex Dual Format DVD Recorder MVDR2102, Oakdale MN, USA and iMovie, Apple Inc., CA, USA). A total of 28 focal cavities and 57 individual *N. bredini* were filmed over the course of 162 hrs. Individual differences in size and color pattern, which were visible in the videos, were used to distinguish individuals from one another.

Animal collection and sample preparation for stable isotope analysis

During the dry season (April 2008), 10 *N. bredini* individuals from coral rubble and 11 individuals from sea grass were collected along with clams, crabs, hermit crabs, and snails collected from both habitats (Table 3.1). During the wet season (October 2008), three *N. bredini* individuals from the coral rubble and five individuals from the sea grass were collected, along with clams, crabs, hermit crabs, snails, alpheid shrimp, brittle stars, and worms collected from both habitats, based on the results from the abundance counts and feeding experiment. *N. bredini* body sizes, measured from rostrum to telson, ranged from 30-46 mm (mean ± standard deviation = 37 ± 4 mm). Prey item body sizes ranged from 5 mm measured from the proximal to distal ends of a snail shell to 40 mm measured from the anterior to posterior ends of a worm.

Upon collection, all animals were frozen and stored at -20°C until dissection and preparation for stable isotope analysis. Prior to dissection, standard body lengths of all animals were measured. Hemolymph was removed from the *N. bredini* samples collected in the wet season with a 27-gauge needle and 1 ml syringe by inserting the needle above the fifth abdominal somite. Hemolymph from the dry season individuals was not analyzed because I was not able to extract enough volume of sample from these individuals. *N. bredini* muscle was also dissected from abdominal somites 2-6. For all prey items, muscle was dissected and separated from the guts to prevent contamination from stomach contents. All samples were freeze-dried (FreezeZone 12 Liter Freeze Dry System, Labconco, Kansas City, MO, USA) for 48 hrs and homogenized before stable isotope analysis.

I did not remove lipids and carbonates from tissue samples even though these constituents are known to have negative $\delta^{13}C$ values relative to proteins (DeNiro & Epstein 1978; reviewed in Boecklen *et al.* 2011). Muscle was dissected from all samples rendering carbonate removal unnecessary (Bunn, Loneragan & Kempster 1995; Mateo *et al.* 2008; Yokoyama *et al.* 2005). Lipids were not removed, because the invertebrates sampled here have low lipid contents (Post *et al.* 2007; Mateo *et al.* 2008) and because an experimental comparison of treated and untreated invertebrate tissues did not reveal significant differences between samples (deVries, *et al*. in review).

All samples were placed in 5 x 9 mm tin capsules and weighed (Costech Analytical Technologies, Valencia, CA, USA; 180 ± 50 μg for all muscle tissue and 220 ± 50 μg for *N. bredini* hemolymph). $\delta^{13}C$ and $\delta^{15}N$ stable isotope ratios were analyzed with elemental analyzer/continuous flow isotope ratio mass spectrometry at the University of California Berkeley Center for Stable Isotope Biogeochemistry using a CHNOS Elemental Analyzer (vario ISOTOPE cube, Elementar, Hanau, Germany) coupled with an IsoPrime100 Isotope Ratio Mass Spectrometer (Isoprime, Cheadle, UK). Isotope ratios are expressed using δ notation as:

$$\delta^{h}X = (R_{sample}/R_{standard}-1) \times 1000 \qquad \text{(Equation 1)}$$

where h is the high mass number, X is the element, R is the high mass-to-low mass isotope ratio, and $R_{standard}$ is Vienna Pee Dee belemnite (VPDB) for carbon and AIR for nitrogen. Units are parts per thousand (per mil, ‰). I used both peach leaves (Standard Reference Material [SRM] No. 1547, n=60, standard deviation [SD] of $\delta^{13}C$ = 0.1‰ and $\delta^{15}N$ = 0.2‰) and bovine liver (SRM No. 1577, n=7, SD of both $\delta^{13}C$ and $\delta^{15}N$ was = 0.1‰) as references and standards and to correct the stable isotope values for drift and linearly of the mass spectrometer.

Statistical analysis of stable isotope data

All stable isotope data were tested for normality using the Shapiro-Wilk test prior to further analysis (R 2.15.0, The R Foundation for Statistical Computing, Vienna, Austria). Differences in $\delta^{13}C$ and $\delta^{15}N$ values between *N. bredini*'s muscle and hemolymph tissue were evaluated using Welch's two-sample t-test. I examined whether $\delta^{13}C$ and $\delta^{15}N$ values in *N. bredini* were affected by habitat, seasonality, and the interaction between the two independent factors using a two-way ANOVA. Tukey's post hoc comparisons were used to assess significant differences between the two habitats and seasons. For prey items, the two-way ANOVA was repeated for the prey collected over both seasons (clams, crabs, hermit crabs, and snails) but a one-way ANOVA that only included habitat as a factor was performed for prey items only collected in the wet season (alpheids, brittle stars, and worms). To provide a visual representation of whether isotopic differences were more pronounced in either sea grass or coral rubble, the mean differences in the $\delta^{13}C$ and $\delta^{15}N$ values between the two habitats within seasons were compared for all animals. Mean differences in the $\delta^{13}C$ and $\delta^{15}N$ values between the wet and dry seasons within habitat types were also compared.

To determine *N. bredini*'s diet within each habitat and season, I calculated the percent contribution of each prey item to the diet using the stable isotope mixing model SIAR v. 4.1.3 (Stable Isotope Analysis in R; Parnell *et al.* 2010). SIAR uses Bayesian statistical inference to approach estimating the probable contributions of each prey item (or source) to a predator's diet when the solution is undefined (the number of sources is greater than the number of isotopes + 1). This method also accounts for uncertainties associated with variation between samples and discrimination factors by assuming that the variability associated with these factors is normally distributed (Parnell *et al.* 2010). Experimentally determined discrimination factors (Δ) for *N. bredini* muscle ($\Delta^{15}N= 0.9 \pm 0.3$ ‰, $\Delta^{13}C= 3.0 \pm 0.6$ ‰) and hemolymph ($\Delta^{15}N= 0.1 \pm 0.2$ ‰, $\Delta^{13}C= 1.7 \pm 0.3$ ‰) were used (deVries *et al.* In review). Concentrations of elemental carbon and nitrogen in each source were also included in the model so that the estimates could be weighted by the amounts of elemental carbon and nitrogen in each prey item (Phillips & Koch 2002). Uninformative priors based on the Dirichlet distribution (a generalized Beta distribution) were used to model each prey item as equally likely to contribute to the stable isotope composition of the consumer (Parnell *et al.* 2010). 1,000,000 simulations were performed with Markov chain Monte Carlo and 100,000 burnins (the initial simulations that are discarded due to variability) to generate estimates of source contributions to the diet (Parnell *et al.* 2010).

For the dry season, the model was run with *N. bredini* as the consumer and the prey items clams, crabs, hermit crabs, and snails as the sources for both habitats. For the wet season, the model was run with *N. bredini* as the consumer and the prey items clams, crabs, hermit crabs, snails, alpheids, brittle stars, and worms as sources for both habitats. Given that more prey items were collected during the wet season, the model also was run with just the hard-shelled prey from the wet season (because these hard-shelled prey, clams, crabs, hermit crabs, and snails, were collected in both seasons) as a sensitivity analysis to determine if the proportional contributions changed when fewer prey were included in the model.

Results

Percent cover and relative abundance

As predicted, *T. testudinum* dominated the sea grass habitat whereas coral rubble, sand, and rocks dominated the coral rubble habitat (Table 3.1). Hermit crabs and snails were the main

prey items present in the sea grass habitat, followed by brittle stars (Table 3.1). In the coral rubble, worms were the most abundant prey item. All hard-shelled prey items (clams, crabs, and hermit crabs), as well as alpheids, were present in similar abundances (Table 3.1). Alpheids were not found in sea grass and brittle stars were not found in coral rubble, but these prey items were included in the subsequent feeding experiment and stable isotope analyses because of their abundances in the other habitats (Table 3.1).

Feeding experiment

In the feeding experiment, all prey items were consumed except for sea grass. Therefore, only data from the animal prey items are presented. The order, from the most to the least number of trials, in which prey were consumed, was: alpheids = worms > clams > crabs = hermit crabs > brittle stars = snails (Table 3.2). Search times ranged from 0 hr to 40 hrs. Handling times ranged from 0 hr to 6 hrs, but the only handling times that were greater than 1 hr were for brittle stars (Table 3.2). Observations of prey capture events revealed that the predatory appendage was used to hammer every prey item, except for brittle stars. It is possible that brittle stars were hammered, but I did not directly observe hammering on brittle star bodies or gather evidence of tissue damage due to hammering (Table 3.2). All prey items were consumed inside mantis shrimp cavities, except for the crabs, which were consumed outside of the cavity in 2 trials.

Field observations of feeding behavior

In 162 hrs of video recordings, only one feeding event of an individual capturing an evasive alpheid prey item with its raptorial appendages was recorded. However, there were 85 instances of individuals acting aggressively towards other organisms. Specifically, I recorded 31 events where individuals produced threat displays or struck at conspecifics over cavity access. In the other 54 aggressive events, individuals produced threat displays towards predators or other competitors. The most common behaviors were peeking from the cavity entrances or remaining in the cavity.

Statistical and mixing model analyses of stable isotope data

The δ-values of all animals shifted at least 1 ‰ between either habitats or seasons or both (Table 3.3, Fig. 3.1), but the directions of these shifts were not consistent between habitats or seasons (Fig. 3.2). As expected, *N. bredini* possessed more enriched $\delta^{15}N$ values relative to its prey, but $\delta^{13}C$ values were generally similar (Table 3.3, Fig. 3.1). There was a significant interaction between habitat and season in the $\delta^{13}C$ values of *N. bredini*, but in the $\delta^{15}N$ values, the interaction between habitat and season in was not significant (Table 3.4). Alpheids showed significant differences in the $\delta^{15}N$ between habitats within the wet season (one-way ANOVA: mean difference ± SE = 0.4 ± 0.1 ‰, $p<0.003$, $F=22.43$, df_1, $n=18$). For the $\delta^{13}N$ values in snails, there was a significant interaction between habitat and season, and for the snail $\delta^{13}C$ values, there were significant differences between habitats (Table 3.4).

Despite these inconsistencies, comparing mean differences in stable isotope values between habitats revealed that, in general, for $\delta^{13}C$, there were greater differences in the wet season compared to the dry season, for $\delta^{15}N$, the differences were greater in the dry season (Fig. 3.2 A, B). Comparing differences between seasons within habitats showed that there were greater differences between mean $\delta^{13}C$ values within coral rubble compared to within sea grass (Fig. 3.2 C, D), but for $\delta^{15}N$, only *N. bredini* in sea grass had a mean difference greater than 2‰

whereby $\delta^{15}N$ was more enriched in the dry season (Fig. 3.2 D), but this difference was not statistically significant (Table 3.4).

Stable isotope values of *N. bredini*'s hemolymph and muscle tissue did not significantly differ (Table 3.3). The mixing model analyses also did not qualitatively differ between tissue types. As such, to simplify the presentation the mixing model results, I focus on the muscle tissue only. The Bayesian mixing model analysis of diet showed that, during the wet season, all prey items contributed about equally to the diet in the coral rubble habitat (contribution range: 13-16 %; Fig. 3.3 D). In sea grass, clams and alpheids were the top contributors to the diet with contributions of 30 % and 24 %, respectively (Fig. 3.3 B). These patterns remained consistent, even when the model was run on just hard-shelled prey items from the wet season (Suppl. Table 3.1). During the dry season, clams were an important food source in both habitats (Fig. 3.3 A, C).

Discussion

Despite the large abundances of snails and hermit crabs in both habitats and the previous research indicating that *N. bredini's* diet consists mostly of those prey (Caldwell, Roderick & Shuster 1989; Full, Caldwell & Chow 1989; Caldwell & Childress 1990), I found that *N. bredini* consumes a wide range of different food sources consisting of both hard- and soft-bodied prey types. Moreover, results indicate that predation patterns vary between habitats and seasons. Here, I examine how *N. bredini*'s diet may relate to spatial and temporal changes in prey abundance and availability. I then connect these findings to raptorial appendage function and to the potential role of *N. bredini* as an opportunistic, generalist predator in the intertidal coral reef food web.

Prey abundance between the two habitats

During the wet season, even though the coral rubble and sea grass habitats are proximate to one another, habitat structures, prey types, and prey abundances differed between the two habitats (Table 3.1). In the sea grass habitat, the most abundant prey items were hermit crabs and snails (Table 3.1), which were generally found aggregating on sand or sea grass blades. In the coral rubble habitat, however, worms were the most abundant prey item (Table 3.1). Thus, mantis shrimp living in either coral rubble or sea grass likely experienced differences in prey abundances between the two habitats. It should be noted that *N. bredini* individuals are known to move between habitats over the course of months to years because of strong storm surges that transport coral rubble cavities to other habitats (Caldwell & Steger 1987). However, it is unlikely that movement between habitats occurs consistently for foraging, as individuals seem to prefer to choose prey items that are close to their home cavities and often do not travel more than several meters to search for prey (Caldwell, Roderick & Shuster 1989; Caldwell & Childress 1990).

Which prey items are **N. bredini** *capable of consuming?*

Regardless of differences in prey abundances between habitats, the feeding experiment demonstrated that *N. bredini* individuals were capable of consuming evasive and soft-bodied prey, in addition to hard-shelled prey. In fact, two relatively soft-bodied prey items, alpheids and worms, were the only prey to be consumed in all trials (Table 3.2). The smashing raptorial strike was almost always employed at some point during the feeding process, whether it was to break

open a hard-shelled prey item, or to capture and subdue a swimming alpheid (Table 3.2). The handling times were similar among prey items, because once the prey was subdued, *N. bredini* spent the majority of its time tearing at muscle tissue with its maxillipeds, as opposed to hammering the prey (Table 3.2). Thus, regardless of whether the prey was hard-shelled or soft-bodied, the time required to consume each prey item was relatively similar in this experiment.

A limitation of the feeding experiment is that all prey items were presented in the same way in a controlled environment. As a result, the search and handling times documented here cannot necessarily be translated to the natural environment, because *N. bredini* individuals face different challenges in the field than they do in an aquarium. However, this experiment still informed what and how *N. bredini* will consume prey when the prey items themselves are the only main differences between the trials. The overall finding suggest that *N. bredini* will strike and consume soft-bodied animals when presented with them, regardless of their morphological specializations for hammering hard-shelled prey.

N. bredini's *diet between two habitats and seasons*

Results from the stable isotope mixing model determined which prey *N. bredini* actually consumed in the field and showed that their diets did not necessarily the reflect the differences in prey abundance between habitats. In the coral rubble during the wet season, worms were the most abundant prey item (Table 3.1), but *N. bredini* consumed all prey in equal proportions (Fig. 3.3). In sea grass during the wet season, hermit crabs and snails were the most abundant prey items (Table 3.1), but *N. bredini* mostly preyed upon alpheids and clams (Fig. 3.3) even though their abundances in were low (Table 3.1). Alpheids and clams are often found in the same coral rubble pieces in which *N. bredini* live (Caldwell & Steger 1987), which was also the case in this study. Thus, *N. bredini* may have consumed those prey in higher proportions in sea grass simply because the prey were easily accessible from their cavities in the coral rubble.

In the dry season, clams were the highest contributor to diet in both habitats but especially in sea grass (Fig. 3.3). Crabs were also important contributors to the diet in coral rubble. Given the extreme low tides that occur during the wet season, which leave the majority of both habitats exposed (Caldwell & Steger 1987), it is possible that clams and crabs could have been the most accessible for mantis shrimp that were confined to small tide pools.

It is interesting to note that during the dry season, both habitats were very similar in appearance, as they both consisted of mainly coral rubble and sand. These observations of habitat similarities are also illustrated by the fact that the mean $\delta^{13}C$ differences of the prey between the two habitats were nearly equivalent in the dry season (Fig. 3.2 A). This result suggests that the two habitats were comparable in structure, because they were receiving similar inputs from primary production (Fry *et al.* 1982; France 1995; Hemminga & Mateo 1996; Vaslet *et al.* 2011). However, the effects of sea grass mortality on the stable isotope values and therefore primary production inputs merits further investigation, because interestingly, the lowest mean differences are seen between seasons within sea grass (Fig. 3.2 D). If sea grass mortality was changing the primary production inputs, then one would expect $\delta^{13}C$ differences between seasons to be the greatest within sea grass.

For both seasons, the possibility that the mixing model analyses were not accurate must be considered. For the wet season analysis, the Bayesian model may have calculated equal likelihood probabilities for each prey item, because too many sources were included in the analysis (Parnell *et al.* 2010). However, the mixing model estimates are more likely a result of natural variation in stable isotope data (Fig, 3.1 D), because high variation can also yield equal

percent contributions to the diet (Parnell *et al.* 2010). For the dry season analysis, fewer prey items were included in this model, which could lead to an overestimation of the proportional contribution of certain prey to the diet (Parnell *et al.* 2010). Clams, however, remained the top contributor to the diet regardless of whether the soft-bodied prey items were included in the analysis (Suppl. Table 3.1), suggesting that clams were an important contributor to *N. bredini's* diet despite habitat differences or seasonality.

Taken together, these findings reinforce the notion that *N. bredini* individuals are not restricted to diets of only hard-shelled prey, because all prey items were represented in the diet. The results further suggest that diet breadth is determined, not necessarily by prey abundance, but by being able to access prey or by the nutritional value of the prey. Caldwell and Steger (1987) noted the importance of prey availability to mantis shrimp diet when they observed that the growth rate of larger mantis shrimp increased after an oil spill affected many of the reef flats surrounding GPML. These researchers also documented a dramatic increase in the hermit crab population and often an abundance of hermit crabs were within centimeters of mantis shrimp cavities. Although mantis shrimp diet was never analyzed post oil spill, it is not difficult to surmise that *N. bredini*'s increase in growth rate was due to individuals being able to consume hermit crabs in great quantities without the abundance of this prey item diminishing (Caldwell & Steger 1987). Caldwell and Childress (1990) later substantiated the idea that prey selection is governed in large part by prey accessibility, by demonstrating that *N. bredini* is more likely to choose snails that are visible and within close proximity to their cavities than snails that are not visible and are farther away from the cavity. Future studies examining encounter rates with different prey items in the field will further elucidate whether prey accessibility contributes to variation in prey consumption between habitats.

In addition to the seasonal and habitat differences affecting prey availability, *N. bredini*'s molt cycle, which is a basic aspect of mantis shrimp biology, likely also contributed to the documented proportional contributions of prey to the diet. For 2-3 weeks after mantis shrimp shed the old exoskeleton and grow a new one, the new exoskeleton has not fully calcified or hardened (Reaka 1975; Caldwell and Steger 1983; R. L. Caldwell pers. comm.). When the exoskeleton has not completely hardened, the ability to generate forceful strikes is reduced, because the exoskeletal components required for generating power strikes are not fully functional (Caldwell and Steger 1983). If strike force is reduced, then *N. bredini* individuals may not be able to crush hard-shelled prey and are therefore limited to a diet of soft-bodied prey that do not require extremely high speeds and accelerations to consume (deVries, Murphy & Patek 2012). Thus, it is possible that some of the individuals sampled in this study had recently molted and consumed soft-bodied prey, which would result in higher proportional contributions of soft-bodied prey to the diet compared to if none of the sampled individuals had molted.

N. bredini *feeding behavior and coral reef trophic dynamics*

The complementary approaches used here to describe mantis shrimp diet demonstrate the importance of examining diet with both field and laboratory experiments. The stable isotope analysis allowed for comparing diet between individuals living in different habitats. Findings from the feeding experiment and field observations strengthened the stable isotope analysis by constraining *N. bredini*'s potential prey items and by providing information on mantis shrimp feeding behavior. In turn, the abundance data gave the necessary context for interpreting these three datasets. This approach builds a foundation for measuring diet breadth in mantis shrimp

that will ultimately yield a richer context for exploring correlations between diet and morphology across mantis shrimp taxa.

In retrospect, the overall finding that *N. bredini* consumes a diverse range of prey, including hard- and soft-bodied organisms, may not be surprising. The high speeds and accelerations generated by *N. bredini*'s raptorial appendage should allow it both to crush hard-shelled prey with high-impact strikes and to move with speeds that are fast enough to capture evasive prey items. Thus, by definition, *N. bredini* is perhaps not an example of a functional specialist, because raptorial appendage morphology does not limit this species to a narrow diet of only hard-shelled prey. Instead, *N. bredini*'s ability to effectively consume hard-shelled prey serves to broaden diet breadth allowing this animal to consume resources that many other animals in its environment cannot.

Besides evolving to consume hard-shelled prey, there are alternative explanations for the evolution of the raptorial strike. Smasher species must be able to manipulate hard coral rubble substrate to construct their cavity dwellings. The evolution of the mantis shrimp strike, therefore, also has been attributed to the need to hammer hard substrates (Ahyong 1997; Ahyong & Harling 2000). However, large smasher species, including those in the genus *Odontodactylus* which produce among the fastest strikes recorded in mantis shrimp to date (Patek, Korff & Caldwell 2004; Patek & Caldwell 2005), burrow in sandy substrates under coral or rocks (Ahyong 2001). Although further investigation examining correlations between appendage morphology and habitat type are required, this observation provides evidence against the need to manipulate hard substrates as being the main selection pressure behind the evolution of the raptorial strike.

Another important characteristic of smasher habitats in the intertidal zone is that the availability of cavity dwellings in both coral rubble and sea grass is very limited. As a result, mantis shrimp are known to frequently fight with conspecifics and other competitors to maintain control over cavities (Dingle & Caldwell 1975; Caldwell & Dingle 1975; Caldwell & Steger 1987; Caldwell 1992; Taylor 2010). Thus, an alternative explanation for the evolution of the forceful appendage strike is that it evolved in response to heightened aggressive intra- and interspecific interactions over limited cavity space.

When *N. bredini* feeding behavior is examined in conjunction with the use of the appendage to strike aggressively, it becomes evident that being an opportunistic, generalist predator presents distinct advantages for *N. bredini*. Recall that in the field recordings of *N. bredini*, only one feeding event was recorded, but there were 85 instances of individuals producing threat displays or striking at other animals over cavity access. Thus, perhaps the prey capture strategy of *N. bredini* allows individuals to rapidly apprehend soft-bodied prey or to gather and then crush hard-shelled prey that are within close proximity to their cavities without losing access to these cavities.

Studies on *N. bredini* feeding behavior showed that *N. bredini* selects medium-sized snails when given snails of varying sizes in a controlled laboratory setting, likely because medium snails are easier to carry back to the cavity than larger snails and because more strikes and longer handling times are required to crush larger snails (Full, Caldwell & Chow 1989; Caldwell & Childress 1990). The former explanation supports the notion that mantis shrimp must gather prey rapidly so as not to lose their cavities. The later explanation suggests that although there are other functional demands on the raptorial appendage, consuming hard-shelled prey does present a challenge to mantis shrimp and is therefore likely a selective pressure on the mantis shrimp strike. Disentangling whether selective pressure for forceful mantis shrimp strikes

can be attributed to maintaining control over cavities or to smashing hard-shelled prey has yet to be accomplished, because both selective pressures are likely acting in concert. Regardless, the results from this study demonstrate that hard-shelled prey items do contribute to mantis shrimp diet even though these prey may be challenging to consume.

An aspect of mantis shrimp anatomy that has not been discussed thus far, are the maxillipeds, which are arguably just as specialized as the raptorial appendages but for different feeding functions (Caldwell & Dingle 1976; Caldwell & Childress 1990). Unlike most crustaceans, mantis shrimp maxillipeds are excellent at rapidly grabbing prey from the water column, manipulating prey before smashing it, and tearing prey apart to expose the tissue for consumption (Caldwell & Childress 1990). In this study, the maxillipeds were observed manipulating and tearing at prey items, not grabbling them from the water column (Table 3.2). However, it is possible that *N. bredini* is able to consume both soft- and hard-bodied prey, because the raptorial appendages and the maxillipeds each perform different functions which, when working together, give mantis shrimp the ability to consume a wide range of prey. To my knowledge, all studies on stomatopod feeding have centered on the raptorial appendage. Thus, future research would benefit greatly from determining exactly how the maxillipeds contribute to mantis shrimp feeding behavior.

Despite their powerful punch, mantis shrimp are the major diet item of common reef animals, such as snappers, lionfish, octopus, and pufferfish (Duarte & Garcia 1999; Layman & Allgeier 2012; R L. Caldwell pers. comm.). *N. bredini* in particular are found in densities as high as 5 individuals per m^2 on the reef flat and are therefore an abundant food source for predators (Caldwell & Steger 1987; Caldwell & Childress 1990). Given that mantis shrimp are very abundant and consumed by a diversity of larger predators, while also consuming many different prey themselves, mantis shrimp may actually be an important link between macro-invertebrates of the intertidal and larger coral reef predators. Future research targeting the strength of trophic interactions involving mantis shrimp would lend unique insight into the current understanding of coral reef food web dynamics. A range of trophic studies using stable isotope analysis have been conducted on coral reef fishes (de la Moriniere *et al.* 2003; Nagelkerken *et al.* 2009; Frédérich *et al.* 2010; Vaslet *et al.* 2011; Layman & Allgeier 2012; McMahon, Berumen & Thorrold 2012 and references therein) and on macro-invertebrates in sea grass habitats (Fry *et al.* 1982; Kennedy *et al.* 2001; Palomar, Junio-Meñez & Karplus 2004; Jeong, Suh & Kang 2012). However, to my knowledge, surprisingly no stable isotope analyses have focused on intertidal coral reef macro-invertebrates. Thus, the results presented here provide baseline information about food web interactions in this important, yet understudied ecosystem.

In summary, this study provides novel insights into how the feeding ecology of smashers is shaped by habitat characteristics and prey availability, as well as by a suite of inherent mantis shrimp characteristics, including raptorial appendage morphology, feeding behavior, and even the molt cycle. The results uncover valuable information about trophic dynamics in coral reefs and contribute to a growing literature suggesting that highly specialized feeding morphology is not necessarily an indicator of diet specialization (Liem 1980; Barnett, Bellwood & Hoey 2006; Bellwood *et al.* 2006; Feranec 2007). Together, these conclusions inform how trophic ecology relates to the discordant relationship between specialized morphology and a generalized diet and will ultimately help to establish whether this pattern as a widespread phenomenon across taxa.

References

Ahyong, S.T. (1997) Phylogenetic analysis of the Stomatopoda (Malacostraca). *Journal of Crustacean Biology,* 17, 695-715.

Ahyong, S.T. (2001) Revision of the Australian stomatopod Crustacea. *Records of the Australian Museum Supplement 26*, 1-326.

Ahyong, S.T. & Harling, C. (2000) The phylogeny of the stomatopod Crustacea. *Australian Journal of Zoology,* 48, 607-642.

Araújo, M.S., Bolnick, D.I. & Layman, C.A. (2011) The ecological causes of individual specialisation. *Ecology Letters,* 14, 948-958.

Barnett, A., Bellwood, D.R. & Hoey, A.S. (2006) Trophic ecomorphology of cardinalfish. *Marine Ecology Progress Series,* 322, 249-257.

Bearhop, S., Adams, C.E., Waldrons, S., Fuller, R.A. & Macleod, H. (2004) Determining trophic niche width: a novel approach using stable isotope analysis. *Journal of Animal Ecology,* 73, 1007-1012.

Bellwood, D.R., Wainwright, P.C., Fulton, C.J. & Hoey, A.S. (2006) Functional versatility supports coral reef biodiversity. *Proceedings of the Royal Society B-Biological Sciences,* 273, 101-107.

Blackwell, P.R.Y., O' Hara, P.D. & Christy, J.H. (1998) Prey availability and selective foraging in shorebirds. *Animal Behavior,* 55.

Boecklen, W.J., Yarnes, C.T., Cook, B.A. & James, A.C. (2011) On the use of stable isotopes in trophic ecology. *Annual Review of Ecology, Evolution, and Systematics,* 42, 411-440.

Bolnick, D.I., Fordyce, J.A., Yang, L.H., Davis, J.M., Hulsey, C.D. & Forister, M.L. (2003) The ecology of individuals: incidence and implications of individual specialization. *The American Naturalist,* 161, 1-27.

Bunn, S.E., Loneragan, N.R. & Kempster, M.A. (1995) Effects of acid washing on stable isotope ratios of C and N in penaeid shrimp and seagrass: omplications for food-web studies using multiple stable isotopes. *Limnology and Oceanography,* 40, 622-625.

Burrows, M. (1969) The mechanics and neural control of the prey capture strike in the mantid shrimps *Squilla* and *Hemisquilla*. *Zeitschrift fur vergleichende Physiologie,* 62, 361-381.

Caldwell, R.L. (1992) Recognition, signalling and reduced aggression between former mates in a stomatopod. *Animal Behavior,* 44, 11-19.

Caldwell, R.L. & Childress, M.J. (1990) Prey selection and processing in a stomatopod crustacean. *Behavioral Mechanisms of Food Selection* (ed. R.N. Hughes). Springer-Verlag, Berlin, Germany.

Caldwell, R.L. & Dingle, H. (1975) Ecology and evolution of agonistic behavior in Stomatopods. *Naturwissenschaften,* 62, 214-222.

Caldwell, R.L. & Dingle, H. (1976) Stomatopods. *Scientific American*, 81-89.

Caldwell, R.L., Roderick, G.K. & Shuster, S.M. (1989) Studies of predation by *Gonodactylus bredini*. *Biology of Stomatopods* (ed. E.A. Ferrero), pp. 117-131. Mucchi, Modena.

Caldwell, R.L. & Steger, R. (1987) Effects of May, 1986 oil spill on gonodactylid stomatopods near Galeta Point *Short-term assesment of an oil spill at Bahia Las Minas, Panama* (eds J.B.C. Jackson, J.D. Cubit, B.D. Keller, V. Batista, K. Burns, H.M. Caffey, R.L. Caldwell, S.D. Garrity, C.D. Getter, C. Gonzalez, H.M. Guzman, K.W. Kaufmann, A.H. Knap, S.C. Levings, M.J. Marshall, R. Steger, R.C. Thompson & E. Weil), pp. 113. Smithsonian Tropical Research Institute, Panama City

Claverie, T., Chan, E. & Patek, S.N. (2011) Modularity and scaling in fast movements: power amplificaiton in mantis shrimp. *Evolution,* 65, 443-461.

Dalerum, F. & Angerbjörn, A. (2005) Resolving temporal variation in vertebrate diets using naturally occurring stable isotopes. *Oecologia,* 144, 647-658.

Darwin, C. (1859) *The Origin of Species*. Oxford University Press, Oxford.

Darwin, C. (1862) *The Various Contrivances by which Orchids are Fertilised by Insects*. John Murray, London.

de la Moriniere, E.C., Pollux, J.A., Nagelkerken, I., Hemming, M.A., Huiskes, A.H.L. & Van der Velde, G. (2003) Ontogenetic dietary changes of coral reef fishes in the mangrove-seagrass-reef continuum: stable isotopes and gut-content analysis. *Marine Ecology Progress Series,* 246, 279-289.

DeNiro, M.J. & Epstein, S. (1978) Influence of diet in the distribution of carbon isotopes in animals. *Geochimica Et Cosmochimica Acta,* 42, 495-506.

deVries, M.S., Martínez del Rio, C., Tunstall, T.S. & Dawson, T.E. (In review) Isotopic incorporation rates and discrimination factors in mantis shrimp: insights into crustacean physiology and life history. *Functional Ecology*.

deVries, M.S., Murphy, E.A.K. & Patek, S.N. (2012) Ambushing prey with a long spear: morphology and kinematics of "spearing" mantis shrimp. *Journal of Experimental Biology,* 215, 4374-4384.

Dingle, H. & Caldwell, R.L. (1975) Distribution, abundance, and interspecific agonisitic behavior of two mudflat stomatopods. *Oecologia,* 20, 167-178.

Dingle, H. & Caldwell, R.L. (1978) Ecology and morphology of feeding and agonistic behavior in mudflat stomatopods (Squillidae). *Biological Bulletin,* 155, 134-149.

Dominguez, J.H. & Reaka, M.L. (1988) Temporal activity patterns in reef-dwelling stomatopods: a test of alternative hypotheses. *Journal of Experimental Marine Biology and Ecology,* 117, 47-69.

Duarte, L.O. & Garcia, C.B. (1999) Diet of the lane snapper, *Lutjanus synagris* (Lutjanidae), in the Gulf of Salamanca, Colombia. *Caribbean Journal of Science,* 35, 54-63.

Ferry-Graham, L.A., Bolnick, D.I. & Wainwright, P.C. (2002) Using functional morphology to examine the ecology and evolution of specialization. *Integrative and Comparative Biology,* 42, 265-277.

France, R.L. (1995) ^{13}C enrichment in benthic compared to planktonic algae - foodweb implications. *Marine Ecology Progress Series,* 124, 307-312.

Frédérich, B., Lehanse, O., Vandewalle, P. & Lepoint, G. (2010) Trophic niche width, shift, and specialization of *Dascyllus aruanus* in Toliara Lagoon, Madagascar. *Copeia,* 2, 218-226.

Fry, B. (2006) *Stable Isotope Ecology*. Springer Science + Business Media, New York, NY.

Fry, B., Lutes, R., Northam, M. & Parker, P.L. (1982) A $^{13}C/^{12}C$ comparison of food webs in Caribbean seagrass meadows and coral reefs. *Aquatic Botany,* 14, 389-398.

Full, R.J., Caldwell, R.L. & Chow, S.W. (1989) Smashing energetics: prey selection and feeding efficiency of the stomatopod, *Gonodactylus bredini*. *Ethology,* 81, 134-147.

Futuyma, D.J. & Moreno, G. (1988) The Evolution of Ecological Specialization. *Annual Review of Ecology and Systematics,* 19, 207-233.

Grant, B.R. & Grant, P.R. (1993) Evolution of Darwin's finches caused by a rare climatic event. *Proceedings of the Royal Society B-Biological Sciences,* 251, 111-117.

Hemminga, M.A. & Mateo, M.A. (1996) Stable carbon isotopes in seagrasses: variability in ratios and use in ecological studies. *Marine Ecology Progress Series,* 140, 285-298.

Hyslop, E.J. (1980) Stomach contents analysis - a review of methods and their application. *Journal of Fish Biology,* 17, 411-430.

Irschick, D.J. & Sherry, T.W. (2005) Phylogenetic methodology for studying specialization. *Oikos,* 110, 404-408.

Jeong, S.J., Suh, H.-L. & Kang, C.-K. (2012) Trophic diversity in amphipods within a temperate eelgrass ecosystem as determined by gut contents and C and N isotope analysis. *Marine Biology,* 159, 1943-1954.

Kennedy, H., Richardson, C.A., Duarte, C.M. & Kennedy, D.P. (2001) Diet and association of *Pontonia pinnophylax* occuring in *Pinna nobilis*: insights from stable isotope analysis. *Journal of the Marine Biological Association of the United Kingdom,* 81, 177-178.

Kunze, J.C. (1981) The functional morphology of stomatopod Crustacea. *Philosophical Transactions of the Royal Society of London,* 292, 255-328.

Layman, C.A. & Allgeier, J.E. (2012) Characterizing trophic ecology of generalist consumers: a case study of the invasive lionfish in The Bahamas. *Marine Ecology Progress Series,* 448.

Layman, C.A., Araújo, M.S., Boucek, R., Hammerschlag-Peyer, C.M., Harrison, E., Jud, Z.R., Matich, P., Rosenblatt, A.E., Vaudo, J.J., Yeager, L.A., Post, D.M. & Bearhop, S. (2011) Applying stable isotopes to examine food-web structure: an overview of analytical tools.

Layman, C.A., Arrington, D., Montana, C.G. & Post, D.M. (2007) Can stable isotope ratios provide for community-wide measures of trophic structure? *Ecology,* 88, 42-48.

Liem, K.F. (1980) Adaptive significance of intra- and interspecific differences in the feeding repertoires of cichlid fishes. *American Zoologist,* 20, 295-314.

Manning, R.B. (1969) *Stomatopod Crustacea of the Western Atlantic*. University of Miami Press, Coral Gables, FL.

Martínez del Rio, C., Anderson-Sprecher, R., Gonzalez, P. & Sabat, P. (2009) Dietary and isotopic specialization: the niche of three Cinclodes ovenbirds. *Oecologia,* 161, 149-159.

Martinez del Rio, C., Wolf, N., Carleton, S. & Gannes, L.Z. (2009) Isotopic ecology ten years after a call for more laboratory experiments. *Biological Review Cambridge Philosophical Society,* 84, 91-111.

Mateo, M.A., Serrano, O., Serrano, L. & Michener, R.H. (2008) Effects of sample preparation on stable isotope ratios of carbon and nitrogen in marine invertebrates: implications for food web studies using stable isotopes. *Oecologia,* 157, 105-115.

McMahon, K.W., Berumen, M.I. & Thorrold, S.R. (2012) Linking habitat mosaics and connectivity in a coral reef seascape. *Proceedings of the National Academy of Sciences,* 109, 15372-15376.

Nagelkerken, I., Van der Velde, G., Wartenbergh, S.L.J., Nugues, M.M. & Pratchett, M.S. (2009) Cryptic dietary components reduce dietary overlap among sympatric butterflyfishes (Chaetodontidae). *Journal of Fish Biology,* 75, 1123-1143.

Newsome, S.D., Martínez del Rio, C., Bearhop, S. & Phillips, D.L. (2007) A niche for isotope ecology. *Frontiers in Ecology and the Environment,* 5, 429-439.

Palomar, N.E., Junio-Meñez, M.A. & Karplus, I. (2004) Feeding habits of the burrowing shrimp *Alpheus macellarius*. *Journal of the Marine Biological Association of the United Kingdom,* 84, 1199-1202.

Parnell, A., Inger, R., Bearhop, S. & Jackson, A. (2010) Source partitioning using stable isotopes: coping with too much variation. *PLoS Biology,* 5, e9672.

Patek, S.N. & Caldwell, R.L. (2005) Extreme impact and cavitation forces of a biological hammer: strike forces of the peacock mantis shrimp (*Odontodactylus scyllarus*). *Journal of Experimental Biology,* 208, 3655-3664.

Patek, S.N., Korff, W.L. & Caldwell, R.L. (2004) Deadly strike mechanism of a mantis shrimp. *Nature,* 428, 819-820.

Phillips, D.L. & Koch, P.L. (2002) Incorporating concentration dependence in stable isotope mixing models. *Oecologia,* 130, 114-125.

Post, D.M., Layman, C.A., Arrington, D.A., Takimoto, G., Quattrochi, J. & Montaña, C.G. (2007) Getting to the fat of the matter: models, methods and assumptions for dealing with lipids in stable isotope analyses. *Oecologia,* 152, 179-189.

Reaka, M.L. (1975) Molting in stomatopod crustaceans. 1. Stages of molt cycle, setagenesis, and morphology. *Journal of Morphology,* 146, 50-80.

Stephens, D.W. & Krebs, J.R. (1986) *Foraging Theory*. Princeton University Press, Princeton, NJ.

Taylor, J.R.A. (2010) Ritualized fighting and biological armor: the impact mechanics of the mantis shrimp's telson. *Journal of Experimental Biology,* 213, 3496-3504.

Tieszen, L.L., Boutton, T.W., Tesdahl, K.G. & Slade, N.A. (1993) Fractionation and turnover of stable carbon isotopes in animal tissues: implications for $\delta^{13}C$ analysis of diet. *Oecologia,* 57, 32-37.

Underwood, A.J., Chapman, M.G. & Crowe, T.P. (2004) Identifying and understanding ecological preferences for habitat or prey. *Journal of Experimental Marine Biology and Ecology,* 300, 161-187.

Van Valen, L. (1965) Morphological variation and width of ecological niche. *The American Naturalist,* 99, 377-390.

Vaslet, A., France, C., Phillips, D.L., Feller, I.C. & Baldwin, C.C. (2011) Stable-isotope analyses reveal the importance of seagrass beds as feeding areas for juveniles of the speckled worm eel *Myrophis punctatus* (Teleostei: Ophichthidae) in Florida. *Journal of Fish Biology,* 79, 692-706.

Wainwright, P.C. & Reilly, S.M. (1994) *Ecological Morphology: Integrative Organismal Biology.* The U. of Chicago Press, Chicago.

Yokoyama, H., Tamaki, A., Harada, K., Shimoda, K., Koyama, K. & Ishihi, Y. (2005) Variability of diet-tissue isotopic fractionation in estuarine macrobenthos. *Marine Ecology Progress Series,* 296, 115-128.

Zack, T.I., Claverie, T. & Patek, S.N. (2009) Elastic energy storage in the mantis shrimp's fast predatory strike. *Journal of Experimental Biology,* 212, 4002-4009.

Tables

Table 3.1. Mean percent cover of common habitat characteristics (sea grass, coral rubble, rocks, and sand) and mean abundance of each potential prey item are presented for sea grass and coral rubble during the wet season. All means represent percent and abundances per 0.25 m^2. 30 quadrats that were 0.25 m^2 were sampled in each habitat. Note that alpheids and brittle stars are categorized as "soft-bodied" because their exoskeletons are much softer than those of the hard-bodied prey items. Bold values indicate significant differences between the two habitats in percent cover or mean relative abundance of habitat characteristics and prey types, respectively ($p < 0.05$). NA is listed for rocks in sea grass, because rocks were not found in the sampled quadrats.

Habitat feature or organism	Sea grass	Coral rubble
Mean percent cover ± SD (%)		
sea grass	**59.33 ± 17.90**	**0.67 ± 2.86**
coral rubble	**2.03 ± 3.71**	**18.43 ± 27.12**
sand	28.40 ± 14.80	32.16 ± 25.33
rocks	**NA**	**40.27 ± 24.50**
Mean abundance ± SD of prey types		
Soft-bodied prey		
alpheid	**0.00 ± 0.00**	**9.67 ± 13.66**
brittle star	**6.67 ± 21.85**	**0.00 ± 0.00**
worm	**0.27 ± 1.01**	**31.85 ± 28.27**
Hard-shelled prey		
clam	**1.85 ± 10.14**	**15.29 ± 19.16**
crab	**0.46 ± 1.64**	**11.20 ± 20.08**
hermit crab	**51.20 ± 35.39**	**14.33 ± 24.65**
snail	**39.60 ± 35.50**	**14.98 ± 25.68**

Table 3.2. The number of trials out of 10 total trials in which prey items were consumed during the feeding experiment are presented, along with estimates of mean ± SD search and handling times for each prey item rounded to the nearest hour, and observations of how each prey item was consumed. Prey types are categorized as soft-bodied and hard-shelled.

Prey type	No. successful trials	Search time (hr)	Handling time (hr)	Feeding observations
Soft-bodied				
alpheid	10	8 ± 12 (n=10)	0 ± 0 (n=5)	Pursued then subdued prey with raptorial appendage hits. Consumed muscle with maxillipeds in cavity.
brittle star	6	7 ± 5 (n=2)	3 ± 3 (n=2)	Prey entered cavity on its own. *N. bredini* consumed the brittle star body and sometimes the legs.
worm	10	4 ± 4 (n=10)	1 ± 0 (n=10)	Captured prey outside of cavity with maxillipeds then subdued with raptorial appendage hits. Consumed in cavity.
Hard-shelled				
clam	9	5 ± 6 (n=6)	0 ± 0 (n=6)	Carried to cavity with maxillipeds. Consumed muscle in cavity using raptorial appendages to smash open shell.
crab	7	10 ± 12 (n=4)	1 ± 1 (n=3)	Pursued then subdued prey with raptorial appendage hits to crab's chelipeds. Consumed muscle under carapace with maxillipeds in or out of cavity.
hermit crab	7	11 ± 14 (n=7)	1 ± 0 (n=5)	Carried prey to cavity with maxillipeds. Consumed muscle in cavity using raptorial appendages to smash open shell.
snail	6	4 ± 3 (n=6)	1 ± 0 (n=6)	Carried prey to cavity with maxillipeds. Consumed muscle in cavity using raptorial appendages to smash open shell.

n = number of trials for which search and handling time was calculated.

Table 3.3. Mean ± SD $\delta^{13}C$ and $\delta^{15}N$ of *N. bredini* and its food sources from both habitats and seasons. Bold indicates significant differences in $\delta^{13}C$ or $\delta^{15}N$ for prey items between habitats within seasons. A Bonferroni corrected significance value of $p < 0.003$ was used to correct for 18 multiple comparisons of stable isotope data.

	Sea grass			Coral rubble		
Animal	n	$\delta^{13}C \pm SD$ (‰)	$\delta^{15}N \pm SD$ (‰)	n	$\delta^{13}C \pm SD$ (‰)	$\delta^{15}N \pm SD$ (‰)
Dry season						
N. bredini muscle	11	**-10.4 ± 1.6**	**7.5 ± 0.9**	10	**-12.3 ± 0.14**	**8.2 ± 0.8**
clam	5	-12.4 ± 0.6	5.2 ± 0.4	5	-14.4 ± 2.2	5.4 ± 0.3
crab	4	-12.5 ± 1.4	3.2 ± 0.9	4	-14.0 ± 1.7	5.0 ± 1.9
hermit crab	4	-10.3 ± 0.8	3.4 ± 0.2	4	-11.2 ± 1.1	3.5 ± 1.0
snail	4	-7.9 ± 0.7	3.6 ± 2.0	5	-9.9 ± 1.4	5.6 ± 0.9
Wet season						
N. bredini						
muscle	5	-9.4 ± 0.6	6.9 ± 0.4	3	-8.5 ± 1.1	6.7 ± 1.1
hemolymph	5	-9.7 ± 0.6	6.3 ± 0.5	2	-8.6 ± 1.6	6.4 ± 0.6
alpheid	8	-11.0 ± 1.4	**6.4 ± 0.2**	10	-10.2 ± 0.6	**6.0 ± 0.2**
brittle star	8	-7.0 ± 2.6	5.0 ± 0.6	6	-7.4 ± 2.4	7.2 ± 1.6
clam	4	-13.3 ± 0.6	5.6 ± 0.2	6	-9.5 ± 1.1	5.1 ± 0.2
crab	12	-12.5 ± 1.4	3.2 ± 0.9	15	-11.3 ± 2.8	3.8 ± 0.8
hermit crab	23	-11.8 ± 1.1	3.8 ± 0.5	9	-10.9 ± 2.0	3.6 ± 0.5
snail	20	**-8.7 ± 0.9**	**4.6 ± 0.3**	26	**-11.5 ± 3.3**	**4.2 ± 0.7**
worm	24	-10.8 ± 0.1	5.1 ± 0.1	5	-9.9 ± 0.9	6.6 ± 1.3

n = number of individuals analyzed for $\delta^{13}C$ and $\delta^{15}N$ values.

Table 3.4. Results of a two-way Analysis of Variance (ANOVA) evaluating differences in mantis shrimp and snail $\delta^{13}C$ and $\delta^{15}N$ values between habitats and seasons. Only these animals are shown, because all other analyses on the other prey items were not significant. Post hoc (HSD) < 0.003 = Tukey's post hoc comparisons with Bonferroni corrected honestly significantly differences (HSD).

Factor	SS	df	MS	*F*	*p*	Post hoc (HSD) < 0.003
Mantis shrimp						
$\delta^{13}C$						
Habitat	13.93	1	13.93	23.49	**<0.003**	sea grass > coral, in dry
Season	18.86	1	18.86	31.38	**<0.003**	dry < wet, in coral
Habitat × Season	10.41	1	10.41	17.56	**<0.003**	
$\delta^{15}N$						
Habitat	2.04	1	2.04	7.18	0.01	
Season	3.58	1	3.58	12.57	**0.002**	dry > wet, in coral
Habitat × Season	1.02	1	1.02	3.59	0.07	
Snail						
$\delta^{13}C$						
Habitat	100.19	1	100.19	17.12	**<0.003**	sea grass > coral, in wet
Season	10.43	1	10.43	1.78	0.19	
Habitat × Season	1.03	1	1.03	0.18	0.68	
$\delta^{15}N$						
Habitat	0.003	1	0.003	0.01	0.91	
Season	1.14	1	1.14	5.67	0.02	
Habitat × Season	11.87	1	11.87	46.84	**<0.003**	

Figure Legends

Figure 3.1. Graphic representation of mean (± SD) $\delta^{13}C$ vs. $\delta^{15}N$ values of mantis shrimp and their potential prey items shows that mantis shrimp have $\delta^{13}C$ and $\delta^{15}N$ values that are more similar to the potential prey items in the wet season compared to the dry season. Animals were collected from sea grass (A, B) and coral rubble (C, D) in the dry season (A, C) and wet season (B, D). The full range of potential prey items was collected during the wet season only. All animals shifted at least 1 ‰ between habitats and seasons.

Figure 3.2. Mean (± propagated SE) differences between δ-values of mantis shrimp and hard-shelled prey from the two habitats and seasons. Coral δ-values minus sea grass δ-values shows the direction of change between habitats and within seasons (A, B). Wet season δ-values minus dry season δ-values shows the direction of change between seasons within habitats (C, D).

Figure 3.3. A Bayesian mixing model analysis of the stable isotope values shows that the mean (± Bayesian 95 % C.I., n values listed in Table 3.3) percent contributions of each prey item to *N. bredini*'s diet were similar for all prey from the wet season (B, D), but that clams dominated the diet in the dry season (A, C). The full range of potential prey items was collected during the wet season only. Symbols correspond to the diet items listed on the x-axes.

Figures

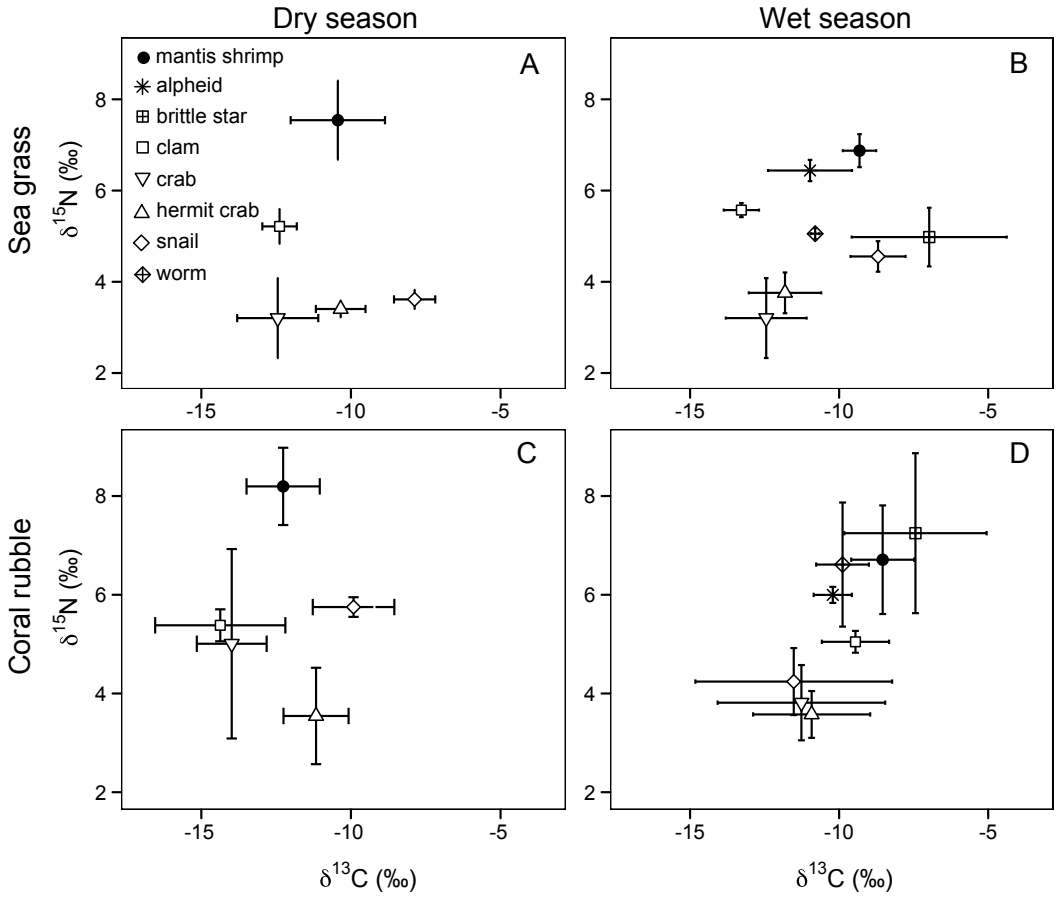

Figure 3.1. Graphic representation of mean (± SD) $\delta^{13}C$ vs. $\delta^{15}N$ values of mantis shrimp and their potential prey items shows that mantis shrimp have $\delta^{13}C$ and $\delta^{15}N$ values that are more similar to the potential prey items in the wet season compared to the dry season. Animals were collected from sea grass (A, B) and coral rubble (C, D) in the dry season (A, C) and wet season (B, D). The full range of potential prey items was collected during the wet season only. All animals shifted at least 1 ‰ between habitats and seasons.

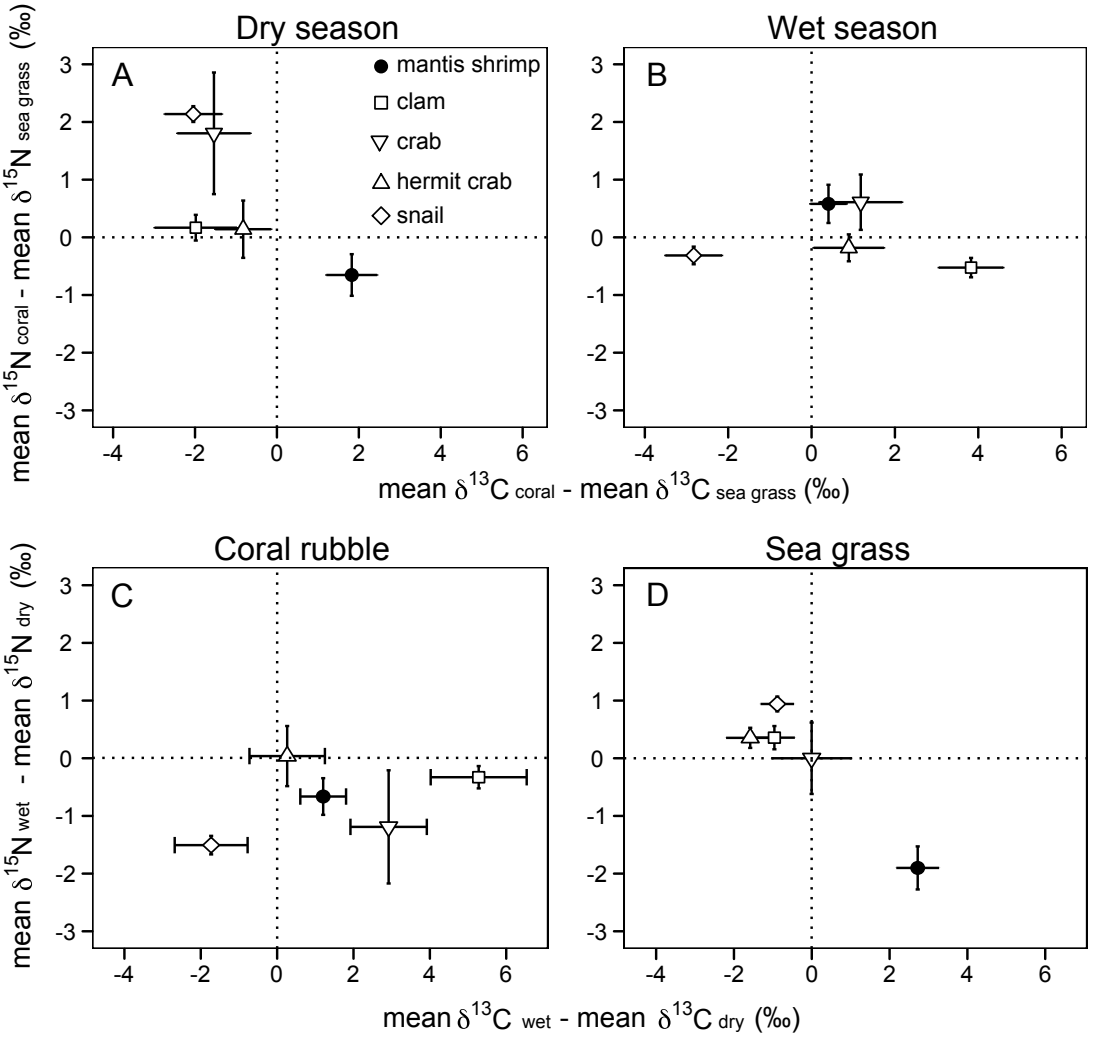

Figure 3.2. Mean (± propagated SE) differences between δ values of mantis shrimp and hard-shelled prey from both habitats and seasons. Coral δ-values minus sea grass δ-values shows the direction of change between habitats and within seasons (A, B). Wet season δ-values minus dry season δ-values shows the direction of change between seasons within habitats (C, D).

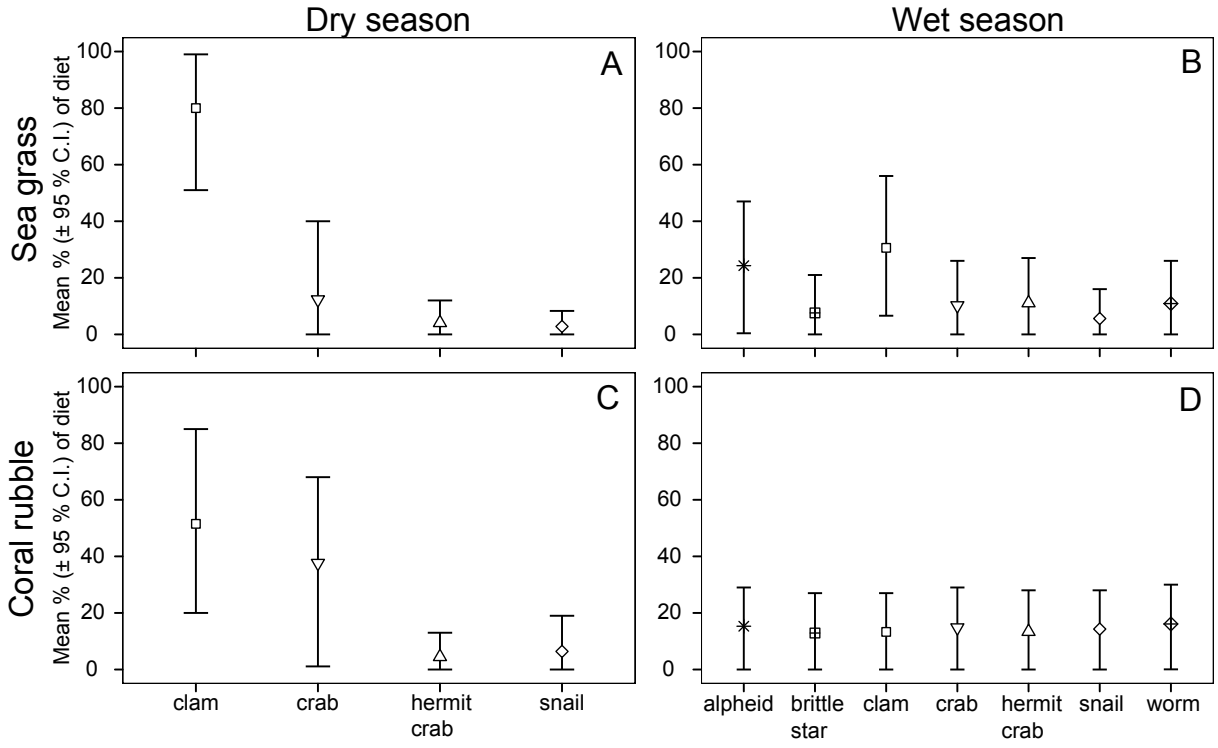

Figure 3.3. A Bayesian mixing model analysis of the stable isotope values shows that the mean (± Bayesian 95 % C.I., n values listed in Table 3.3) percent contributions of each prey item to *N. bredini*'s diet were similar for all prey from the wet season (B, D), but that clams dominated the diet in the dry season (A, C). The full range of potential prey items was collected during the wet season only. Symbols correspond to the diet items listed on the x-axes.

Supplementary Material

Supplementary Table 3.1. Mean (Bayesian 95% confidence intervals) percent contributions to *N. bredini's* diet calculated with the program, Stable Isotope Analysis in R (SIAR), for muscle tissue of (a) hard-shelled prey items collected from each habitat during the wet and dry seasons and (b) soft-bodied prey items collected from each habitat during the wet season only. For the wet season, results are presented for the SIAR model run on the complete dataset with all prey items included (full model) and on only the hard-shelled prey items. Running the model two ways on the wet season data showed that while the percent contributions to the diet changed when the soft-bodied prey items were included in the analysis, the order of importance of each prey to the diet remained the same. Important source contributions are shown in bold.

	Wet season (full model)		Wet season (hard-shelled prey)		Dry season	
Prey item	Sea grass (%)	Coral rubble (%)	Sea grass (%)	Coral rubble (%)	Sea grass (%)	Coral rubble (%)
Hard-shelled						
clam	**30.6 (6.5-56.0)**	13.3 (0-27.0)	**47.3 (20.0-78.0)**	24.4 (0-47.0)	**80.8 (51.0-99.0)**	**51.5 (20.0-85.0)**
crab	10.2 (0-26.0)	14.8 (0-29.0)	17.7 (0-40.0)	25.2 (0.08-47.0)	12.3 (0-40.0)	37.6 (1.1-68.0)
hermit crab	11.1 (0-27.0)	13.4 (0-28.0)	20.6 (0-43.0)	24.2 (0-48.0)	4.1 (0-12)	4.5 (0-13.0)
snail	5.6 (0-16.0)	14.3 (0-28.0)	14.4 (0.2-28.0)	26.2 (0.1-49.0)	2.8 (0-8.3)	6.4 (0-19.0)
Soft-bodied						
alpheid	**24.3 (0.4-47.0)**	15.3 (0-29.0)				
brittle star	7.6 (0-21.0)	12.9 (0-27.0)				
worm	10.9 (0-26)	16.1 (0.06-30.0)				

Conclusion

In this dissertation, I measured the kinematics of spearing mantis shrimp and the diet breadth of smashing mantis shrimp, by examining feeding mechanics, metabolism, and feeding behavior.

In Chapter I, I examined the feeding mechanics and behavior of the spearing mantis shrimp, *Lysiosquillina maculata*. I found that spearer strikes were slower, but had a farther reach than smasher strikes. This result suggests that there is a trade-off between reach and kinematic output, because it may be more important for spearers to reach far outside of their burrows to capture fast moving prey, as opposed to spearing with extremely high speeds.

In Chapter II, I measured the rate at which carbon and nitrogen incorporated into the tissue of *Neogonodactylus bredini*, a smashing mantis shrimp. Although there was variation in incorporation rates between muscle and hemolymph, N. *bredini*'s rate of carbon incorporation was consistent with those predicted by an allometric equation correlating incorporation rate with body mass for teleost fishes and sharks. Interestingly, the incorporation rate of $\delta^{15}N$ in hemolymph was faster than the incorporation rate of $\delta^{13}C$. This finding suggests that *N. bredini* leads an energetically demanding lifestyle, which requires absorbing high amounts of protein.

In Chapter III, I examined the feeding ecology and diet of *N. bredini*. In contrast with the hypothesis that specialized feeding morphology corresponds to a narrow diet, *N. bredini*'s smashing appendage does not limit this predator to a diet of only hard-shelled prey. *N. bredini* consumed both hard- and soft-bodied prey available in the habitat, likely because it seeks the prey that are most available and easy to access. Being able to consume a range of available prey, regardless of whether it is hard- or soft-bodied, could help *N. bredini* individuals to reduce the risk of losing their home cavity to other competitors.

This body of research forms the foundation for constructing an overarching definition of diet specialization applicable across taxa (Ferry-Graham, Bolnick & Wainwright 2002; Irschick & Sherry 2005). Given that diet specialization is a relative term and I only explored the diet breadth of one smashing species, I was unable to determine how general *N. bredini's* diet is relative to other mantis shrimp. However, my findings provide the first step towards creating a standard diet breadth continuum that can be used to define degree of diet specialization across taxa. These results provide the essential foundation with which to test the diet breadth continuum in mantis shrimp using stable isotope analysis.

In addition to mantis shrimp, there are other observations of animals with specialized feeding morphology consuming types of prey that would not necessarily require specialized mechanics. As mentioned in the Introduction, the scale-eating cichlid, which has remarkably specialized jaws for nipping scales off of other fish, also consumes zooplankton (Liem 1980). Additionally, labroid fish species have jaw morphologies that range from aggressive suction feeders to algal scrapers, yet these species appear to have broad diets (Bellwood *et al.* 2006). Similarly, fossil records of ungulates moving into grasslands show that the evolution of specialized dentition for consuming grass did not prevent ungulates from eating other plants (Feranec 2007).

In Chapter III, I introduced the idea that consumers exhibiting a tight link between feeding morphology and diet are usually categorized as *functional specialists*, because their morphology restricts them to a subset of available resources (Ferry-Graham, Bolnick & Wainwright 2002). When associations between smashing morphology and diet are examined in

conjunction with other examples of animals with specialized morphology, however, it becomes evident that having feeding morphology which performs one ecological function may have two ecological ramifications. Specialized morphology can either narrow diets, or it can broaden diets by making it possible for consumers to feed on prey items that other animals in its habitat cannot. Thus, mantis shrimp, along with the other examples described herein, cannot be defined as functional specialists because specialized morphology does not appear to limit diet breadth. Instead, I propose that these animals be termed *functional generalists*, because their specialized morphology allows them to access a subset of available resources unavailable to other animals, but it does not limit them to just this resource subset.

Smashing mantis shrimp provide an excellent example of functional generalists. Their raptorial appendages, which are highly specialized to produce high speeds and accelerations yielding high force, allow smashers to consume hard-shelled prey items that are very difficult for other animals to process. The result is that smashers are able to consume a wider range of prey than would otherwise be possible without the capacity to produce forceful strikes. This discovery, coupled with evidence from the other animals described herein, suggest that functional generalists are more prevalent in nature than is thought. Future research may show that the ability of "specialized" morphology to increase diet breadth is a widespread phenomenon across animals once considered to be diet specialists (Barnett, Bellwood & Hoey 2006, Bellwood *et al.* 2006, Liem 1980).

References

Barnett, A., Bellwood, D.R. & Hoey, A.S. (2006) Trophic ecomorphology of cardinalfish. *Marine Ecology Progress Series,* 322, 249-257.

Bellwood, D.R., Wainwright, P.C., Fulton, C.J. & Hoey, A.S. (2006) Functional versatility supports coral reef biodiversity. *Proceedings of the Royal Society B-Biological Sciences,* 273, 101-107.

Bolnick, D.I., Fordyce, J.A., Yang, L.H., Davis, J.M., Hulsey, C.D. & Forister, M.L. (2003) The ecology of individuals: incidence and implications of individual specialization. *The American Naturalist,* 161, 1-27.

Feranec, R.S. (2007) Ecological generalization during adaptive radiation: evidence from Neogene mammals. *Evolutionary Ecology Research,* 9, 555-557.

Ferry-Graham, L.A., Bolnick, D.I. & Wainwright, P.C. (2002) Using functional morphology to examine the ecology and evolution of specialization. *Integrative and Comparative Biology,* 42, 265-277.

Futuyma, D.J. & Moreno, G. (1988) The Evolution of Ecological Specialization. *Annual Review of Ecology and Systematics,* 19, 207-233.

Hutchinson, G.E. (1957) Concluding Remarks. *Cold Spring Harbour Symposia on Quantitative Biology*, pp. 415-427.

Irschick, D.J. & Sherry, T.W. (2005) Phylogenetic methodology for studying specialization. *Oikos,* 110, 404-408.

Liem, K.F. (1980) Adaptive significance of intra- and interspecific differences in the feeding repertoires of cichlid fishes. *American Zoologist,* 20, 295-314.